

# Tunnel and multiphoton ionization of atoms and ions in a strong laser field (Keldysh theory)

V S Popov

DOI: 10.1070/PU2004v047n09ABEH001812

## Contents

1. Introduction	855
2. Early papers	856
3. Further development of the Keldysh theory	859
4. Ionization in the field of an ultrashort laser pulse	864
5. Adiabatic case	866
6. Effect of a magnetic field on the ionization probability	867
7. Lorentz ionization	867
8. Exactly solvable model	869
9. Keldysh theory and experiment	871
10. Relativistic tunneling theory	873
11. Electron – positron pair production from a vacuum by the field of high-power optical and X-ray lasers	875
12. Conclusion	878
13. Appendices	879
13.1 Asymptotic coefficients for atoms and ions; 13.2 The Keldysh function and its expansions; 13.3 Remarks on the ‘ADK theory’	
References	883

**Abstract.** The theoretical description of the nonlinear photoionization of atoms and ions exposed to high-intensity laser radiation is underlain by the Keldysh theory proposed in 1964. The paper reviews this theory and its further development. The discussion is concerned with the energy and angular photoelectron distributions for the cases of linearly, circularly, and elliptically polarized laser radiation, with the ionization rate of atomic states exposed to a monochromatic electromagnetic wave and to ultrashort laser pulses of various shape, and with momentum and angular photoelectron spectra in these cases. The limiting cases of tunnel ( $\gamma \ll 1$ ) and multiphoton ( $\gamma \gg 1$ ) ionization are discussed, where  $\gamma$  is the adiabaticity parameter, or the Keldysh parameter. The probability of above-barrier ionization is calculated for hydrogen atoms in a low-frequency laser field. The effect of a strong magnetic field on the ionization probability is discussed. The process of Lorentz ionization occurring in the motion of atoms and ions in a constant magnetic field is considered. The properties of an exactly solvable model — the ionization of an  $s$ -level bound by zero-range forces in the field of a circularly polarized electromagnetic wave — are

described. In connection with this example, the Zel’dovich regularization method in the theory of quasistationary states is discussed. Results of the Keldysh theory are compared with experiment. A brief discussion is made of the relativistic ionization theory applicable when the binding energy of the atomic level is comparable with the electron rest mass (multiply charged ions) and the sub-barrier electron motion can no longer be considered to be nonrelativistic. A similar process of electron-positron pair production from a vacuum by the field of high-power optical or X-ray lasers (the Schwinger effect) is considered. The calculations invoke the method of imaginary time, which provides a convenient and physically clear way of calculating the probability of particle tunneling through time-varying barriers. Discussed in the Appendices are the properties of the asymptotic coefficients of the atomic wave function, the expansions for the Keldysh function, and the so-called ‘ADK theory’.

## 1. Introduction

Ionization of atoms, ions, and semiconductors exposed to high-intensity laser radiation has been considered in hundreds of papers. The theory of these processes originates with the work by Keldysh [1], who showed for the first time that the tunnel effect in a variable electric field  $\mathcal{E}(t) = \mathcal{E} \cos \omega t$  and the multiphoton ionization of atoms are the two limiting cases of nonlinear photoionization, whose character depends strongly on the value of the adiabaticity parameter  $\gamma$ . This parameter, also introduced by Keldysh, is the ratio between the frequency of laser light  $\omega$  and the frequency  $\omega_t$  of electron tunneling through a

V S Popov Russian State Research Center ‘Institute of Theoretical and Experimental Physics’,  
ul. B. Chermushkinskaya 25, 117259 Moscow, Russian Federation  
Tel. (7-095) 129 96 14  
E-mail: markina@itep.ru

Received 15 April 2004, revised 24 May 2004  
*Uspekhi Fizicheskikh Nauk* 174 (9) 921–951 (2004)  
Translated by E N Ragozin; edited by M V Chekhova

potential barrier,

$$\gamma = \frac{\omega}{\omega_t} = \frac{\omega\sqrt{2mI}}{e\mathcal{E}} = \frac{1}{2K_0F}, \quad (1.1)$$

where  $I = \kappa^2 m e^4 / 2\hbar^2$  is the ionization potential of the atomic level,  $\mathcal{E}$  is the amplitude of the electric wave field,  $F = \mathcal{E}/\kappa^3 \mathcal{E}_a$  is the reduced field, and  $K_0 = I/\hbar\omega$  is the multiquantumness parameter of the process, i.e., the minimal number of photons required for ionization. Further, as a rule, atomic units  $\hbar = m = e = 1$  are used, where  $m$  is the electron mass. We note that  $\kappa = \sqrt{I/I_H}$ ,  $F$ ,  $K_0$ , and  $\gamma$  are dimensionless quantities; here,  $I_H = m e^4 / 2\hbar^2 = 13.6$  eV is the ionization potential of the hydrogen atom,  $\mathcal{E}_a = m^2 e^5 / \hbar^4 = 5.14 \times 10^9$  V cm<sup>-1</sup> is the atomic unit of electric field intensity (in this case,  $\kappa = 1$  and  $F \equiv \mathcal{E}$  for the ground state of the hydrogen atom), and the ionization rate  $w$  of a level is measured in the units  $m e^4 / \hbar^3 = 4.13 \times 10^{16}$  s<sup>-1</sup>.

Tunnel ionization of atomic states takes place when  $\gamma \ll 1$ , while for  $\gamma \gg 1$  the ionization is a multiphoton process [1]. When calculating the matrix element for the transition from the initial atomic state, which belongs to a discrete spectrum, to the final state, which belongs to a continuum, Keldysh employed the Volkov wave function [2, 3], in which the interaction between the electron and the field of a light wave is exactly taken into account while the Coulomb interaction between the ejected electron and the atomic core is neglected. As a result, analytical formulas were obtained for the ionization rate  $w$ , which describe not only the two limiting cases ( $\gamma \ll 1$  and  $\gamma \gg 1$ ), but also the intermediate range of parameter values  $\gamma \sim 1$ , where the formulas become significantly more complicated. The results obtained by Keldysh laid the foundation for subsequent investigations (both theoretical and experimental) in this area of atomic physics.

2004 marks forty years since the pioneering work of L V Keldysh [1] first appeared. We believe that the present time is appropriate for reviewing this theory and its present-day status.

## 2. Early papers

Shortly after the appearance of Ref. [1], Nikishov and Ritus [4] and Perelomov, Popov, and Terent'ev [5, 6] obtained analytical expressions for energy and momentum photoelectron spectra, as well as the exact form of the pre-exponential factor in the Keldysh formula for the ionization rate  $w$ . These results are valid for arbitrary values of the  $\gamma$  parameter and refer to the ionization of a state bound by a short-range potential, or a  $\delta$ -potential (which is a good approximation in the case of ionization of singly charged negative ions such as H<sup>-</sup>, Na<sup>-</sup>, I<sup>-</sup>, etc.). The inclusion of the Coulomb interaction in the final state was considered in Refs [6–9]. Also considered, with an exponential accuracy,<sup>1</sup> was the effect of a constant magnetic field on the ionization rate of a level [10]. The ionization probability is proportional to the squared asymptotic coefficient  $C_{\kappa l}$ , which is determined from independent calculations (see Refs [11–15], as well as

<sup>1</sup> The rate of tunnel ionization  $w$  depends extremely sharply on the intensity of the applied field [see, for instance, formula (2.5)]. Calculation of the exponential factor in  $w$  alone provides a qualitative description of ionization, and in some cases a quantitative description.

Appendix 13.1). Here, we mention only some of the results obtained in these works.<sup>2</sup>

For a linearly polarized monochromatic electromagnetic wave, the differential ionization probability, i.e., the momentum photoelectron spectrum, is of the form

$$dw(\mathbf{p}) = P \exp \left\{ -2K_0 \left[ f(\gamma) + c_1(\gamma)q_{\parallel}^2 + c_2(\gamma)q_{\perp}^2 \right] \right\} \frac{d^3p}{(2\pi)^3}, \quad (2.1)$$

where  $\mathbf{q} = \mathbf{p}/\kappa$  and  $f(\gamma)$  is the Keldysh function [1, 16]:

$$f(\gamma) = \left( 1 + \frac{1}{2\gamma^2} \right) \operatorname{arcsinh} \gamma - \frac{\sqrt{1+\gamma^2}}{2\gamma} \\ = \begin{cases} \frac{2}{3}\gamma - \frac{1}{15}\gamma^3, & \gamma \ll 1, \\ \ln 2\gamma - \frac{1}{2}, & \gamma \gg 1 \end{cases} \quad (2.2)$$

(for more details, see Appendix 13.2), the coefficients of the photoelectron momentum distribution are [5]

$$c_1(\gamma) = \operatorname{arcsinh} \gamma - \gamma(1+\gamma^2)^{-1/2}, \quad (2.2') \\ c_2(\gamma) = \operatorname{arcsinh} \gamma,$$

and  $P(\gamma)$  is the pre-exponential factor. Implied in this case is the fulfillment of the conditions

$$F \ll 1 \quad \text{and} \quad K_0 \gg 1, \quad (2.3)$$

which are required for the quasiclassical approximation to be applicable, while the Keldysh parameter  $\gamma$  may be arbitrary. Here,

$$\operatorname{arcsinh} \gamma \equiv \ln(\gamma + \sqrt{1+\gamma^2}),$$

$\mathbf{p} = (p_{\parallel}, p_{\perp})$  is the photoelectron momentum, with  $p_{\parallel}$  being the momentum component along the direction of the electric field  $\mathcal{E}$ ,  $p_{\perp}$  being perpendicular to it, and  $\kappa = \sqrt{2I}$  being the characteristic momentum of the bound state.

In the adiabatic limit ( $\gamma \ll 1$ ), the angular photoelectron distribution has a sharp peak along the field  $\mathcal{E}$ :  $p_{\parallel} \sim \gamma^{-1} p_{\perp} \gg p_{\perp} \sim \kappa\sqrt{F}$ . At the same time, in the opposite case  $\gamma \gg 1$  we have

$$p_{\parallel} \approx p_{\perp} \sim \kappa(K_0 \ln \gamma)^{-1/2} \ll \kappa,$$

and the angular distribution approaches the isotropic one. For the ionization rate of a level (i.e., the probability of ionization per unit time) we have with an exponential accuracy

$$w(F, \omega) \propto \begin{cases} \exp \left\{ -\frac{2}{3F} \left[ 1 - \frac{1}{10} \left( 1 - \frac{1}{3} \xi^2 \right) \gamma^2 \right] \right\}, & \gamma \ll 1, \\ (K_0 F)^{2K_0} \sim J^{K_0}, & \gamma \gg 1, \end{cases} \quad (2.4)$$

where  $J = (c/8\pi)(1 + \xi^2)\mathcal{E}^2$  is the intensity of laser radiation and  $\xi$  is its ellipticity [ $\xi^2 \leq 1$ , see formula (3.2)].

The pre-exponential factor  $P$  in Eqn (2.1) was also calculated in Refs [4, 5]. For instance, for  $\gamma \ll 1$  the ionization rate of a state  $|lm\rangle$  with the orbital angular momentum  $l$  by

<sup>2</sup> An extensive account of the calculations was published in Refs [8, 9]. When comparing formulas from Refs [1, 5, 6] with Refs [4, 7, 9] one should remember the relation between the designations:  $\xi = 1/\gamma$ .

**Table 1.** Asymptotic coefficients for the ground states of atoms and ions ( $l = 0$ ).

$Z = 1$	$I, \text{eV}$	$n^*$	$A$	$C_\kappa$		$c_1 \cdot 100$	Grade of accuracy
				HF	H		
H	13.60	1.000	2	1.000	1.000	0	A
Li	5.392	1.588	0.82	1.07	1.061	1.87	B
Na	5.139	1.627	0.74	1.04	1.058	1.64	B
K	4.341	1.770	0.52	0.95	1.043	0.71	C
Rb	4.177	1.804	0.48	0.94	1.038	0.51	C
Cs	3.894	1.869	0.42	0.92	1.027	0.23	B
Sr	5.695	1.545	0.86	1.05	1.063	2.02	C
He	24.59	0.744	2.87	0.993	0.912	4.83	A
Ne	21.57	0.794	1.75	1.18	0.932	3.02	C
Ar	15.76	0.929	2.11	0.950	0.998	0.29	B
Kr	14.00	0.986	2.22	1.13	0.979	0.01	B
Xe	12.13	1.059	2.4	1.3	1.015	0.15	C
U	6.194	1.484	0.99	1.08	1.064	2.31	A

$Z = 2$	$I, \text{eV}$	$n^*$	$A$	$C_\kappa$		$c_1 \cdot 100$	Grade of accuracy
				HF	H		
Li <sup>+</sup>	75.64	0.848	6.5	1.02	0.952	1.49	C
Sr <sup>+</sup>	11.03	2.221	1.39	0.93	0.942	0.42	B
Xe <sup>+</sup>	20.98	1.610	3.2	1.01	1.059	1.69	C

$Z = 0$	$I, \text{eV}$	$\kappa$	$A$	$C_\kappa$		$c_1$	Grade of accuracy
				HF	H		
H <sup>-</sup>	0.7542	0.235	1.11	1.15	0.5	1.0	B
Li <sup>-</sup>	0.618	0.212	1.0	1.09	0.5	1.0	D
Na <sup>-</sup>	0.548	0.201	1.0	1.12	0.5	1.0	D
K <sup>-</sup>	0.502	0.192	0.9	1.03	0.5	1.0	E
Rb <sup>-</sup>	0.486	0.189	0.8	0.92	0.5	1.0	E

Note.  $Z$  is the charge of the atom or ion core,  $n^*$  is the effective principal quantum number,  $A$  are coefficients from handbook [14], HF and H are the values of  $C_\kappa$  calculated by the self-consistent field (Hartree–Fock) method and by the Hartree formula (2.7), and  $c_1$  is the coefficient in the expansion (13.1.3). Grades of accuracy for  $A$  and  $C_\kappa$ : error of calculation  $\delta < 1\%$  (grade A),  $\delta = 1-3\%$  (B),  $\delta = 3-10\%$  (C),  $\delta = 10-30\%$  (D), and  $\delta > 30\%$  (E).

linearly polarized ( $\xi = 0$ ) light is [5]

$$w_{lm} = \kappa^2 \sqrt{\frac{3}{\pi}} (2l+1) \frac{(l+m)!}{2^m m! (l-m)!} C_{\kappa l}^2 2^{2n^*-m} \times F^{m+1.5-2n^*} \exp\left[-\frac{2}{3F} \left(1 - \frac{1}{10} \gamma^2\right)\right], \quad m \geq 0, \quad (2.5)$$

with  $w_{l,-m} = w_{lm}$ . In the case of ionization by a constant electric field, in expression (2.5) one needs to put  $\gamma = 0$  and remove the factor  $\sqrt{3F/\pi}$ , which emerges [5] when the static ionization rate is averaged over a period of laser radiation. Here,  $m = 0, \pm 1, \dots$  is the projection of the angular momentum  $l$  on the electric wave field,  $n^*$  is the effective principal quantum number of the level [11–15], which is calculated from the experimentally measured energy  $E_0 = -I$  of the atomic state:

$$n^* = \frac{Z}{\kappa} = \frac{Z}{\sqrt{2I}}, \quad (2.6)$$

$Z$  is the atomic or ion core charge, and  $C_{\kappa l}$  is the dimensionless asymptotic coefficient of the atom wave function<sup>3</sup> away

<sup>3</sup> The atomic potential is of the form  $U(r) \approx Z/r$  for  $r \gg r_c$ , where  $r_c$  is the atomic core radius; the values  $Z = 1, 2$ , and 0 refer to neutral atoms, singly charged positive ions, and negative ions. For the ground state of atomic hydrogen,  $\kappa = n^* = 1$  and  $C_{\kappa 0} = 1$ . As regards the valence  $s$  electrons in neutral atoms, the values of  $n^*$  vary between 0.744 for He ( $I = 24.588$  eV) and 1.869 for Cs ( $I = 3.894$  eV).

( $\kappa r \gg 1$ ) from the nucleus [for more details, see Appendix 13.1, in particular formulas (13.1.1), (13.1.3), and (13.1.5)].

Hartree [11] proposed a simple and sufficiently precise expression for this coefficient as far back as 1927:

$$C_{\kappa l}^2 = \frac{2^{2n^*-2}}{n^*(n^*+l)!(n^*-l-1)!}, \quad x! \equiv \Gamma(x+1) \quad (2.7)$$

(see also Refs [12–15]). This formula is a natural generalization of the expression following directly from the exact solution of the Schrödinger equation for the hydrogen atom [16], where  $n^* = n = 1, 2, 3, \dots$ . Other approximations for the coefficient  $C_{\kappa l}$  were obtained by means of the quantum defect method [17, 18] and the effective range expansion [19]. The numerical values of  $C_{\kappa l}$  for neutral atoms and several positive and negative ions were calculated by the Hartree–Fock method and may be borrowed, for instance, from handbook [14]. In the case of valence  $s$  electrons these coefficients are rather close (to within  $\sim \pm 10\%$ ) to unity, as is evident from Table 1. That is why Eqns (2.1) and (2.5) are almost model-independent. It also follows from Table 1 that the Hartree approximation (2.7) exhibits a satisfactory accuracy for the  $s$  state for all atoms, from hydrogen to uranium.

Equation (2.5) is asymptotically exact when  $F \rightarrow 0$ . In the case of the ground state of the hydrogen atom it corresponds to the well-known asymptotics  $w_{st}(\mathcal{E}) = 4\mathcal{E}^{-1} \exp(-2/3\mathcal{E})$  for a constant electric field  $\mathcal{E}$  obtained with the semiclassical method [16]. Since it is assumed that the reduced field  $F \ll 1$ ,

the ionization rate of the sublevel  $|lm\rangle$  decreases rapidly [4, 5] with  $|m|$ . As a result, the ionization probability averaged with statistical weights

$$\bar{w}_l = (2l + 1)^{-1} \sum_{m=-l}^l w_{lm} \quad (2.5')$$

is almost the same as for the  $s$  level, with the exception of the asymptotic coefficient  $C_{kl}^2$ .

Equation (2.5) is valid for low-frequency laser radiation, i.e., for  $\omega \ll \omega_t$ . For an arbitrary  $\gamma$ , the rate of ionization of the  $s$  level bound by a short-range ( $Z = 0$ ) potential is represented in the form of the sum of  $n$ -photon process probabilities:

$$w(\mathcal{E}, \omega) = \sum_{n > n_{th}} w_n, \quad n_{th} = K_0 \left( 1 + \frac{1}{2\gamma^2} \right), \quad (2.8)$$

where  $l = 0$ ,  $w_n$  is the partial probability of  $n$ -photon ionization:

$$w_n = \frac{\kappa^2}{\pi} |C_{\kappa}|^2 K_0^{-3/2} \beta^{1/2} F(\sqrt{\beta(n - n_{th})}) \times \exp \left\{ - \left[ \frac{2}{3F} g(\gamma) + 2c_1(n - n_{th}) \right] \right\}, \quad (2.8')$$

$g(\gamma) = 3f(\gamma)/2\gamma$ , the functions  $f(\gamma)$  and  $c_1(\gamma)$  were defined by expressions (2.2) and (2.2') above,  $n_{th}$  is the photoionization threshold for linearly polarized radiation,  $\beta = 2(c_2 - c_1) = 2\gamma/\sqrt{1 + \gamma^2}$ , and

$$F(x) = \int_0^x \exp[-(x^2 - y^2)] dy = \begin{cases} x - \frac{2}{3}x^2 + \dots, & x \rightarrow 0, \\ \frac{1}{2x} + \frac{1}{4x^3} + \dots, & x \rightarrow \infty \end{cases}$$

[the so-called Dawson function, see 7.1.16 in handbook [20], which attains its maximum for  $x_m = 0.9241$ , with  $F(x_m) = 0.541\dots$ ]. It is easily shown that Eqns (2.8) and (2.8') in the limiting cases  $\gamma \ll 1$  and  $\gamma \gg 1$  lead to estimates (2.4). Furthermore, these equations coincide with formula (2.5) when it is assumed that  $\gamma \ll 1$  and  $l = 0$ . Therefore, they provide a continuous connection between the cases of low- and high-frequency laser radiation. For states with an arbitrary angular momentum  $l$ , expressions for the partial probabilities  $w_n$  are similar to expression (2.8') but are more cumbersome in form [5].

In the case of circularly polarized radiation, the energy photoelectron spectrum is Gaussian. In particular, the  $n$ -photon ionization probability for  $\gamma \ll 1$  is [4]

$$w_n = w_{max} \exp \left[ - \frac{\gamma(n - n_0)^2}{2n_0} \right] \propto \exp \left[ - \frac{\omega^4 \kappa}{\mathcal{E}^3} (n - n_0)^2 \right], \quad (2.9)$$

where  $n_0 \approx 2n_c$  and  $n_c = n_{th}(\xi = \pm 1) = K_0(1 + \gamma^{-2})$  is the ionization threshold, i.e., the minimum number of absorbed  $\hbar\omega$  photons required for the ionization of an atomic level with a binding energy  $I = \kappa^2/2$  by a circularly polarized wave. The distribution (2.9) has a peak for  $n = n_0$  and is relatively narrow:  $\Delta n/n_0 \sim \omega/\sqrt{\kappa\mathcal{E}} = \gamma\sqrt{F} \ll 1$ , although its width is

not small by itself:

$$\Delta n = \sqrt{\frac{\mathcal{E}^3}{\omega^4 \kappa}} \sim \sqrt{\frac{n_0}{\gamma}} \gg 1.$$

The angular distribution of the ejected photoelectrons is of the form [5]

$$w(\psi, \gamma) = \text{const} \cdot [J_{n_0}(n_0 \zeta)]^2, \quad (2.10)$$

$$\zeta = \frac{p_{\perp}}{F\gamma^2 \kappa n_0} = 2 \sqrt{\frac{v(1-v)}{1+\gamma^2}} \cos \psi,$$

where  $J_n(z)$  is the Bessel function,  $v = n_c/n_0$  ( $1/2 < v < 1$ ),  $\psi$  is the angle between the electron momentum  $\mathbf{p}$  and the plane of polarization of laser radiation,  $p_{\perp} = p_{n_0} \cos \psi$ ,  $p_{n_0} = \sqrt{2\omega(n_0 - n_c)} \approx \kappa/\gamma$ , and  $n_0$  is the most probable number of absorbed photons:

$$n_0 = \begin{cases} 2n_c \left( 1 - \frac{1}{3} \gamma^2 \right), & \gamma \ll 1, \\ n_c [1 + (2 \ln \gamma)^{-1}], & \gamma \gg 1. \end{cases} \quad (2.11)$$

Since  $n_0 > n_c \gg 1$ , the majority of photoelectrons are ejected near the plane of polarization of the light wave, as follows from the asymptotics for the Bessel function [20]. Although the angular photoelectron distribution is appreciably broadened with increasing  $\gamma$ , it nevertheless remains rather narrow for  $\gamma \gg 1$  as well [21], which is clear from Fig. 1.

The Coulomb interaction between the ejected electron and the atomic core was taken into account in Ref. [6] employing the quasiclassical theory of the Coulomb potential perturbation. However, the authors failed to completely consider the  $\gamma \gg 1$  case: the validity condition of the perturbation theory is of the form [6]

$$\gamma \ll \gamma_* = (n_* F)^{-1/2}, \quad (2.12)$$

and since  $n_* \sim 1$  (see Table 1) and  $F \ll 1$ , this condition is fulfilled in the range of values  $\gamma \lesssim 1$ . The corresponding

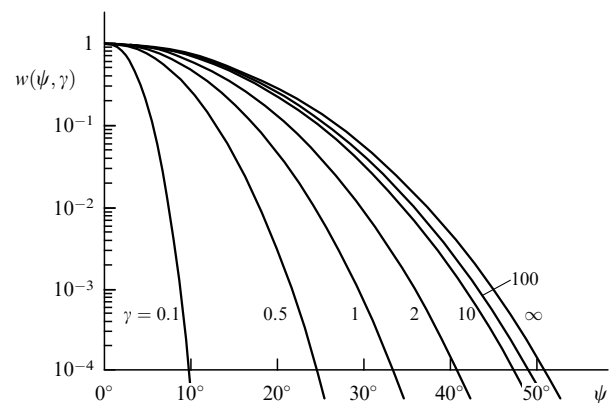


**Figure 1.** The case of circular polarization. The angular photoelectron distribution is normalised to unity for  $\psi = 0$ . Here,  $K_0 = 10$  and  $\psi$  is the angle between the ejected-electron momentum and the plane of polarization of laser radiation. The values of the Keldysh parameter  $\gamma$  are indicated by the curves.

calculation of the Coulomb correction for different light ellipticities  $\xi$  was performed in Ref. [6]. Also noteworthy is Ref. [7], in which a special diagram technique was developed for this problem and some formulas were obtained for the Coulomb correction, but again not for all values of  $\xi$  and  $\gamma$ . A simple expression was derived for the case of circular polarization [7]:

$$w(\mathcal{E}, \omega) = w_{\text{sr}}(\mathcal{E}, \omega) (F\sqrt{1+\gamma^2})^{-2n_*}, \quad \xi = \pm 1, \quad (2.13)$$

where  $w_{\text{sr}}$  is the probability of ionization from a short-range potential. The inclusion of the Coulomb interaction increases the electron cloud density at  $\kappa r \gg 1$  [see formula (13.1.1) in Appendix 13.1]; furthermore, the effective barrier width decreases as  $\gamma$  increases [5]. This causes the Coulomb correction for  $F \sim 0.01-0.1$  to raise the ionization probability by several orders of magnitude (for neutral atoms).

The results obtained in Refs [1, 4–9] provide a rather detailed description of nonlinear photoionization in a wide range of  $\gamma$  values. Nevertheless, these results were not analyzed in full detail at that time, which is partly explained by the lack of reliable experimental data (the multiphoton ionization of atoms itself was experimentally discovered in Ref. [22]).

To calculate the transition amplitude in Keldysh's approach, as well as in numerous subsequent papers, advantage was taken of the saddle-point technique with the Volkov wave function, while in Refs [5, 6, 8] use was made of the 'imaginary time' method (the correspondence between these methods is discussed in the concluding Section 12). These approximations are justified when the frequency and intensity of the electromagnetic wave are small in comparison with the ionization potential  $I$  and the characteristic atomic field  $\kappa^3 \mathcal{E}_a$ ; in this case, the barrier width is large in comparison with the radius of the bound state  $1/\kappa$  and its penetrability is exponentially small. More recently, Faisal [23] and Reiss [24, 25] invoked a somewhat different approach to obtain more precise but more cumbersome formulas for the transition amplitude and the photoelectron spectrum. In this approach, the saddle-point technique is not employed and the wave function of the final state is expanded into a Fourier series, which eventually leads to infinite sums in the number of absorbed photons and necessitates numerical calculations. The corresponding approximation is known in the literature as the KFR theory (Keldysh, Faisal, and Reiss). This theory is frequently employed in the analysis of different experiments in this area (concerning this issue, see Refs [25–27] as well as Section 9).

In concluding this section we make several remarks.

(1) Formula (2.5) is valid for the  $|lm\rangle$  states of any atom, with the exception of excited ( $n \geq 2$ ) levels of the hydrogen atom, for which the pre-exponential factor  $F^{-\beta}$  and the constant  $C_{kl}$  change owing to the specific accidental degeneracy<sup>4</sup> of the states with  $l = 0, 1, \dots, n-1$ . In particular, for a constant electric field we have, according to Refs [33, 5],  $\beta = 2n_2 + |m| + 1$ , while the corresponding exponent in Eqn (2.5) is  $\beta' = 2n - |m| - 1 = \beta + 2n_1$ . Here,  $n_1$ ,  $n_2$ , and  $m$  are parabolic quantum numbers and  $n = n_1 + n_2 + |m| + 1$  is the principal quantum number of the level [16].

(2) If the adiabatic factor  $\sqrt{3F/\pi}$  is omitted in expression (2.5), in the limit  $\omega \rightarrow 0$  this equation turns into the well-

known formula for the rate of negative-ion ( $n^* = 0$ ) ionization by a constant electric field [16, 34].

(3) In the derivation of expression (2.1), the action function  $S(p)$  is expanded near the saddle point in the final electron momentum up to the second-order terms  $p^2/\kappa^2$ . Gribakin and Kuchiev [35], who reproduced (in a somewhat different way) the results obtained in Ref. [5], indicated that the quadratic approximation for  $S(p)$  is insufficient in some cases. In particular, the angular photoelectron distribution in the  $n$ -photon absorption,  $dw_n/\sin\theta d\theta$ , for the case of  $\text{H}^-$  ions ionization by laser light with  $\omega = 0.0043$  a.u. (a  $\text{CO}_2$  laser) and  $J = 10^{11} \text{ W cm}^{-2}$  ( $\gamma \approx 0.6$ ) agrees well with formula (53) from Ref. [5] for the first three photopeaks ( $n = 16, 17$ , and  $18$ ). However, upon further increase in  $n$ , the ratio  $p/\kappa$  increases and the fit becomes worse (see Fig. 2 in Ref. [35]).

(4) The accuracy of quadratic approximation was recently investigated [36] for the case of  $s$ -level ionization by linearly polarized radiation. The spectrum of direct above-threshold ionization  $w(p)$  calculated in the framework of the Keldysh model employing the saddle-point technique but without expansion in powers of  $p/\kappa$  was compared with formula (2.1). It was shown that the domain of applicability of this expansion is restricted to finite energies  $\varepsilon \lesssim 1.5 U_p$ , where  $U_p = F^2/4\omega^2$  is the average energy of electron oscillations in the wave field (or the ponderomotive potential). For  $\varepsilon > 2U_p$ , the ionization probability decreases with momentum  $p$  much more steeply than according to expression (2.1), especially after getting over the point  $\varepsilon_0 = 2U_p - I = (1/2)\kappa^2(\gamma^{-2} - 1)$  (in the tunnel regime, i.e., for  $\gamma < 1$ ). However, the values of  $w(p)$  themselves in this region are several orders of magnitude smaller than  $w(0)$ , and therefore the total ionization probability is hardly changed upon introducing this improvement.

The quadratic expansion in  $p$  employed in Refs [1, 4, 5] is not fundamental to the ionization theory, but it is valid for  $p \lesssim \kappa$  and the formulas without it become much more complicated and call for numerical computer-assisted calculations.

### 3. Further development of the Keldysh theory

We will consider several recent papers which furnish the further development of the Keldysh theory.

First, the energy and angular photoelectron distributions were calculated and analyzed in detail in the general case of an elliptically polarized incident wave for arbitrary values of the parameter  $\gamma$ . In particular, the angular distribution in the case of circularly polarized laser radiation was shown to concentrate about the plane in which the field vector  $\vec{\mathcal{E}}(t)$  rotates and to remain rather narrow not only for low-frequency radiation  $\gamma \ll 1$ , but for large  $\gamma$  as well (see Fig. 1). With increasing  $\gamma$ , the distribution of  $w_n$  in the number of absorbed photons, i.e., the photoelectron energy spectrum, remains Gaussian, as in formula (2.9), but its relative width decreases:

$$\frac{\Delta n}{\sqrt{n_0}} = \begin{cases} \gamma^{-1/2}, & \gamma \ll 1, \\ 1, & \gamma \approx 0.47, \\ (2 \ln \gamma)^{-1}, & \gamma \gg 1. \end{cases} \quad (3.1)$$

When  $\gamma \ll 1$ , this distribution is significantly broader than the Poisson distribution with the same average value of  $n_0$  and for  $\gamma \gg 1$  it is, conversely, narrower than the Poisson one. The exact formulas and further details can be found elsewhere [21].

<sup>4</sup> Related to the so-called 'hidden' symmetry group of the Coulomb field [16, 28–32].

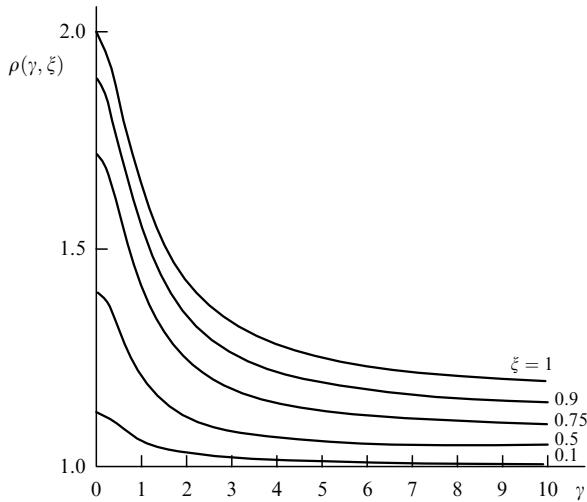


**Figure 2.**  $\rho(\gamma, \xi) = n_0/n_{th}$  ratio versus  $\gamma$  for different ellipticities  $\xi$ :  $n_0$  is the most probable and  $n_{th}$  is the threshold number of absorbed photons ( $\xi = 0$  corresponds to linearly and  $|\xi| = 1$  to circularly polarized radiation).

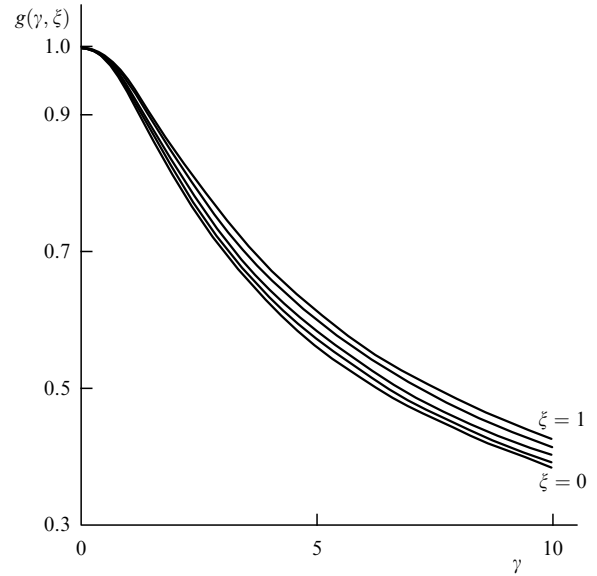


**Figure 3.** Function  $g(\gamma, \xi)$  from formula (3.4) for the ionization rate  $w$ . The curves (from bottom to top) correspond to the values of light ellipticity  $\xi = 0, 0.5, 0.7, 0.9$ , and  $1$ .

The case of elliptical polarization,

$$\vec{\mathcal{E}}(t) = \mathcal{E} \cos \omega t \mathbf{e}_x + \xi \mathcal{E} \sin \omega t \mathbf{e}_y, \quad -1 \leq \xi \leq 1 \quad (3.2)$$

(here,  $\xi$  is the ellipticity of laser radiation), for which the photoionization threshold is

$$n_{th} = K_0 \left( 1 + \frac{1 + \xi^2}{2\gamma^2} \right) \quad (3.3)$$

(Fig. 2), was considered in Refs [5, 37–39]. The principal (exponential) factor in the formula for the ionization rate,

$$w \propto \exp \left[ -\frac{2}{3F} g(\gamma, \xi) \right] = \exp \left[ -\frac{2I}{\omega} f(\gamma, \xi) \right], \quad (3.4)$$

was calculated in Ref. [5]. The expression obtained therein was recast to a more convenient form in Refs [8, 39], where it was shown that all the formulas are significantly simplified by selecting for the variable  $\tau_0 = \tau_0(\gamma, \xi)$  — the ‘time’ (purely imaginary) of sub-barrier electron motion —

$$f(\gamma, \xi) = \left( 1 + \frac{1 + \xi^2}{2\gamma^2} \right) \tau_0 - \frac{1}{\gamma^2} \left[ \frac{1 - \xi^2}{4} \sinh 2\tau_0 + \xi^2 \frac{\sinh^2 \tau_0}{\tau_0} \right], \quad (3.5)$$

with  $\tau_0$  being determined from the transcendental equation

$$\sinh \tau_0 \left[ 1 - \xi^2 \left( \coth \tau_0 - \frac{1}{\tau_0} \right)^2 \right]^{1/2} = \gamma. \quad (3.6)$$

In the two limiting cases we have: if  $\gamma \ll 1$ , then

$$\tau_0 = \gamma - \frac{1}{18} (3 - \xi^2) \gamma^3 + \dots, \quad (3.7)$$

$$f(\gamma, \xi) = \frac{2}{3} \gamma \left[ 1 - \frac{1}{10} \left( 1 - \frac{\xi^2}{3} \right) \gamma^2 + \dots \right],$$

and if  $\gamma \gg 1$ , then

$$\tau_0(\gamma, \xi) = \begin{cases} \ln \left( \frac{2\gamma}{\sqrt{1 - \xi^2}} \right), & 1 - \xi^2 \gg \frac{1}{\ln 2\gamma}, \\ \ln(\gamma\sqrt{2 \ln \gamma}), & \xi = \pm 1, \end{cases} \quad (3.8)$$

$$f(\gamma, \xi) = \tau_0 - \frac{1}{2} + \xi^2 \Delta + O\left(\frac{\ln \gamma}{\gamma^2}\right), \quad (3.8)$$

where

$$\Delta = \left\{ 2\tau_0^2 \left[ 1 - \xi^2 \left( 1 - \frac{1}{\tau_0} \right)^2 \right] \right\}^{-1}$$

(since  $\tau_0 \gtrsim \ln 2\gamma \gg 1$ ,  $\Delta$  is a small correction). With an increase in the ellipticity of light, the functions  $\tau_0$  and  $g$  rise monotonically for a fixed  $\gamma$  (Fig. 3), and the ionization probability accordingly decreases, especially for  $|\xi| \rightarrow 1$ , i.e., for polarizations close to the circular one. In the low-frequency ( $\gamma \ll 1$ ) domain, the ionization rate for the  $s$  level is [5]

$$w_a = \kappa^2 C_\kappa^2 \sqrt{\frac{3F^3}{\pi(1 - \xi^2)}} \left( \frac{F}{2} \right)^{-2n_s} \exp \left[ -\frac{2}{3F} \left( 1 - \frac{3 - \xi^2}{30} \right) \gamma^2 \right], \quad (3.8')$$

if the ellipticity  $\xi$  is not too close to the circular one ( $1 - \xi^2 \gtrsim F$ ).

The dependence of the energy and angular spectra of photoelectrons on the ellipticity  $\xi$  in the case of tunnel ionization was considered in Refs [37, 38]. However, part of the statements in these papers is incorrect.<sup>5</sup> These inaccuracies were corrected in the next paper [39], and we now turn to the description of results obtained in it.

<sup>5</sup> This applies, in particular, to the statement that the formulas for the electron momentum distribution derived in Ref. [5] have only a very narrow domain of applicability near  $\xi \approx 0$ .

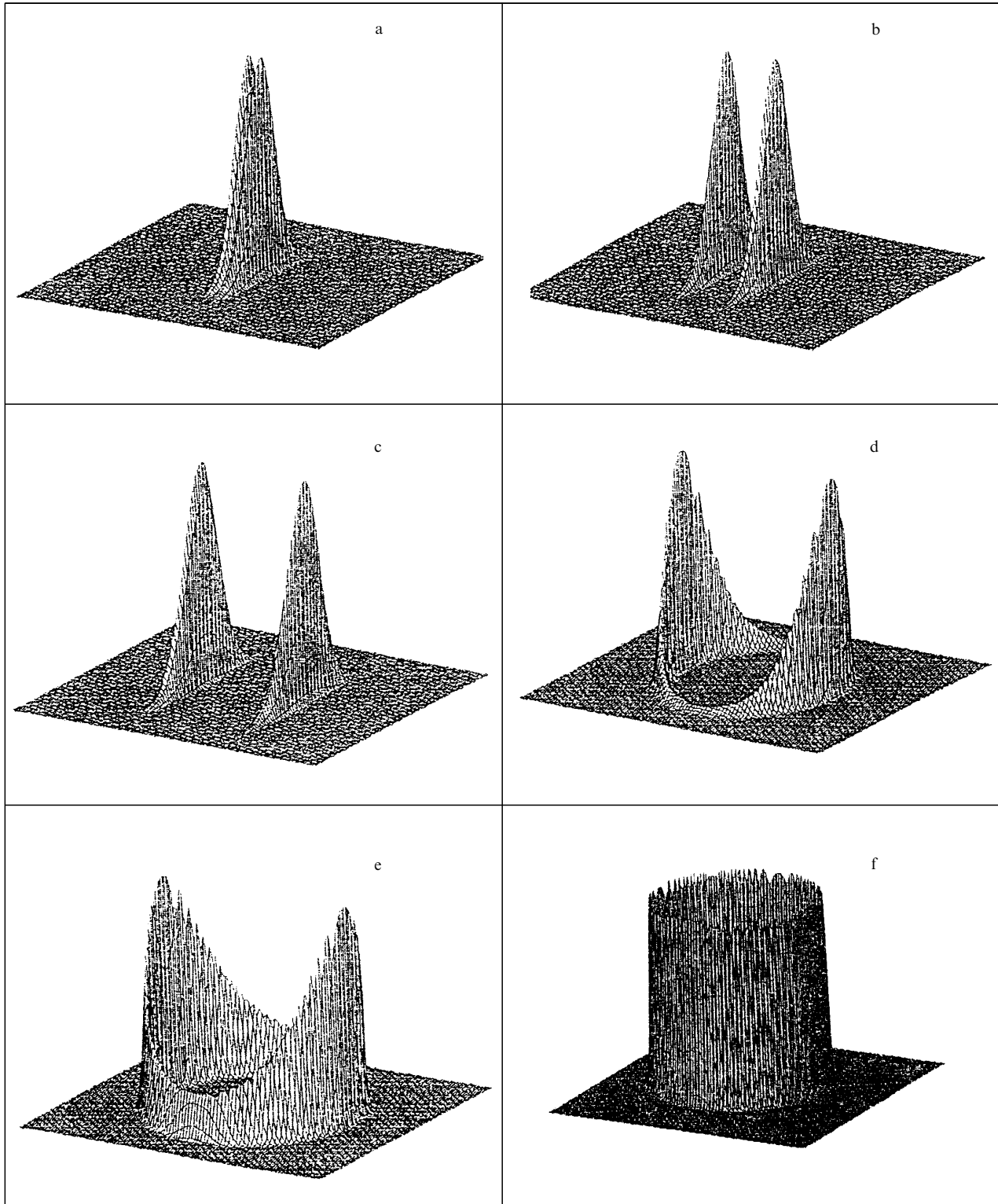


**Figure 4.** The case of elliptical polarization. Evolution of the photoelectron momentum distribution in the plane of the electric field ( $p_z = 0$ ) for  $\xi = 0.05, 0.25, 0.5, 0.8, 0.95,$  and  $1$  (Figs a–f, respectively). The calculations were made for the ionization of  $\text{Ne}^{3+}$  ( $I = 97.1$  eV) by the field of a Ti:Sapphire laser ( $\hbar\omega = 1.58$  eV,  $J = 2 \times 10^{16}$  W cm $^{-2}$ ,  $\gamma = 0.2$ ).

When  $0 < \xi^2 < 1$ , the most probable momentum of the ejected photoelectrons  $\mathbf{p}_{\text{max}}$  is directed along the minor axis of the field ellipse [the  $y$ -axis in expression (3.2)], for  $\xi = 0$  (linear polarization) it is directed along the peak of the electric field (the  $x$ -axis), and the photoelectron distribution for the case of circular polarization becomes isotropic in the

plane of the vector  $\vec{\mathcal{E}}$ . Figure 4, borrowed from Ref. [39], shows the evolution of photoelectron momentum distribution  $w(p_x, p_y, p_z = 0)$  in the plane of  $\vec{\mathcal{E}}$  as the ellipticity of light varies. When the polarization is close to the linear one,  $|\xi| \lesssim \gamma\sqrt{F} \ll 1$ , the distribution possesses a sharp peak along the principal axis of the field ellipse as in Eqn (2.1). Next, a

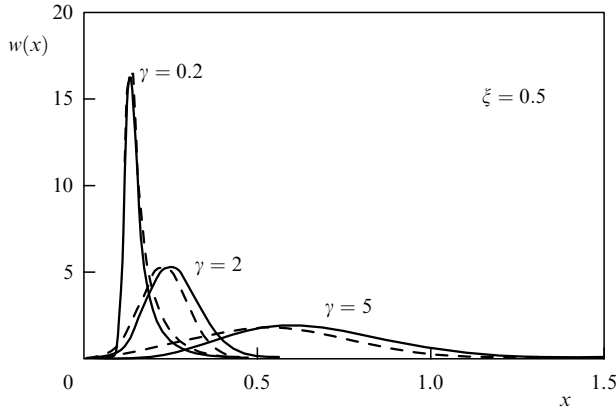


**Figure 5.** Photoelectron energy spectrum in the ionization of  $\text{Ne}^{3+}$  by the field of a Ti:Sapphire laser  $J = 3.2 \times 10^{13}$ ,  $2 \times 10^{14}$ , and  $2 \times 10^{16} \text{ W cm}^{-2}$ , curves with  $\gamma = 5$ , 2, and 0.2, respectively (the dashed curves represent calculations by the formulas of Ref. [34]). Here,  $x = E/E_0$ , where  $E_0 = F^2/\omega^2$  is proportional to the average energy of electron oscillations in the wave field, the ionization probability is  $w(x) = dW/dx$ .

two-peak structure is formed [5, 39]:

$$dw(\mathbf{p}) \propto \exp \left[ (1 - \xi^2) \frac{\omega^2 \kappa^3}{3\mathcal{E}^3} p_x^2 + \frac{\kappa}{\mathcal{E}} p_z^2 \right] \times \left\{ \exp \left[ -\frac{\kappa}{\mathcal{E}} \left( p_y - \xi \frac{\mathcal{E}}{\omega} \right)^2 \right] + \exp \left[ -\frac{\kappa}{\mathcal{E}} \left( p_y + \xi \frac{\mathcal{E}}{\omega} \right)^2 \right] \right\} \frac{d^3 p}{(2\pi)^3}, \quad \gamma \ll 1, \quad (3.9)$$

which is clearly seen for  $|\xi| \gtrsim \sqrt{F}$  and persists up to values  $|\xi| \approx 1 - F$ . Lastly, the photoelectron distribution for  $\xi \rightarrow \pm 1$  becomes isotropic in the plane  $\psi = 0$ :

$$dw \propto \exp \left\{ -\frac{\kappa}{\mathcal{E}} \left[ \left( p_{\perp} - |\xi| \frac{\mathcal{E}}{\omega} \right)^2 + p_z^2 \right] - \frac{1 - \xi^2}{3F} \sin^2 \varphi \right\} \frac{d^3 p}{(2\pi)^3}. \quad (3.10)$$

Here,  $p_{\perp} = (p_x^2 + p_y^2)^{1/2} = p \cos \psi$ ,  $\psi$  is the angle between  $p$  and the polarization plane,  $0 \leq \psi \leq \pi/2$ , and  $\varphi = \arctan(p_x/p_y)$ ,  $0 \leq \varphi \leq 2\pi$ . Hence it is clear that  $\Delta p_z \sim \Delta p_{\perp} \sim \kappa \sqrt{F} \ll \kappa$ . For  $\xi^2 = 1$ , the dependence of  $dw(\mathbf{p})$  on the azimuth angle  $\varphi$  vanishes, and expression (3.10) grades into the momentum distribution for the case of circular polarization [40]:

$$dw(p_{\perp}, p_z) \propto \exp \left\{ -\frac{2}{3\mathcal{E}} \left[ \kappa^2 + \left( p_{\perp} - \frac{\mathcal{E}}{\omega} \right)^2 + p_z^2 \right]^{3/2} \right\} \approx \exp \left\{ -\frac{2\kappa^3}{3\mathcal{E}} - \frac{\kappa}{\mathcal{E}} \left[ \left( p_{\perp} - \frac{\mathcal{E}}{\omega} \right)^2 + p_z^2 \right] \right\} \quad (3.11)$$

(the light wave travels along the  $z$ -axis).

For the photoelectron energy spectrum  $w_n$  Mur et al. [39] obtained analytical formulas possessing a good accuracy for all values of the Keldysh parameter, including the intermediate case  $\gamma \sim 1$  (compare the solid and dashed curves in Fig. 5, which shows the evolution of the distribution  $w_n$  when the parameter  $\gamma$  is varied from 0.2 to 5 for  $\xi = 0.5$ ; for other values of  $\xi$ , the picture is similar [39]). In particular, for  $\gamma \ll 1$  and  $1 - \xi^2 \gg F$  the distribution in the number of absorbed

photons has the form

$$w_n \propto a(\gamma(n - n_0)) \exp \left[ -\frac{2}{3}(1 - \xi^2)\gamma^3(n - n_0) \right], \quad n > n_0, \quad (3.12)$$

where  $n_0 = F^2(1 + 3\xi^2)/4\omega^3 = (1 + 3\xi^2)(1 + \xi^2)^{-1}n_{\text{th}}$ ,

$$a(x) = \exp(-x) I_0(x) = \begin{cases} 1 - x + \frac{3}{4}x^2 + \dots, & x \rightarrow 0, \\ (2\pi x)^{-1/2}, & x \gg 1, \end{cases} \quad (3.12')$$

and  $I_0(x)$  is the Bessel function of an imaginary argument. We note that elliptically polarized radiation is quite often employed in photoionization experiments today [41–45].

During the last 10–15 years, considerable attention has been attracted to the study of ionization by a low-frequency laser field,  $\gamma \ll 1$ , owing to the development of infrared lasers in the tera- and petawatt power range (for which  $\omega < 0.05 \sim 1 \text{ eV}$ ,  $F \gtrsim 0.1$ , and  $\gamma \lesssim 0.1$ ). Here, in theoretical calculations advantage is quite often taken of the adiabatic Landau–Dykhne approximation [16, 46–51]. In this case, the formulas given above are significantly simplified. In particular, the momentum distribution (2.1) takes on the form

$$w(\mathbf{p}) = w(0) \exp \left\{ -\left[ \frac{\omega^2(2I)^{3/2}}{3\mathcal{E}^3} p_{\parallel}^2 + \frac{(2I)^{1/2}}{\mathcal{E}} p_{\perp}^2 \right] \right\}, \quad \xi = 0, \quad (3.13)$$

$$w(0) = C_{\kappa}^2 \frac{\omega^2}{\pi^2 \mathcal{E}} \left( \frac{F}{2} \right)^{-2n^*} \exp \left( -\frac{2}{3F} \right),$$

while for the case of circular polarization

$$w(\psi) \propto \exp(-c\psi^2), \quad c = \frac{\kappa \mathcal{E}}{\omega^2} = \frac{2K_0}{\gamma}, \quad (3.14)$$

with the coefficient  $c \gg 1$  and  $\Delta\psi \sim \omega/\sqrt{\kappa \mathcal{E}} \ll 1$ .

It is noteworthy that these formulas, which are given<sup>6</sup> in Refs [48, 49], follow directly from the general equations (2.1), (2.3), and (2.10). These equations are valid for arbitrary values of the Keldysh parameter when the quantities appearing in them are expanded in powers of  $\gamma$ . For instance,

$$c_1(\gamma) = \frac{1}{3}\gamma^3 + \dots, \quad c_2(\gamma) = \gamma - \frac{1}{6}\gamma^3 + \dots,$$

after which Eqn (2.1) takes on the form

$$w(\mathbf{p}) = w(0) \exp \left[ -\frac{1}{\omega} \left( \frac{1}{3}\gamma^3 p_{\parallel}^2 + \gamma p_{\perp}^2 \right) \right], \quad \gamma = \frac{\omega \sqrt{2I}}{\mathcal{E}}, \quad (3.15)$$

which is in perfect agreement with the distribution (3.13). For the case of circular polarization, the formula

$$\frac{w(\psi, \gamma)}{w(0, \gamma)} = \frac{\gamma}{\sqrt{\gamma^2 + \psi^2}} \exp \left\{ -\frac{2}{3F} \left[ \left( 1 + \frac{\psi^2}{\gamma^2} \right)^{3/2} - 1 \right] \right\} \quad (3.16)$$

<sup>6</sup> Unfortunately, it is necessary to mention that the role of early investigations [4–8] is covered in a heavily biased manner in Refs [47–51], as in other works of these authors. For more details on this issue, see article [52] and Appendix 13.3.

is somewhat more accurate [21] than expression (3.14). To derive it, one should take into account in relations (2.10) that the variable  $\zeta = 1 - (\gamma^2 + \psi^2)/2 \rightarrow 1$  in the small-angle domain and employ the Langer asymptotics [20] for the Bessel function  $J_n(n\zeta)$  with  $n \gg 1$  (for more details, see Ref. [21]). When  $\psi \ll \gamma \ll 1$ , expressions (3.14) and (3.17) are almost identical, but the number of photoelectrons for  $\psi > \gamma$  decreases faster with an increase in the angle  $\psi$  than according to expression (3.14).

The results presented in Eqns (3.9)–(3.16) and in Figs 4 and 5 relate to the case of ionization of singly charged negative ions ( $Z = 0$ ). For  $Z \neq 0$ , the angular photoelectron distribution may be distorted due to the effect of the Coulomb field of the residual ion on the electron motion in the continuum [53, 54]. The ejected electron momentum (at infinity) is [55]

$$\mathbf{p}(t \rightarrow \infty) = \mathbf{p}(t_0, v_0) - Z \int_{t_0}^{\infty} dt \frac{\mathbf{r}_L(t; t_0, v_0)}{r_L^3(t; t_0, v_0)}, \quad (3.17)$$

where  $\mathbf{r}_L(t)$  is the electron trajectory in the laser field upon passing through the barrier (at time  $t_0$  with a velocity  $v_0$ ) defined by the Newtonian equation of motion, the Coulomb interaction being taken into account by the perturbation theory.<sup>7</sup> The photoelectron momentum distribution is obtained by recalculating the spectrum  $dW/d^3p$  at the instant of ejection, which is expressed in terms of the variables  $t_0$  and  $v_0$ , to the asymptotic momentum values using relation (3.17). The Coulomb interaction in the final state breaks the symmetry of the distribution (3.9) relative to the axes of the field ellipse, shifting its peak away from the  $y$ -axis. This follows from numerical calculations for the  $s$ -photon ionization of xenon atoms by the radiation of a Ti:Sapphire laser (for  $\gamma = 1.12$  and  $\zeta = 0.36$  and  $0.56$ ). The calculation of Ref. [55] is in satisfactory agreement with experiment [43] for high ( $s \geq 4$ ) peaks.

We also note that the following relation between the adiabatic  $w_a$  and static (in a constant field,  $w_{st}$ ) ionization rates is valid in the case of low-frequency radiation [5]:

$$w_a(F, \zeta) = (\zeta^2)^{-1/2} a\left(\frac{1 - \zeta^2}{6F\zeta^2}\right) w_{st}(F), \quad (3.18)$$

where  $a(x)$  is the same function as in expression (3.12'). This expression is asymptotically exact in the limit  $F \rightarrow 0$ . When the polarization is not too close to the circular one, the equation is simplified:

$$w_a(F, \zeta) = \sqrt{\frac{3F}{\pi(1 - \zeta^2)}} w_{st}(F), \quad 1 - \zeta^2 \gg F. \quad (3.19)$$

On the other hand,  $w_a(F, \zeta = \pm 1) = w_{st}(F)$ . In the narrow transition region ( $1 - \zeta^2 \lesssim F \ll 1$ ) near the circular polarization, the dependence of  $w_a(F, \zeta)$  on the field amplitude  $F$  is not of a simple power form.

When  $\gamma \ll 1$ , the rate of ionization by a low-frequency field can be calculated by averaging  $w_{st}(F(t))$  over a field period:

$$w_a(F) = \frac{1}{T} \int_0^T w_{st}(F(t)) dt, \quad (3.20)$$

<sup>7</sup> Compare with Ref. [6], in which the Coulomb potential  $\delta V_C = -Z/r$  was taken into account in the sub-barrier section of the trajectory, which makes a contribution to  $\text{Im } S$ . By contrast, the time  $t$  in expression (3.17) is real, and  $\text{Im } S$  is no longer changed for  $t > t_0$ .

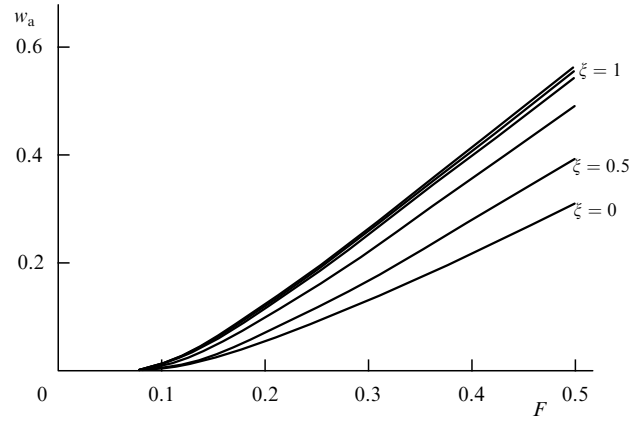


**Figure 6.** Rate of above-barrier ionization  $w_a$  for the ground state of the hydrogen atom and low-frequency laser radiation [21]. The curves correspond to the values of the ellipticity of light  $\xi = 0, 0.5, 0.8, 0.9, 0.95,$  and  $1$ ; the quantities  $w_a$  and  $F$  are given in atomic units.

which leads [5] to expression (3.18) in the weak-field domain. This formula can also be used for strong fields when the numerical values of  $w_{st}(F)$  are known. These calculations for the hydrogen atom were performed by many authors (see, in particular, Refs [56–62]). In view of these results, we obtain the values of  $w_a(F, \xi)$  presented in Fig. 6. It is noteworthy that the dependence of  $w_a$  on the field amplitude in the above-barrier domain is surprisingly close to the linear one:

$$w_a(F, \xi) \approx k(F - F_0), \quad F > F_0, \quad (3.21)$$

where the parameters  $k$  and  $F_0$  depend on the quantum numbers of the level (in particular,  $k = 1.47$ ,  $F_0 = 0.122$  for the ground state of the hydrogen atom and  $k = 0.81$ ,  $F_0 = 0.260$  for Rydberg states; the values of  $k$  and  $F_0$  are given in atomic units). A similar behavior of  $w_{st}(F)$  for the Stark effect in a constant electric field (Fig. 7) was discovered in the numerical calculations of Refs [60, 61] for the states of the hydrogen atom with different parabolic quantum numbers  $(n_1, n_2, m)$ . In this case, use was made of summation of the (divergent) perturbation theory series in powers of  $F$  with the aid of Pade–Hermite approximation formulas. Formula (3.21) applies to the domain  $F > F_0$ , the value of  $F_0$  somewhat exceeding the critical field  $F_{cr}$ , for which the energy of the

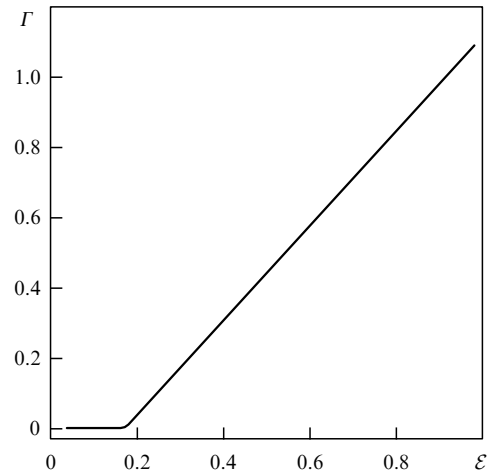


**Figure 7.** Stark effect in the hydrogen atom: dependence of the Stark width  $\Gamma$  on the field  $\mathcal{E}$  for the ground state [61]. The domain of intermediate asymptotics (3.22) is clearly seen for  $\mathcal{E} \gtrsim 0.2$ .

Stark level coincides with the peak of the potential barrier. The level width  $\Gamma = w(F)$  for  $F < F_{\text{cr}}$  is asymptotically small, while for  $F \gtrsim F_{\text{cr}}$  (the above-barrier domain) it approaches the asymptotics (3.21).

Equation (3.21) is an example of ‘intermediate asymptotics’,<sup>8</sup> which is not valid in either weak or superstrong ( $F \gg F_{\text{cr}}$ ) fields: in the latter case,  $\Gamma(F) \propto (F \ln F)^{2/3}$  (see Ref. [65]). An explanation for the intermediate asymptotics in the theory of ionization of atoms by a strong field was given in Ref. [66] with the aid of the  $1/n$  expansion known from quantum mechanics [67–69].

#### 4. Ionization in the field of an ultrashort laser pulse

We next consider the ionization of atoms by an ultrashort laser pulse. As is well known, high-intensity electromagnetic fields can be obtained in practice by way of significant shortening of the laser pulse, when its duration becomes comparable to the optical period and the spectrum contains a large number of higher harmonics. Because of the strong nonlinearity of multiphoton ionization, it cannot be reduced to the sum of contributions from separate harmonics. The problem of calculating the ionization rate and the photoelectron spectrum for nonmonochromatic laser radiation of arbitrary form is therefore a topical problem. In Ref. [70] Keldysh employed essentially the same method of calculation as in his pioneering work [1], while in Ref. [71] use was made of the so-called ‘imaginary time method’ (ITM), which we discuss quite briefly here. The principles of the ITM are discussed in greater detail in Refs [8, 72], as well as in Chapter V of monograph [73].

To describe the sub-barrier particle motion, use is made of classical equations of motion, though with the imaginary time<sup>9</sup>:  $t \rightarrow it$ . The trajectory obtained in this case cannot be realized in classical mechanics because of the imaginary values of the ‘time’ and momentum. However, on going over to quantum mechanics it is precisely this trajectory that allows describing the sub-barrier electron transition from the initial bound state in the atom to the final state in the continuum. After deriving the sub-barrier trajectory and calculating the imaginary part of the function  $W$  along this trajectory (the so-called ‘shortened action’ [78]) it is possible to obtain explicit expressions for the ionization rate  $w$  of the level:

$$w \propto \exp\left(-\frac{2}{\hbar} \text{Im} W\right), \quad W = \int_{t_0}^0 (\mathcal{L} + E_0) dt, \quad (4.1)$$

$$\mathcal{L} = \frac{1}{2} \dot{\mathbf{r}}^2 + \vec{\mathcal{E}}(t)\mathbf{r} - U(r), \quad E_0 = -\frac{\kappa^2}{2}.$$

<sup>8</sup> Interesting examples of intermediate asymptotics in problems of fluid dynamics and mathematical physics are considered in Refs [63, 64].

<sup>9</sup> The ITM for the description of particle tunneling across time-varying barriers was first proposed in Ref. [5], elaborated in Ref. [8], and generalized to the relativistic case in Ref. [74]. We note that the ITM is the generalization of the method of complex classical trajectories developed by Landau as early as 1932 for the calculation of quasiclassical matrix elements with rapidly oscillating wave functions [however, only for static fields, where the introduction of the complex time  $t$  is not required because  $t$  can be excluded from the quasiclassical momentum  $p = \sqrt{2(E - U(x))}$ ]. In Landau’s approach it is the coordinate  $x$  rather than the time  $t$  that resides in the complex plane. For further details concerning the Landau method, the reader is referred to Refs [75–77] and to §§ 51–53 in the book [16].

To calculate the photoelectron energy and momentum spectra, one should consider the set of ‘classical’ paths close to the extremal sub-barrier trajectory (which minimizes  $\text{Im} W$  and defines the most probable path of particle tunneling) and calculate the imaginary part of the action function up to quadratic terms in the deviation of such a trajectory from the extremal path. This approach is applicable to a broad class of pulsed fields for arbitrary values of the Keldysh parameter  $\gamma$ . Equation (2.1) can be shown to remain valid in the case of linear polarization, with [71]

$$f(\gamma) = \int_0^\gamma \chi(u) \left(1 - \frac{u^2}{\gamma^2}\right) du, \quad (4.2)$$

$$c_1(\gamma) = c_2 - \gamma c_2' = \int_0^\gamma [\chi(u) - \chi(\gamma)] du, \quad c_2(\gamma) = \int_0^\gamma \chi(u) du,$$

the function  $\chi(u)$  in expression (4.2) being completely defined by the shape of the laser pulse. In the case where the external field is spatially uniform and is linearly polarized,

$$\mathcal{E}(t) = \mathcal{E} \varphi(\omega t), \quad -\infty < t < \infty, \quad \varphi(\pm\infty) \rightarrow 0, \quad (4.3)$$

it is possible to suggest a simple analytical procedure, described in detail in Ref. [71], for determining  $\chi(u)$  from the pulse shape. For instance,  $\chi(u) = (1 + u^2)^{-1/2}$  corresponds to the monochromatic laser light with  $\varphi(t) = \cos t$ ,  $\chi(u) = 1/(1 + u^2)$  to a soliton-like pulse with  $\varphi(t) = 1/\cosh^2 t$ , etc. (Table 2). For different fields in the form (4.3), including those taken directly from experimental data, the function  $\chi(u)$  can be found numerically. After that, as is seen from expression (4.2), the problem reduces to quadratures. The photoelectron momentum spectrum is defined by the formula

$$dw(\mathbf{p}) \propto \exp\left\{-\frac{2}{3F} g(\gamma) - \frac{\kappa}{\mathcal{E}} \left[ b_1(\gamma)(p_{\parallel} - p_{\text{max}})^2 + b_2(\gamma) p_{\perp}^2 \right]\right\} \frac{d^3 p}{(2\pi)^3}, \quad (4.4)$$

where  $g(\gamma) = 3f(\gamma)/2\gamma$ ,  $b_{1,2}(\gamma) = \gamma^{-1} c_{1,2}(\gamma)$ , and  $p_{\text{max}} = (\mathcal{E}/\omega) \int_0^\infty \varphi(t) dt$  is the momentum which the field transfers to the electron on its escape from the barrier,<sup>10</sup>  $0 < t < \infty$ .

We note that the expression (4.4) for the spectrum is valid, strictly speaking, only for short laser pulses, where  $v\lambda/cL \ll 1$  ( $v$  is the electron velocity,  $\lambda = 2\pi/\omega$  is the wavelength, and  $L$  is the length of the laser radiation beam waist,  $L \gtrsim \lambda$ ). For long pulses, account should be taken of the change in the electron drift momentum induced by the gradient force [79–81]. To calculate the distribution of electrons over their final kinetic energies in this case, it is required to consider their motion in the spatially nonuniform field in the laser beam waist and include the effect of ponderomotive acceleration. In simple models this can be done analytically [81], but for realistic profiles of the laser field this can be done numerically. We will not expand on these issues because the electron motion for  $t > 0$  is classically allowed and the total ionization probability (rate) is no longer changed in this case (although the momentum and angular distributions may undergo significant distortions).

<sup>10</sup> Formula (4.4) defines the spectrum of photoelectrons outgoing to infinity (provided the external field is turned off adiabatically), while expressions (2.1) and (3.13) pertain to the moment the electron is just emerging from the barrier ( $t = 0$ ).

**Table 2.** Models of laser pulses.

No.	$\varphi(t)$	$\tau_0(\gamma)$	$\chi(u)$
1	1	$\gamma$	1
2	$\cos t$	$\operatorname{arcsinh} \gamma$	$(1 + u^2)^{-1/2}$
3	$1/\cosh^2 t$	$\arctan \gamma$	$(1 + u^2)^{-1}$
4	$1/\cosh t$	$\arctan(\sinh \gamma)$	$1/\cosh u$
5	$(1 + \delta)/(\cosh t + \delta),$ $-1 < \delta \leq 1$	—	$(1 - \delta)/(\cosh \rho u - \delta),$ $\rho = \sqrt{(1 - \delta)/(1 + \delta)}$
6	$(\cosh^2 t + \beta^2 \sinh^2 t)^{-1}$	—	$\left(\cosh^2 u + \frac{\sinh^2 \beta u}{\beta^2}\right)^{-1}$
7	$(1 + t^2)^{-1}$	$\tanh \gamma$	$1/\cosh^2 u$
8	$(1 + t^2)^{-3/2}$	$\gamma/\sqrt{1 + \gamma^2}$	$(1 + u^2)^{-3/2}$
9	$\operatorname{cn}(t, q)$	—	$[1 + (\sinh qu/q)^2]^{-1/2}$
10	$\frac{1 - t^2}{(1 + t^2)^2}$	$\frac{2\gamma}{1 + \sqrt{1 + 4\gamma^2}}$	$\frac{1}{2u^2} [1 - (1 + 4u^2)^{-1/2}]$

*Note.* The function  $\varphi(t)$  defines the shape of a pulse (4.3),  $\tau_0$  is the initial moment (dimensionless) of sub-barrier motion,  $\operatorname{cn}$  is elliptic cosine [20]. In this case, No. 1 corresponds to a constant field; for Nos 2, 9, and 10, the momentum  $p_{\parallel}$  transferred from the external field to the electron upon passing through the barrier is zero.

The functions  $g(\gamma)$ , which correspond to various pulsed fields of the form (4.3), are plotted in Fig. 8, which also shows this function for a monochromatic field (curve 1). In particular, curve 3 corresponds to a Gaussian pulse and curve 5 to a Lorentzian pulse. We note that the time axis in Fig. 8 is so reduced that all pulses have the same curvature at the peak,  $\varphi''(0) = -1$ , which is convenient for the comparison of variously shaped pulses.

The results of calculations for a modulated laser pulse with the Gaussian envelope

$$\varphi(t) = \exp\left(-\frac{t^2}{2\sigma^2}\right) \cos t \tag{4.5}$$

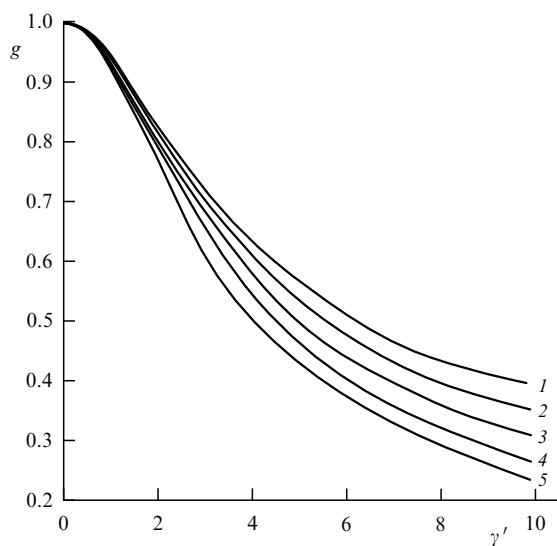


**Figure 8.** Dependence of the function  $g(\gamma)$  from formula (4.4) on the form of the field pulse. Curves 1–5 correspond to  $\varphi(t) = \cos t, 1/\cosh^2 t, \exp(-t^2), (1 + t^2)^{-3/2},$  and  $(1 + t^2)^{-1}$ , respectively. Plotted on the abscissa is the scaled variable  $\gamma' = \sqrt{a_2} \gamma$ .

(a model rather close to experiment and quite frequently used in laser physics) are given in Fig. 9. In this case, the function  $\chi(u)$  can be defined in the parametric form:

$$\chi = \frac{\exp(-s^2/2\sigma^2)}{\cosh s}, \quad u = \frac{1}{2} \int_{-s}^s \exp\left(\frac{t^2}{2\sigma^2} + t\right) dt, \tag{4.5'}$$

where  $s$  is a parameter,  $0 < s < \infty$ .

The pulse (4.5) shortens with a decrease in  $\sigma$ , the value of  $f(\gamma, \sigma)$  also decreases in this case, and the ionization rate in the  $\gamma \gg 1$  domain rises sharply. From the physical standpoint this is attributable to the increase in the relative weight of higher harmonics in the spectrum of the pulse. This effect becomes appreciable when the pulse comprises about five field cycles or fewer. In all cases considered, the shortening of a laser pulse results in a significant rise in the ionization rate (for the same field amplitude  $\mathcal{E}$ ) when  $\gamma \gtrsim 1$ . The dependence

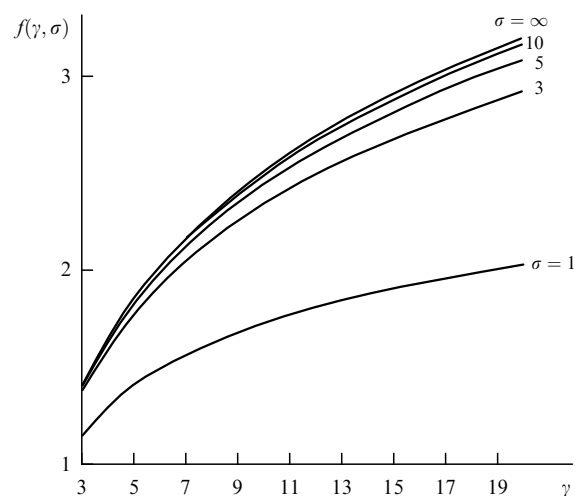


**Figure 9.** Function  $f(\gamma, \sigma)$  from expression (2.1) for the case of a modulated pulse (4.5). The parameter  $\sigma$  defines the envelope width ( $\sigma = 1, 3, 5, 10,$  and  $\infty$ , curves from bottom to top).

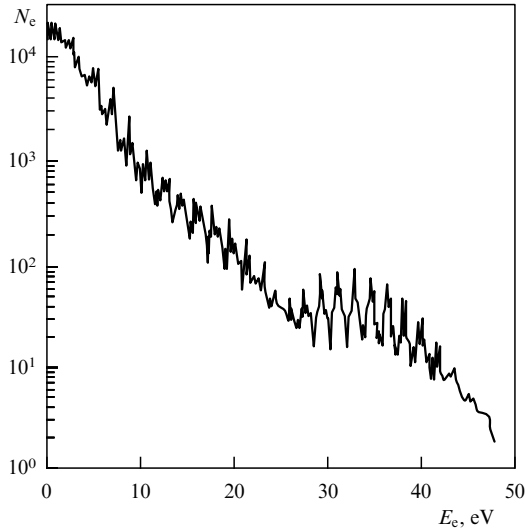


**Figure 10.** Photoelectron energy spectrum for the above-barrier ionization of xenon [43] (the case of linear polarization).  $N_e$  is the number of photoelectrons.

of the photoelectron momentum spectrum on the laser pulse shape, as well as the effect of tunnel ionization in the energy spectrum, was considered at length in Ref. [71].

This effect was noted [5] for the case of linear polarization of monochromatic radiation. It arises from the interference of transition amplitudes which correspond to two saddle points in the complex plane  $t$  residing within one period of the electric field  $\mathcal{E}(t) = \mathcal{E} \cos \omega t$ . When the longitudinal component of the electron momentum  $p_{\parallel}$  is nonzero, there emerges a (real) phase shift between these amplitudes, which is responsible for an additional factor in the momentum spectrum. In the case of  $n$ -photon ionization,

$$dw(\mathbf{p}_n) \rightarrow dw(\mathbf{p}_n) [1 + (-1)^n \cos \phi_n], \quad (4.6)$$

where, according to Refs [5] and [35],

$$\phi_n = \frac{2\kappa p_{\parallel} \sqrt{1 + \gamma^2}}{\omega \gamma}, \quad (4.7)$$

with  $p = p_n = \sqrt{2\omega(n - n_{\text{th}})}$  and  $n_{\text{th}} = K_0(1 + 2\gamma^2)/2\gamma^2$  [see formula (3.3)].

In the quasiclassical case, the phase  $\phi_n$  is large:  $\phi_n \sim F^2/\omega^3 \gg 1$  for  $\gamma \ll 1$  and  $\phi_n \sim \sqrt{K_0/\ln \gamma}$  for  $\gamma \gg 1$ . Therefore, in the integral of expression (4.6) over the photoelectron exit angle, the contribution of the term with  $\cos \phi_n$  decreases sharply. It can be neglected when calculating the ionization rate, but it gives rise to the rapid oscillations in  $n$ -photon ionization probabilities  $w_n = w(E_n)$  depicted in Fig. 10. Experimental investigations of the interference effect in the case of elliptically polarized radiation were performed in Refs [41–43]. We note that expression (4.6) predicts the threshold behavior of the probabilities  $w_n$ , namely [4]  $w_n \propto (n - n_{\text{th}})^{1/2} \propto \sqrt{E_n}$  for even  $n$  and  $w_n \propto (n - n_{\text{th}})^{3/2}$  for odd  $n$ , for  $n \rightarrow n_{\text{th}}$ .

A similar interference effect may show up in the case of ionization by an ultrashort laser pulse when the pulse shape is such that the transition amplitude has contributions from several saddle points with a given momentum  $\mathbf{p}$  and with equal (or close) values of the imaginary part of the action. In particular, rapid oscillations in the photoelectron energy

spectrum were predicted [70] for pulses of the form  $\varphi(t) = 3^{3/2} \sinh t/2 \cosh^3 t$  and  $t \exp[(1 - t^2)/2]$ , which can serve as models of a one-cycle laser field [here, the normalization is so selected that  $\varphi(t_m) = \pm 1$  at the peak].

## 5. Adiabatic case

The ionization of atoms in a low-frequency laser field ( $\gamma \rightarrow 0$ ,  $F \ll 1$ ) occurs at the points in time when the electric field is close to its peak value. In expression (4.3) for  $t \approx 0$  we put

$$\varphi(t) = 1 - \frac{a_2}{2!} t^2 + \frac{a_4}{4!} t^4 - \dots, \quad a_2 > 0, \quad (5.1)$$

to arrive at formula (4.4), in which

$$g(\gamma) = 1 - \frac{a_2}{10} \gamma^2 - \frac{1}{280} (a_4 - 10a_2^2) \gamma^4 - \frac{1}{15120} (a_6 - 56a_4a_2 + 280a_2^3) \gamma^6 + \dots, \quad (5.2)$$

$$b_1(\gamma) = \frac{1}{3} a_2 \gamma^2 + \dots, \quad b_2(\gamma) = 1 - \frac{1}{6} a_2 \gamma^2 + \dots$$

Hence, for monochromatic light we obtain

$$g(\gamma) = \frac{3}{2\gamma} f(\gamma) = \sum_{n=0}^{\infty} (-1)^n g_n \gamma^{2n} = 1 - \frac{1}{10} \gamma^2 + \frac{9}{280} \gamma^4 - \frac{5}{336} \gamma^6 + \dots \quad (5.3)$$

(for more details, see Appendix 13.2).

Passing to the scaled variable  $t' = \sqrt{a_2} t$  makes it possible to compare variously shaped pulses:

$$g(\gamma) = 1 - \frac{1}{10} \gamma'^2 + \frac{9}{280} k \gamma'^4 + \dots, \quad (5.4)$$

$$k = 1 - \frac{a_4 - a_2^2}{9a_2^2}, \quad \gamma' = \sqrt{a_2} \gamma.$$

The dependence on the specific pulse shape manifests itself here beginning with terms of order  $\gamma^4$ . The coefficient  $k$  depends only on the shape of the laser pulse and not on its duration. As a rule<sup>11</sup>,  $0 < k \leq 1$  and therefore the coefficients of expansion (5.4) are numerically small. Hence, we can conclude that the situation for  $\gamma \sim 1$  is closer to the tunnel situation than to the multiphoton one, and the domain of applicability of the asymptotic expansions extends up to values  $\gamma \gtrsim 1$ . Interestingly, the radius of convergence of these expansions is defined by the position of the nearest singular point of the function  $\chi(u)$  in the complex plane [71].

In the adiabatic domain, the longitudinal momentum of a photoelectron far exceeds the transverse one:

$$p_{\parallel} \sim a_2^{-1/2} \gamma^{-1} p_{\perp} \sim \kappa \sqrt{\frac{F}{a_2} \frac{F}{\omega}}, \quad p_{\perp} \sim \sqrt{F} \kappa \ll \kappa, \quad (5.5)$$

which is attributed to the possibility of electron acceleration along the slowly varying electric field  $\mathcal{E}(t)$ . Here,  $a_2 = -\varphi''(0)$  is the curvature of the laser pulse in the vicinity of its peak.

<sup>11</sup> However, this coefficient may exceed unity when the pulse is flattened at its summit. A specific example:

$$\varphi(t) = \frac{1 + (1/2)(1 - a)t^2}{\cosh t} = 1 - \frac{a}{2} t^2 + \frac{1}{24} (6a - 1)t^4 + \dots,$$

for which  $k > 1$  for  $0 < a < 3 - \sqrt{8} = 0.172$ .

## 6. Effect of a magnetic field on the ionization probability

We now consider time-constant fields  $\mathcal{E}$  and  $\mathcal{H}$ . Let  $\theta$  be the angle between them and  $\gamma_c$  be the adiabaticity parameter:

$$\gamma_c = \frac{\omega_c}{\omega_t} = \frac{\kappa \mathcal{H}}{c \mathcal{E}}, \quad (6.1)$$

where  $\omega_c = e\mathcal{H}/mc$  is the cyclotron, or Larmor, frequency related to the gyration of a particle in the magnetic field and  $\omega_t = e\mathcal{E}/\kappa$  is the tunneling frequency in the electric field. As in the case of ionization by a laser field, in this problem there are two frequencies,  $\omega_c$  [which plays the same part as the frequency of light  $\omega$  in formula (1.1)] and  $\omega_t$ . The ratio of these frequencies significantly affects the ionization rate  $w$ . The extremal sub-barrier path derived with the aid of the ITM has the form [10, 82]

$$\begin{aligned} x &= i \frac{\mathcal{E}}{\omega_c^2} \left( \tau - \frac{\tau_0}{\sinh \tau} \sinh \tau \right) \sin \theta, \\ y &= \frac{\mathcal{E}}{\omega_c^2} \frac{\tau_0}{\sinh \tau_0} (\cosh \tau - \cosh \tau_0) \sin \theta, \\ z &= \frac{\mathcal{E}}{2\omega_c^2} (\tau_0^2 - \tau^2) \cos \theta, \end{aligned} \quad (6.2)$$

where  $\tau = i\omega_c t$  and  $-\tau_0 \leq \tau \leq 0$  in the sub-barrier motion. The initial moment  $\tau_0$  is determined from the equation

$$\tau_0^2 - \sin^2 \theta (\tau_0 \coth \tau_0 - 1)^2 = \gamma_c^2. \quad (6.3)$$

The formula for the ionization rate is similar in form to formula (3.6). The function  $g = g(\gamma_c, \theta)$  in the exponent has the form

$$g(\gamma_c, \theta) = \frac{3\tau_0}{2\gamma_c} \left[ 1 - \frac{1}{\gamma_c^2} \left( \sqrt{\tau_0^2 - \gamma_c^2} \sin \theta - \frac{1}{3} \tau_0^2 \cos^2 \theta \right) \right]. \quad (6.4)$$

We note that this expression coincides with that obtained in Ref. [10] but is written in a more compact form. With an increase in  $\gamma_c$ , the function  $g$  increases monotonically and the ionization probability accordingly decreases steeply. Therefore, the magnetic field stabilizes the bound level. In terms of the ITM, this is easily explained by the fact that the sub-barrier electron path is affected by the Lorentz force and ‘becomes twisted’, with the result that the barrier width increases.

Also calculated in the context of this problem were the Coulomb correction  $Q(\gamma_c, \theta)$  and the preexponential factor  $P$  [72]. The inclusion of the Coulomb interaction significantly increases the ionization probability of a neutral atom in comparison with the case of a negative ion (for the same value of the binding energy  $|E_0| = \kappa^2/2$ ). We give the expansions in the  $\gamma_c \ll 1$  domain (a ‘weak’ magnetic field):

$$\tau_0(\gamma_c, \theta) = \gamma_c + \frac{1}{18} \gamma_c^3 \sin^2 \theta + O(\gamma_c^5), \quad (6.5)$$

$$\begin{aligned} g(\gamma_c, \theta) &= 1 + \frac{1}{30} \gamma_c^2 \sin^2 \theta \\ &\quad - \frac{\gamma_c^4}{315} \sin^2 \theta \left( \cos^2 \theta - \frac{11}{24} \sin^2 \theta \right) + \dots, \end{aligned} \quad (6.6)$$

$$Q(\gamma_c, \theta) = 1 + \frac{2}{9} \gamma_c^2 \sin^2 \theta + \dots, \quad P(\gamma_c, \theta) = 1 - \frac{1}{6} \gamma_c^2 + \dots$$

For  $\theta = 0$  (the case  $\mathcal{E} \parallel \mathcal{H}$ ) we have  $\tau_0 = \gamma_c$ ,  $g(\gamma_c, 0) \equiv 1$ , and  $Q(\gamma_c, 0) = (2\kappa^3/\mathcal{E})^{2Z/\kappa}$ . In the other limiting case,  $\theta = \pi/2$ , the formulas are somewhat simpler (this case will be considered in the following section). We note that the ionization probability for  $\gamma_c > 1$  is exponentially small and yet nonzero (in contrast to the statement made in Ref. [83]).

In concluding this section we point out one more application of the ITM. As is well known, the series of the perturbation theory (PT) in quantum mechanics and field theory exhibit factorial divergence (the so-called ‘Dyson phenomenon’ [84–87]). In Refs [88, 89], the ITM was applied to the investigation of higher orders of the PT (in powers of  $\mathcal{E}$  and  $\mathcal{H}$ ) for the hydrogen atom in constant external fields. It was shown [89] that the PT series turned, for some value of the ratio  $\mathcal{H}/\mathcal{E}$  depending on the angle  $\theta$  between the fields, from a series of constant sign (as in the case of the Stark effect) into an alternating series (as for the Zeeman effect). In Refs [89, 90], the ITM was successfully employed to determine the asymptotics of the higher orders of the  $1/n$  expansion in multidimensional problems of quantum mechanics, including those for the molecular hydrogen ion  $\text{H}_2^+$  (see also Refs [91, 92]).

We shall not go into further detail, because these issues are outside of the scope of our review.

## 7. Lorentz ionization

When an atom or an ion enters a magnetic field  $\mathcal{H}$ , in its rest frame  $K_0$  there emerges (due to the Lorentz transformation) an electric field  $\mathcal{E}_0$ , which may cause the ionization of the atom. This process has come to be known as the Lorentz ionization. We consider the quasiclassical theory of the Lorentz ionization [93], which is applicable in the domain of weak (in comparison with atomic) fields:

$$\epsilon = \frac{\mathcal{E}_0}{\kappa^3 \mathcal{E}_a} \ll 1, \quad h = \frac{\mathcal{H}_0}{\kappa^2 \mathcal{H}_a} \ll 1, \quad (7.1)$$

where  $\kappa = \sqrt{2I}$  and  $\mathcal{H}_a = m^2 e^3 c / \hbar^3 = 2.35 \times 10^9$  G. We restrict ourselves to the case of ionization of the  $s$  level ( $l = 0$ ).

When an atom travels with a velocity  $v$  at an angle  $\varphi$  to the direction of magnetic field  $\mathcal{H}$ , the fields  $\mathcal{E}_0$  and  $\mathcal{H}_0$  in the rest frame are

$$\begin{aligned} \mathcal{E}_0 &= q\mathcal{H} = (\Gamma^2 - 1)^{1/2} \mathcal{H} \sin \varphi = \frac{v \sin \varphi}{\sqrt{1 - v^2}} \mathcal{H}, \quad \vec{\mathcal{E}}_0 \perp \vec{\mathcal{H}}_0, \\ \mathcal{H}_0 &= (1 + q^2)^{1/2} \mathcal{H} = (\Gamma^2 \sin^2 \varphi + \cos^2 \varphi)^{1/2} \mathcal{H} \\ &= \sqrt{\frac{1 - v^2 \cos^2 \varphi}{1 - v^2}} \mathcal{H}, \end{aligned} \quad (7.2)$$

where  $q = p_\perp/mc$ ,  $p_\perp$  is the transverse (relative to the magnetic field) particle momentum and  $\Gamma = (1 - v^2)^{-1/2}$  is the Lorentz factor. An important parameter defining the sub-barrier electron motion is<sup>12</sup>  $\gamma_L = \omega_c/\omega_t$  [a special case of expression (6.1)], where  $\omega_c = e\mathcal{H}_0/mc$  is the cyclotron frequency and  $\omega_t = \mathcal{E}_0/\kappa$  is the tunneling

<sup>12</sup> This parameter is similar to the Keldysh parameter  $\gamma$  in the theory of multiphoton ionization. Note that  $\gamma_L = 2b/r_L$ , where  $b$  is the barrier width in the electric field and  $r_L = c\kappa/e\mathcal{H}$  is the Larmor radius. At  $r_L \lesssim b$ , or  $\gamma > 1$ , the magnetic field bends the sub-barrier trajectory and hampers tunneling.

frequency:

$$\gamma_L = \frac{\kappa \mathcal{H}_0}{c \mathcal{E}_0} = \frac{\kappa}{v} \left( 1 + \frac{\cot^2 \varphi}{\Gamma^2} \right)^{1/2} = \frac{\kappa}{v \sin \varphi} \sqrt{1 - v^2 \cos^2 \varphi} \tag{7.3}$$

(the velocity  $v$  is expressed in atomic units  $e^2/\hbar = 2.19 \times 10^8$  cm s<sup>-1</sup>). For nonrelativistic particles,  $\mathcal{E}_0/\mathcal{H}_0 = v_{\perp}/c \ll 1$  and  $\gamma_L = \kappa/v_{\perp}$  may assume arbitrary values. On the other hand, in the case of ultrarelativistic,  $\Gamma \gg 1$ , particles,  $\mathcal{E}_0/\mathcal{H}_0 = 1 - (2q^2)^{-1} \rightarrow 1$ , and in the frame  $K_0$  crossed fields emerge, i.e.,  $\vec{\mathcal{E}}_0 \perp \vec{\mathcal{H}}_0$  and  $\mathcal{E}_0 \approx \mathcal{H}_0$ . In this case,  $\mathcal{E}_0$  can be many times greater than the initial magnetic field  $\mathcal{H}$ .

Invoking the quasiclassical solution [72] of the problem of ionization of atoms in electric and magnetic fields, for the Lorentz ionization probability in the laboratory frame of reference  $K$  we find

$$w_L = \Gamma^{-1} \kappa^2 C_{\kappa}^2 \left( \frac{\epsilon}{2} \right)^{1-2\eta} P(\gamma_L) [Q(\gamma_L)]^{\eta} \exp \left[ -\frac{2}{3\epsilon} g(\gamma_L) \right]. \tag{7.4}$$

Here,  $C_{\kappa}$  is the asymptotic coefficient of the wave function for a free atom (see Appendix 13.1),  $\eta = Z/\kappa$  is the Sommerfeld parameter,  $Z$  is the charge of the atom core,

$$\epsilon = \frac{\mathcal{E}_0}{\kappa^3} = \Gamma \frac{v_{\perp} \hbar}{137 \kappa}, \quad g(\gamma) = \frac{3\tau_0}{2\gamma} \left( 1 - \sqrt{\frac{\tau_0^2 - \gamma^2}{\gamma^2}} \right), \tag{7.5}$$

and we omit the more cumbersome expressions [93] for the preexponential factor  $P$  and the Coulomb correction  $Q$ . All these quantities are expressed most simply in terms of  $\tau_0$  — the imaginary ‘time’ of sub-barrier electron motion determined from the equation [compare with Eqn (3.6)]

$$\tau_0^2 \left[ 1 - \left( \coth \tau_0 - \frac{1}{\tau_0} \right)^2 \right] = \gamma_L^2, \tag{7.6}$$

or  $\tanh \tau_0 = \tau_0/[1 + (\tau_0^2 - \gamma_L^2)^{1/2}]$ . The principal (exponential) factor in formula (7.4) was found in Ref. [10]. We give its expansions:

$$g(\gamma) = \begin{cases} 1 + \frac{1}{30} \gamma^2 + \frac{11}{7560} \gamma^4 + \dots, & \gamma \ll 1, \\ \frac{3}{8} [\gamma + 2\gamma^{-1} + \gamma^{-3} + \dots], & \gamma \gg 1. \end{cases} \tag{7.7}$$

Although the functions  $P(\gamma)$  and  $Q(\gamma)$  exhibit a rather strong dependence on the parameter  $\gamma$  (Fig. 11), the probability  $w_L$  is most sensitive namely to the variations of  $g(\gamma)$ , because this function enters in the exponent in expression (7.4) and, what is more, with a large coefficient  $2/3\epsilon \gg 1$ . The functions  $g(\gamma)$ ,  $P(\gamma)$ , and  $Q(\gamma)$  have been tabulated [93]. The probability  $w_L$  is conveniently represented in the following form:

$$w_L = \Gamma^{-1} S w_{st}(\mathcal{E}_0), \tag{7.8}$$

where  $w_{st}(\mathcal{E}_0)$  is the static ionization probability in the electric field  $\mathcal{E}_0$  and  $S$  is the stabilization factor which takes into account the magnetic field-induced suppression of bound-state decay probability. The effect of the Coulomb interaction

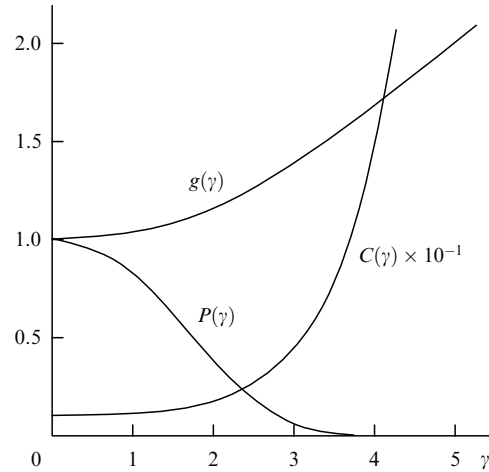


Figure 11. The case of the Lorentz ionization. Plots of the functions appearing in Eqn (7.4), with  $C(\gamma) = \sqrt{Q(\gamma)}$  and  $\gamma \equiv \gamma_L$ .

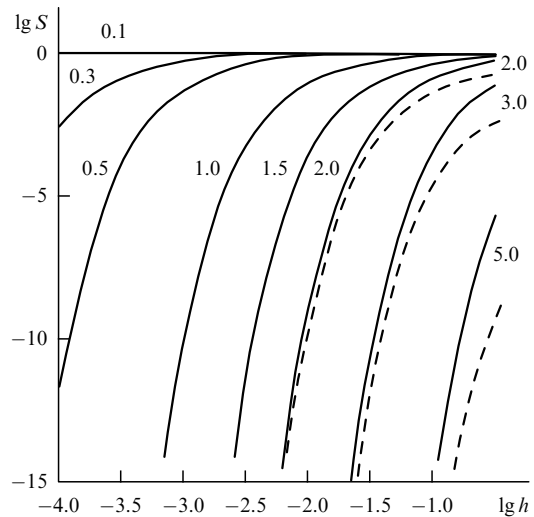


Figure 12. Stabilization factor  $S$  for the ground state of the hydrogen atom (solid curves) and for a negative ion with the same binding energy ( $\kappa = 1$ ,  $Z = 0$ , dashed lines). The values of the parameter  $\gamma_L$  are indicated by the curves;  $h = \mathcal{H}/\kappa^2 \mathcal{H}_a$  is the reduced magnetic field. The curves are plotted on a log – log scale.

on the magnitude of  $S$  becomes appreciable for  $\gamma_L = 1.5$ , as is evident from Fig. 12.

The static magnetic fields obtained in laboratory conditions do not exceed 1 MG. The method of magnetic cumulation (explosion-assisted compression of an axial magnetic field), proposed by A D Sakharov in 1951 [94, 95], made it possible to obtain the record-high values  $\mathcal{H} = 25$  MG in the USSR and  $\mathcal{H} = 15$  MG in the USA. Further progress in this area gives the hope of achieving<sup>13</sup> 30–100 MG fields. Referring to Table 3, when the velocity of hydrogen atoms in the  $\mathcal{H} = 25$  MG field is changed from 1 to 10 a.u., the situation changes from nearly perfect stability of the atom to its instantaneous ionization in a time comparable to the atomic time.

<sup>13</sup> See Ref. [96]. We note that Karnakov et al. [93] gave a description of magnetic cumulation, which is a certain development of the estimates made by Sakharov [95].

**Table 3.** Probability of the Lorentz ionization for the ground state of atomic hydrogen.

$\mathcal{H} = 25 \text{ MG}$			$\mathcal{H} = 350 \text{ MG}$		
$v$	$\mathcal{E}_0 \cdot 100$	$w_L$	$v$	$\mathcal{E}_0 \cdot 100$	$w_L$
1.0	1.06	1.03(-9)	0.167	2.48	7.6(-12)
1.25	1.33	6.41(-4)	0.20	2.98	8.05(-3)
1.67	1.77	2.40	0.22	3.28	50.4
2.0	2.13	1.55(5)	0.25	3.77	1.06(5)
2.5	2.66	5.56(7)	0.3	4.47	5.22(8)
5.0	5.32	6.24(12)	0.4	5.96	1.33(12)
10	10.7	7.73(14)	0.5	7.45	3.54(13)

Note. Here, the angle  $\varphi = \pi/2$ , the velocity  $v$  of the atoms and the field  $\mathcal{E}_0$  are given in atomic units, and the ionization rate  $w_L$  in  $s^{-1}$ .

For negative ions with a low binding energy (for instance, the  $H^-$  ion with  $I = 0.7542 \text{ eV}$  and  $\kappa = 0.236$ ), the dependence of the probability  $w_L$  on  $\mathcal{H}$  and  $v$  is qualitatively similar in form to that for neutral atoms, but the transition region between  $w_L \approx 0$  and  $w_L \rightarrow 1$  is located at lower values of  $\mathcal{H}$  and  $v$ . Weakly bound states with  $\kappa \ll 1$  are known in solid-state physics (the Wannier–Mott excitons in semiconductors; for instance, for germanium crystals,  $\kappa \sim 0.01$ ). In all these cases, significantly weaker fields are required for ionization than in the case of the hydrogen atom.

Superstrong magnetic fields are also encountered in astrophysics. The field  $\mathcal{H}$  on the surface of magnetic white dwarfs varies from 2 MG to  $\sim 1000 \text{ MG}$  (see the table on p. 35 in Ref. [97] containing a list of 50 such objects). In particular, the magnetic field for the Grw + 70°08247 star changes from its maximum value  $\mathcal{H}_{\max} = 350 \text{ MG}$  at the poles to  $0.5\mathcal{H}_{\max}$  at the equator. Lorentz ionization can also occur when a star in its motion penetrates a cloud of neutral hydrogen (see estimates in Ref. [93]).

The sub-barrier electron motion in the magnetic field is characterized by two frequencies,  $\omega_L$  and  $\omega_t$ . In this respect, the situation is similar to that which occurs in the ionization of atoms by the laser field (there are two characteristic frequencies,  $\omega$  and  $\omega_t$ ). This analogy is not superficial; suffice it to compare Eqns (3.6) and (7.6) for the imaginary time  $\tau_0$  and the corresponding expressions for sub-barrier trajectories. However, there is a distinction between these two problems. In a magnetic field, the sub-barrier path ‘twists’ and the barrier width increases with an increase in the parameter  $\gamma_L$ :

$$b = \frac{\kappa^2}{2\mathcal{E}} \begin{cases} 1 + \frac{1}{36} \gamma^2 + \dots, & \gamma \ll 1, \\ \gamma(1 + \gamma^{-2} + \dots), & \gamma \gg 1, \end{cases} \quad (7.9)$$

while in the case of laser-induced ionization [5], the barrier width becomes smaller with increasing  $\gamma$ , for instance,

$$b = \frac{\kappa^2}{2\mathcal{E}} \left( 1 - \frac{1}{4} \gamma^2 \right) \text{ for } \gamma \ll 1.$$

That is why the function  $g(\gamma)$  and the ionization rate in the region  $\gamma \gg 1$  behave in opposite ways (compare Figs 3 and 11).

In the foregoing it was assumed that the atom velocity  $v \ll c$ . In the relativistic theory of Lorentz ionization developed by Nikishov [98] on the basis of the Klein–Gordon equation (without taking into account the electron spin), the formulas are significantly more complicated. It was possible

to obtain a simple result for  $Z = 0, \mathbf{v} \perp \vec{\mathcal{H}}$ , and  $\gamma_L \ll 1$ :

$$w_L(\mathcal{H}, v) \propto \mathcal{E}_0 \exp \left[ -\frac{2\eta^3}{3\mathcal{E}_0} \left( 1 + \frac{1}{30} \tilde{\gamma}_L^2 \right) \right], \quad (7.10)$$

where  $\mathcal{E}_0 = \mathcal{H}v/\sqrt{1-v^2}$  is the electric field in the rest frame of the atom,  $\tilde{\gamma}_L = \gamma_L \sqrt{1-v^2}$ ,  $\eta = (m^2 - \epsilon_0^2)^{1/2}$ ,  $\epsilon_0$  is the bound-state energy, and  $c = 1$ . Since  $\tilde{\gamma}_L \ll 1$ , the ionization in this case is determined only by the field  $\mathcal{E}_0$  and the effect of the magnetic field  $\mathcal{H}_0$  is insignificant (the stabilization factor  $S \approx 1$ ). In the nonrelativistic limit we have  $\eta = \kappa = \sqrt{2I}$ ,  $\mathcal{E}_0/\eta^3 = \epsilon$ , and formula (7.10) turns into formula (7.4), the coefficient  $1/30$  in the correction being in agreement with the first term of expansion (7.7).

### 8. Exactly solvable model

As usual, of interest is the investigation of models which allow the exact solution of the Schrödinger equation. In our case, such a model is the decay problem of a shallow-lying state bound by short-range attractive forces exposed to a circularly polarized electromagnetic wave.<sup>14</sup> Considering this model allows tracing in detail the tunnel-to-multiphoton ionization transition, discussing the accuracy of the quasiclassical approximation, etc.

Passing to the frame of reference co-rotating with the field [100] leads to the stationary Schrödinger equation with the Hamiltonian

$$H_\omega = -\frac{1}{2} \Delta + U(r) - \omega L_z + \mathcal{E}x, \quad (8.1)$$

where  $\omega$  and  $\mathcal{E}$  are the frequency and amplitude of the electric field of the wave and  $L_z$  is the projection of the orbital angular momentum of the electron on the direction of its propagation (the  $z$ -axis). The spectrum of complex quasi-energy [101, 102] states coincides with the quasistationary level spectrum of the Hamiltonian  $H_\omega$ . Its Green function, which satisfies the Sommerfeld radiation condition at infinity, can be derived in the analytical form. Employing the  $\delta$ -potential approximation, which is equivalent to the introduction of a boundary condition at zero [73], for the quasi-energy  $E = E_r - i\Gamma/2$  of the quasistationary state it is possible to obtain the closed equation [103, 104]

$$I(\epsilon; \gamma, K_0) = \sqrt{\epsilon} - 1, \quad (8.2)$$

where  $l = 0$ ,

$$I = \frac{1}{(2\pi i K_0)^{1/2}} \int_0^\infty \frac{du}{u^{3/2}} \left[ \exp \left( i \frac{2K_0 \sin^2 u}{\gamma^2} - u \right) - 1 \right] \times \exp(-2iK_0 \epsilon u), \quad (8.3)$$

$$\epsilon = \epsilon + \gamma^{-2}, \quad \epsilon = \frac{E}{E_0} = 1 + \delta + i\eta,$$

$$E_r = E_0(1 + \delta), \quad \Gamma = \kappa_0^2 \eta, \quad (8.4)$$

$$\gamma = \frac{\omega \kappa_0}{\mathcal{E}} = \frac{1}{2K_0 F}, \quad \kappa_0 = \sqrt{2I_0},$$

<sup>14</sup> This problem by itself is of interest for the theory of multiphoton ionization of negative ions of the type  $H^-$ ,  $Li^-$ ,  $Na^-$ , etc. The earlier results obtained in this area were discussed in monograph [17] and review [99].

$\epsilon$  is the reduced quasi-energy,  $\delta = (\text{Re } E - E_0)/E_0$  is the relative level shift in the laser field,  $I_0 = -E_0 = \kappa_0^2/2$  is the binding energy in the absence of the wave,  $\gamma$  is the Keldysh parameter,  $F = \mathcal{E}/\kappa_0^3$  is the reduced field, and  $K_0 = I_0/\omega$  is the multiquantumness parameter. Equation (8.2) is formally valid for arbitrary  $F$  and allows going beyond the weak-field domain bounds (hereinafter, without loss of generality we assume that  $\kappa_0 = 1$ ). Although this equation has been known for 30 years, for a long time it resisted numerical solution (outside the framework of the perturbation theory in the field  $F$ ). The reason lies with the fact that, since  $\Gamma > 0$  and  $\text{Im } \epsilon = \Gamma/2I_0 > 0$ , the integral (8.3) diverges at the upper limit<sup>15</sup> and necessitates determination, i.e., regularization. For such regularization Mur et al. [105] proposed the use of the Zel'dovich method [106], which had been developed for applying the perturbation theory to quasistationary states (see also Ref. [73], Chapter VII).

The heart of this method can be explained by the example of calculating the normalization integral

$$N = \int_0^\infty |\chi_k(r)|^2 dr.$$

For the Gamow wave function  $\chi_k(r) = rR_k(r) \propto \exp(ikr)$ , and therefore  $|\chi_k|^2 \propto \exp(2k_2r)$  for  $r \rightarrow \infty$ , where  $k = \sqrt{2E} = k_1 - ik_2$  and  $k_2 > 0$ , and the normalization integral  $N$  diverges. As shown by Zel'dovich, in the regularized sense it should be treated as the limit

$$N = \lim_{\alpha \rightarrow +0} \int_0^\infty \chi_k^2(r) \exp(-\alpha r^2) dr, \quad (8.5)$$

which plays the part of the norm of this state (as noted in Ref. [106], in the integral (8.5) there enters precisely the square of the complex wave function  $\chi_k^2(r)$  rather than its squared modulus, which ensures convergence of the integral). In accordance with this recipe, for the solution of Eqn (8.2) we will consider the  $\alpha \rightarrow +0$  limit of the solutions to the equation

$$I_\alpha(\epsilon; \gamma, K_0) = \sqrt{\epsilon} - 1, \quad (8.2')$$

where  $I_\alpha(\epsilon)$  is obtained from expression (8.3) with the replacement

$$\exp(-2i\epsilon K_0 u) \rightarrow \exp(-2i\epsilon K_0 u - \alpha u^2), \quad \alpha > 0. \quad (8.6)$$

The practical execution of the above procedure imposes certain requirements on computational capability, which was hardly possible in the 1960s. For instance, to calculate the width  $\Gamma$  from Eqn (8.2') with a relative accuracy on the order of  $10^{-4}$  was found to require reaching the regularization parameter values  $\alpha \sim 10^{-6} - 10^{-7}$ , which now is entirely feasible with a personal computer. The problems of convergence of the Zel'dovich method and the conditions of its validity are considered in Ref. [105].

<sup>15</sup> This is precisely the case with another equation, obtained by Demkov and Drukarev [34] for the problem of  $s$ -level ionization by a constant electric field; however, the regularization of this equation is achieved simply by shifting the contour of integration from the real axis to the lower half-plane [87]. We emphasize that the divergences occurring here are by no means accidental and are directly related to the exponential growth of the Gamow wave function of the quasistationary state at infinity.

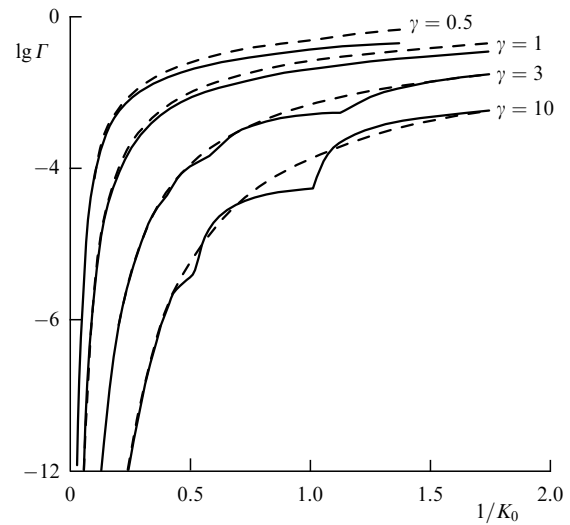


**Figure 13.** The width  $\Gamma$  of a quasistationary level in the case of a  $\delta$ -potential ( $r_c = 0$ ). The solid lines  $\Gamma = \Gamma(\gamma, \omega)$  represent the numerical solution of Eqn (8.2) with the use of the Zel'dovich method and the dashed lines represent the quasiclassical approximation [4, 5].

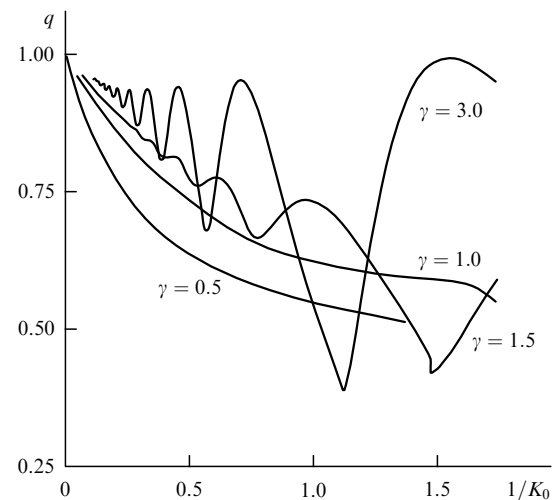


**Figure 14.** Accuracy of the quasiclassical approximation for the level width in the case of the  $\delta$ -potential:  $q = \Gamma/\Gamma_Q$ ; the values of the Keldysh parameter  $\gamma$  are indicated by the curves.

The results of calculation of the level width  $\Gamma$  versus  $1/K_0 = \omega/I_0$  are presented in Fig. 13 for several values of the parameter  $\gamma$ . The dashed lines show the quasiclassical approximation  $\Gamma_Q$  corresponding to the Keldysh theory [4, 5]. One can see that, when  $\gamma \leq 1$ , it is always valid for  $K_0 \gtrsim 1$ ; when  $\gamma \gg 1$ , it is required that  $K_0 \gg 2 \ln \gamma$ . With a decrease in the Keldysh parameter there occurs transition from the multiphoton ionization mode to the tunnel one. Indeed, at  $\gamma \gtrsim 3$ , in the dependence of the width  $\Gamma$  on  $\omega$  there emerges a structure related to the opening of  $n$ -photon ionization channels. This is clearly seen in Fig. 14, which shows the ratio  $q = \Gamma/\Gamma_Q$ , where  $\Gamma_Q(\gamma, \omega)$  is the result obtained in the quasiclassical approximation [4, 5]. For  $\gamma > 5$  and  $K_0 \sim 1$ , the magnitudes of  $\Gamma$  and  $\Gamma_Q$  for the same frequency  $\omega$  may differ by an order of magnitude. With decreasing  $\gamma$ , the threshold oscillations smooth out rapidly as we enter the adiabatic domain  $\gamma \lesssim 1$ .

Equation (8.2) corresponds to the zero range of force action; however, a correction  $\Delta(\epsilon, \kappa_0 r_s)$  for the effective interaction radius is easily introduced in it [107]. The numerical solution of this equation permits determining the shifts and widths of the levels of singly charged negative ions (in this case, the expansion parameter  $\kappa_0 r_s$  varies from 0.62 for  $\text{H}^-$  to 0.54 for  $\text{Rb}^-$ ). The results of calculation [108] of the width  $\Gamma$  suggest that, although the approximation of zero-range forces provides a qualitatively adequate description of the situation, the correction of the order of  $r_s$  is nevertheless rather significant and should be included in the comparison of the theory with experiment.

We also note that the results of earlier numerical calculations [103] of the width  $\Gamma$  as a function of parameters  $\gamma$  and  $\omega$  in the  $\delta$ -potential model are at variance with Fig. 13 and, as already noted [107], are erroneous. A technique for regularizing Eqn (8.2) was recently proposed [109, 110], which is substantially different from the Zel'dovich method<sup>16</sup> and takes advantage of the specific form of this integral equation. The widths  $\Gamma$  obtained with its aid are in agreement with our calculations; however, the Zel'dovich regularization method is more universal and will undoubtedly find further use in atomic and nuclear physics.

Andreev et al. [107] generalized Eqns (8.2) and (8.3) to the case of states with a nonzero orbital angular momentum  $l$  by considering the effective interaction radius  $r_l$  (which is significant for  $l \geq 1$  because the approximation of zero-range forces is valid only for  $s$  states [73]). On this basis they solved the problem of ionization of a weakly bound  $p$  level by the field of a circularly polarized wave and derived the analytical expressions for the shifts and widths of three quasi-energy states originating from the initial  $p$  level in the wave field [107]. All three widths  $\Gamma_{lm}$  in the antiadiabatic case ( $K \gg 1, \gamma \gtrsim 1$ ) were shown to be different from each other, the width of the  $m = 0$  state being the smallest of them. Therefore, the situation here is significantly different from the case of linear polarization (2.5), the probabilities  $w_{lm}$  being nonsymmetrical relative to the sign of  $m$  (here,  $m = 0, \pm 1$  is the projection of the orbital angular momentum on the direction of wave propagation).

## 9. Keldysh theory and experiment

We briefly consider the issue of experimental verification of the Keldysh theory. During the last 10–15 years, many works have been concerned with the observation of single and multiple ionization of rare-gas atoms from the optical to near-ultraviolet spectral regions, but the accuracy of these experiments is still not high enough. Significantly more accurate data were obtained employing high-power infrared lasers, for which  $\omega \ll I$ ,  $\gamma \lesssim 1$ , and  $\mathcal{E} < \mathcal{E}_a$  (a  $\text{CO}_2$  laser with  $\lambda = 10.6 \mu\text{m}$ ,  $\hbar\omega = 0.117 \text{ eV} = 0.0043 \text{ a.u.}$  is a typical example). A tunnel ionization mode was realized in these experiments, whereby the Keldysh parameter is smaller than unity, the experimental data being compared, as a rule, with the predictions of the so-called ‘ADK theory’ [50, 51], which we discuss in Appendix 13.3. In the subsequent discussion the results of some experiments will also be compared with the formulas from Ref. [5]. On averaging the ionization probabilities  $w_{lm}$  with statistical weights, these formulas assume

<sup>16</sup> In Refs [109, 110] this technique was employed to consider the stabilization of atomic decay probability in a strong field and to calculate the rate of laser radiation-induced ionization of negative hydrogen ions.

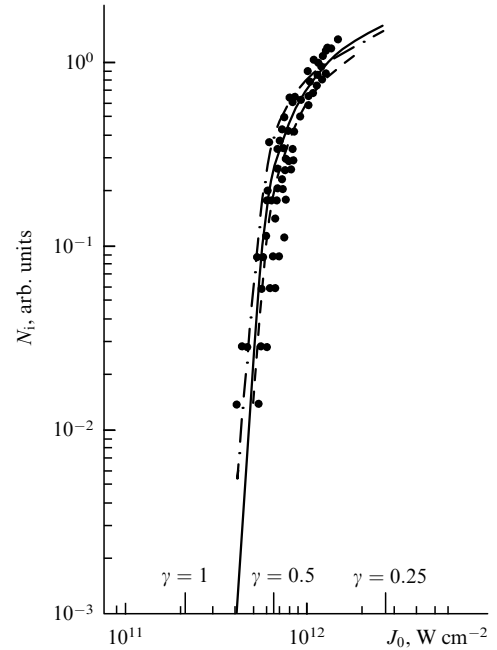


**Figure 15.** Number of  $\text{K}^+$  ions (in arbitrary units) as a function of light intensity  $J_0$ ,  $\text{W cm}^{-2}$ , according to Ref. [111] ( $\text{CO}_2$  laser,  $\xi = 0$ ,  $K_0 = 37.2$ ). The solid curve was calculated by formula (13.3.1) (see explanation in the text). The points at which the Keldysh parameter is  $\gamma = 1.0, 0.5$ , and  $0.25$  are indicated on the ordinate axis.

the form (13.3.1) from Appendix 13.3. Not pretending to present a complete review of the experimental data, we will consider just a few of the many dozens of papers concerned with this problem.

Figure 15 shows the number  $N_i$  of potassium ions (in arbitrary units) as a function of laser radiation intensity: the experimental data of Ref. [111] are represented by points, the curves having been plotted by the ADK formula (13.3.4) (the solid curve) and by formula (13.3.1) without the correction of the order of  $\gamma^2$  in the exponent (the dashed curve) and with the inclusion of this correction (the dash-dotted curve). We note that the adiabatic correction  $\propto \gamma^2$  is more significant than the difference between the coefficients  $C_\kappa$  and  $C_\kappa^{\text{ADK}}$  (although  $0.1\gamma^2 \ll 1$ , this term in the exponent is large because of the coefficient  $2/3F$ ). Points at which the Keldysh parameter is  $\gamma = 1, 0.5$ , and  $0.25$  are marked on the ordinate axis (all experimental points pertain to the domain in which  $\gamma < 0.4$ , and therefore advantage can be taken of the formulas relating to the tunnel ionization mode). One can see from Fig. 15 that both formulas, (13.3.1) and (13.3.4), are consistent with the experimental data. This comes as no surprise, because the difference between them for  $\gamma \ll 1$  is entirely related to the difference between the coefficients  $C_\kappa$  and  $C_\kappa^{\text{ADK}}$ , which is small (in this case,  $C_\kappa/C_\kappa^{\text{ADK}} = 0.87$ ).

We give the formulas which provide an easy way of calculating the electric field  $\mathcal{E}$  and the parameter  $\gamma$ :

$$\mathcal{E} = 0.169\sqrt{J}, \quad \gamma = \frac{\omega\kappa}{\mathcal{E}} = \sqrt{\frac{J_1}{J}}, \quad J_1 = \frac{35\omega^2 I}{I_H}, \quad (9.1)$$

with  $\gamma^2/15F = 0.133K_0(J_1/J)^{3/2}$ , and the multiquantumness parameter is

$$K_0 = 0.011 \frac{\lambda I}{I_H} = \frac{I}{2\omega I_H}. \quad (9.2)$$

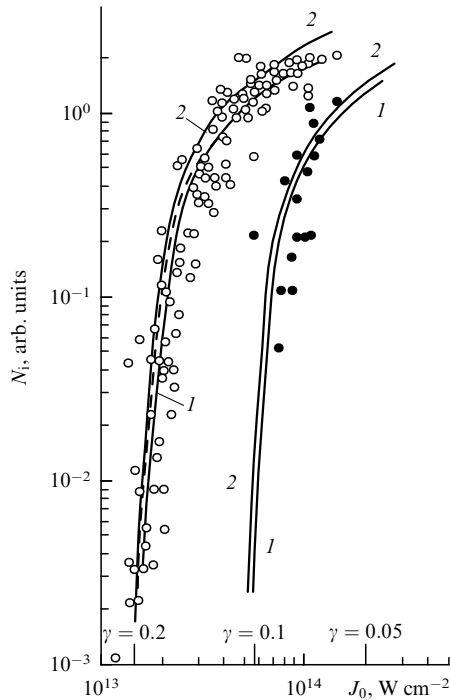


**Figure 16.** Experimental data [111] on the tunnel ionization of atomic xenon with the production of  $\text{Xe}^+$  ( $\circ$ ) and  $\text{Xe}^{++}$  ( $\bullet$ ) ions. Curves 1 correspond to formula (13.3.4), curves 2 were plotted by formula (13.3.1).

Here,  $\mathcal{E}$  is measured in atomic field units  $\mathcal{E}_a$ , the intensity of laser radiation  $J$  in  $10^{15} \text{ W cm}^{-2} = 1 \text{ PW cm}^{-2}$ , the frequency  $\omega$  in atomic units  $me^4/\hbar^3 = 4.13 \times 10^{16} \text{ s}^{-1}$ , and the wavelength  $\lambda$  in nm, with  $\xi = 0$  (linear polarization). To move to the general case of elliptical polarization it would suffice to make the change  $J \rightarrow J/(1 + \xi^2)$ . The tunnel ionization domain corresponds to intensities  $J > J_1$ .

Similar results were obtained [111] in experiments carried out to produce xenon ions in the field of  $\text{CO}_2$ -laser radiation (Fig. 16) as well as in the case of ionization of atomic helium [112] by the field of Ti:Sapphire laser radiation. The curves constructed by formulas (13.3.1) and (13.3.4) are very close (see Figs 15 and 16) and provide a fairly good description of the experimental data (in this case, the curves for  $\text{Xe}^{++}$  were calculated assuming a cascade mechanism of tunnel ionization, which is evidently justified in this case). Since for atomic helium  $C_\kappa/C_\kappa^{\text{ADK}} = 0.98$ , without the inclusion of the correction  $\propto \gamma^2$  the curves corresponding to formulas (13.3.1) and (13.3.4) are indistinguishable to within the accuracy of the drawing.

Recently, measurements were made [113] of the momentum spectrum of the particles produced in the course of tunnel ionization of neon atoms. Figure 17, which was borrowed from Ref. [113], shows the distribution of  $\text{Ne}^+$  ions ejected along ( $p_{\parallel}$ ) and across ( $p_{\perp}$ ) the direction of the polarization vector of linearly polarized Ti:Sapphire laser radiation ( $\lambda = 795 \text{ nm}$ ,  $K_0 = 13.9$ ). The solid curves in Fig. 17 correspond to formula (3.13) derived by expanding expressions (2.1) in the parameter  $\gamma$ . In this case,  $\gamma = 0.35$ , and therefore the difference between these formulas does not go beyond the limits of experimental error [in particular, the coefficients of the momentum spectra by Eqns (2.1) and (3.13) are  $c_2 = 0.343$  and  $0.350$ , respectively]. The energy distribution of tunnel electrons [44] in the ionization of xenon atoms ( $\mathcal{E} = 0.051\mathcal{E}_a$ ,  $\gamma = 0.01$ ) is also consistent with Eqn (3.13).

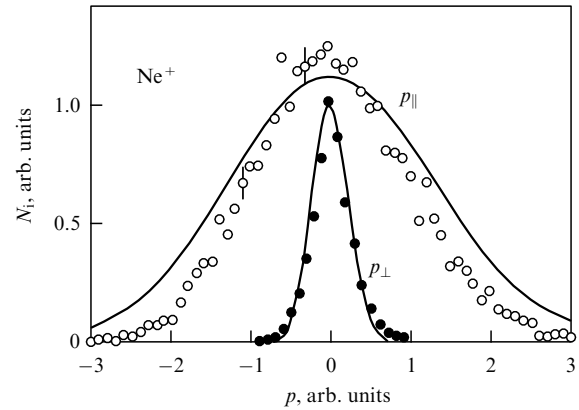


**Figure 17.** Momentum distribution of  $\text{Ne}^+$  ions (linear polarization). The experimental data of Ref. [113] are represented by points; the solid curves were plotted by formula (3.13).

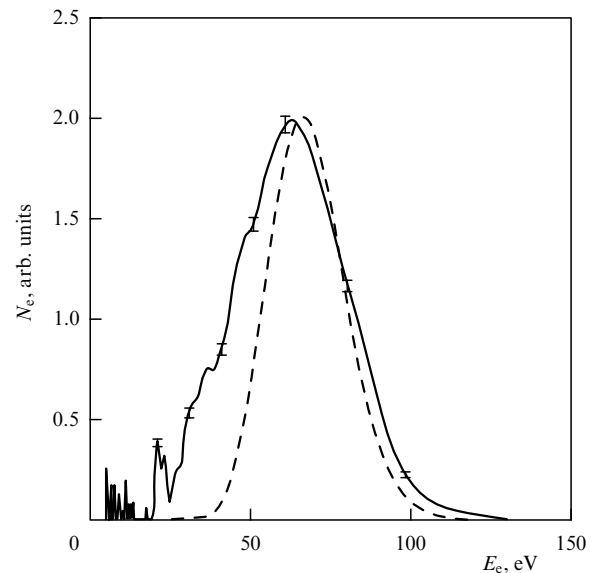


**Figure 18.** Photoelectron energy spectrum in the above-barrier ionization of helium atoms by the circularly polarized light of a  $\text{CO}_2$  laser with the intensity  $J = 6 \times 10^{15} \text{ W cm}^{-2}$  (solid line, Ref. [114]). Results of numerical calculations by the KFR model (dashed line).

Finally, we outline the results of Ref. [114] concerned with the investigation of above-threshold ionization of helium atoms. Figure 18 shows the photoelectron energy spectrum and the results of calculations by the KFR (Keldysh–Faisal–Reiss) theory for circularly polarized laser radiation. The forms of both distributions are in qualitative agreement with each other. The photoelectron distribution possesses a peak at an energy  $E_e^{\text{max}} = 64 \text{ eV}$ , which is significantly higher than the peak energy in the case of linear polarization,  $E_e^{\text{max}} \approx 10 \text{ eV}$ . The difference is attributed to the fact that electrons in the field of a circularly polarized wave acquire a significantly higher orbital momentum than for a linearly polarized wave.

We restrict ourselves to the above examples although they could easily be raised in number. On the whole, the ionization of atoms in the tunnel domain  $\gamma \lesssim 1$ , where it is nonresonant in nature, is adequately described (both qualitatively and quantitatively) by the Keldysh theory. In the literature this is

commonly formulated as the experimental confirmation of the ‘ADK theory’ [115, 51]. However, since the ‘ADK theory’ can be reduced to a trivial modification of the results obtained in Refs [4–7] long before the publication of Ref. [115], this statement does not appear to be unbiased (in this connection see Ref. [52] and Appendix 13.3).

The situation is more complicated in the  $\gamma > 1$  domain, in which transition from the tunnel ionization mechanism to the multiphoton one occurs. Here, the ionization of atoms may be substantially affected by the resonances with the excited states adjacent to the continuum boundary. At the same time, the analytical theory of Keldysh and his followers considers only one (initial) bound state and the continuum and does not take into account explicitly the structure of the upper levels of a specific atom. In this case, in general the theory cannot pretend to be a direct comparison with experimental data, and more adequate are numerical calculations based on the perturbation theory of high order in the field which includes resonance energy denominators. Many authors have carried out such calculations, including those for hydrogen atoms, alkali atoms, etc. for different numbers of absorbed photons. This generates the need for calculating complex multiple sums over intermediate states typical of high orders of the perturbation theory. To this end, special methods of calculation have been elaborated, including the use of Green functions as well as quantum defect and model potential methods. On all these issues we refer the reader to monograph [17], which also gives further references.

However, it is pertinent to note that the values  $\gamma > 1$  correspond to strong fields, in which atomic levels acquire large widths and overlap with each other, so that the resonance structure does not always become apparent. That is why the Keldysh theory quite often turns out to be applicable in the region  $\gamma \gtrsim 1$  as well.

In summary, one can say that the Keldysh ionization theory provides convenient analytical formulas for atom ionization rates, the energy and momentum spectra of photoelectrons, their angular distribution, and so forth, furnishes a qualitative and, sometimes, quantitative description of the tunnel ionization of atoms and ions, and is valid in the intermediate ( $\gamma \sim 1$ ) domain as well. On the other hand, numerical calculations on the basis of the transient high-order perturbation theory can yield rather accurate values of the above quantities, which apply, however, to a specific atom and to specific values of the frequency  $\omega$ , electric field intensity  $\mathcal{E}$ , and ellipticity  $\xi$ . That is why these two approaches complement each other and a comprehensive understanding of the problem of atom ionization in a strong laser field calls for a combination of analytical and numerical approaches.

## 10. Relativistic tunneling theory

The rapid progress of laser physics and technology has made it possible to achieve record-high intensities  $J \sim 10^{21} \text{ W cm}^{-2}$ , and their increase by 1–2 orders of magnitude is planned for the immediate future [116]. Such a strong field can produce ions with a charge  $Z \sim 40–60$ , for which the electron-level binding energy  $E_b = m_e c^2 - E_0$  becomes comparable to the rest energy  $m_e c^2$ . In this case, the sub-barrier electron motion responsible for ionization can no longer be treated as nonrelativistic, and a generalization of the Keldysh ionization theory is called for.

A linearly polarized plane electromagnetic wave is defined by the potentials<sup>17</sup>

$$\mathbf{A} = \left( 0, -\frac{\mathcal{E}_0}{\omega} a(\eta), 0 \right), \quad \varphi \equiv 0, \quad (10.1)$$

where  $\mathcal{E}_0$  is the wave field amplitude,  $\mathcal{E} = \mathcal{H} = \mathcal{E}_0 a'(\eta)$ ,  $\eta = \omega(t - x)$ , the  $x$ -axis coincides with the direction of wave propagation, the electric field is directed along the  $y$ -axis and the magnetic field along the  $z$ -axis. The function  $a(\eta)$  defines the pulse shape. In particular,  $a(\eta) = \sin \eta$  corresponds to monochromatic laser light,  $a(\eta) = \eta$  to a constant crossed field,  $a(\eta) = \tanh \eta$  to a soliton-like pulse  $\mathcal{E}(t, x) = \mathcal{E}_0 / \cosh^2 \eta$ , etc. The equations of motion for the electron four-momentum  $p^i = (\mathbf{p}, E)$  take the form

$$\begin{aligned} \dot{p}_x &= e\mathcal{E}v_y, & \dot{p}_y &= e\mathcal{E}(1 - v_x), & \dot{p}_z &= 0, \\ \dot{E} &= e(\vec{\mathcal{E}}\mathbf{v}) = e\mathcal{E}v_y, \end{aligned} \quad (10.2)$$

where the point denotes a derivative with respect to laboratory time  $t$ . For any dependence  $\mathcal{E}(\eta)$  there exists the integral of motion [2, 3]

$$J = E - p_x = \frac{1 - v_x}{\sqrt{1 - v^2}} = \frac{\eta}{\omega\tau}, \quad (10.3)$$

where  $\tau = \int^t \sqrt{1 - v^2} dt$  is the proper time of the particle. The second equation in (10.2) gives

$$\frac{dp_y}{d\eta} = \frac{e\mathcal{E}_0}{\omega} a'(\eta), \quad p_y(\eta) = \frac{e\mathcal{E}_0}{\omega} a(\eta) = -eA_y(\eta)$$

(when selecting the constant of integration we take into account that upon passing to the imaginary time,  $t \rightarrow it$ , the variable of the light wave front  $\eta$  and the momentum  $p_y$  become purely imaginary). Next,

$$\begin{aligned} \frac{dy}{d\eta} &= \frac{1}{J\omega} \frac{dy}{d\tau} = \frac{p_y(\eta)}{J\omega}, \\ y(\eta) &= \frac{e\mathcal{E}_0}{J\omega^2} \int_{\eta_0}^{\eta} a(\eta') d\eta', \quad y(\eta_0) = 0, \end{aligned}$$

and  $p_x(\eta)$ ,  $x(\eta)$  are defined in a similar way. The solution can be obtained in explicit form for any dependence of the wave field on  $\eta$ .

The sub-barrier trajectory for the case of monochromatic laser radiation, where  $a(\eta) = \sin \eta$ , has the form

$$\begin{aligned} p_x(\eta) &= \frac{1}{4\beta^2 J} \left( \frac{\sinh 2\eta_0}{2\eta_0} - \cosh 2\eta \right), & p_y(\eta) &= i\beta^{-1} \sinh \eta, \\ x &= \frac{i\eta}{4\omega\beta^2 J^2} \left( \frac{\sinh 2\eta_0}{2\eta_0} - \frac{\sinh 2\eta}{2\eta} \right), \\ y &= \frac{1}{\omega\beta J} (\cosh \eta_0 - \cosh \eta), & z &\equiv 0, \end{aligned} \quad (10.4)$$

where  $\beta = \omega/e\mathcal{E}_0$  and we have made the substitution  $\eta \rightarrow i\eta$  corresponding to the ITM. In this case,  $\eta_0 = -i\omega t_0$ , where  $t_0$  is the initial (imaginary) instant of time for sub-barrier motion.

<sup>17</sup> In this section, use is made of the relativistic units  $\hbar = m = c = 1$  and the ellipticity of radiation is denoted by the letter  $\rho$ .

The quantities  $\eta_0$  and  $J$  are determined from the initial conditions

$$E(\eta_0) = \sqrt{p_x^2(\eta_0) + p_y^2(\eta_0) + 1} = \epsilon, \quad p_x(\eta_0) = \epsilon - J \quad (10.5)$$

(here,  $\epsilon = E_0/m_e c^2$ ,  $0 < \epsilon < 1$ , and  $E_0$  is the initial level energy, including the rest energy of the electron), whence

$$\sinh^2 \eta_0 = \gamma^2 \frac{1 - 2\epsilon J + J^2}{1 - \epsilon^2}, \quad \frac{\sinh 2\eta_0}{2\eta_0} = 1 + 2\gamma^2 \frac{1 - J^2}{1 - \epsilon^2}, \quad (10.6)$$

where  $\gamma$  is the adiabaticity parameter, which is the relativistic generalization of the Keldysh parameter,

$$\gamma = \omega T_t = \frac{\omega}{e\mathcal{E}_0} \sqrt{1 - \epsilon^2}, \quad (10.7)$$

and  $T_t$  is the typical tunneling time in the electric field  $\mathcal{E}_0$ . From the system of equations (10.6) it is easy to determine  $\eta_0$  and  $J$  as functions of the parameters of the problem  $\gamma$  and  $\epsilon$ .

We calculate the function of ‘shortened action’

$$W = \int_{t_0}^0 [-\sqrt{1 - v^2} + e(\mathbf{A}\mathbf{v}) + \epsilon_0] dt,$$

along the sub-barrier trajectory to find with an exponential accuracy the ionization rate for a relativistic bound state:

$$w_R \propto \exp(-2\hbar^{-1} \text{Im } W) = \exp\left[-\frac{2}{3F} g(\gamma, \epsilon)\right], \quad (10.8)$$

where

$$g = \frac{\sqrt{1 + (2/3)\xi^2 - (1/3)\xi^4}}{\xi^2 \gamma} \eta_0 (J - \epsilon),$$

$F = \mathcal{E}_0/\mathcal{E}_{\text{ch}}$ , and  $\mathcal{E}_{\text{ch}}$  is the characteristic field defined by the initial level energy:

$$\mathcal{E}_{\text{ch}} = \frac{(\sqrt{3}\xi)^3}{1 + \xi^2} \mathcal{E}_{\text{cr}}, \quad \xi = \left[1 - \frac{1}{2}\epsilon(\sqrt{\epsilon^2 + 8} - \epsilon)\right]^{1/2}, \quad (10.9)$$

$\mathcal{E}_{\text{cr}} = m_e^2 c^3 / e\hbar = 1.32 \times 10^{16}$  V cm<sup>-1</sup> is the ‘critical’, or Schwinger, field in quantum electrodynamics [117–120].

The value of  $\mathcal{E}_{\text{ch}}$  monotonically increases as the bound level becomes deeper. In the nonrelativistic limit,  $\epsilon \rightarrow 1$  and  $\mathcal{E}_{\text{ch}} = (2I)^{3/2} \mathcal{E}_a$ , where  $\mathcal{E}_a = \alpha^3 \mathcal{E}_{\text{cr}}$ ,  $\alpha = 1/137$ , and  $I$  is the ionization potential (in atomic units). In this case, formula (10.8) turns into the Keldysh formula (2.1). Equations (10.6)–(10.8) furnish its extension to the case of deep-lying levels and are easily solved with a computer (Fig. 19).

In a similar way it is possible to calculate the rate of  $s$ -level ionization by an elliptically polarized electromagnetic wave (the general case of monochromatic radiation). In lieu of expressions (10.6) we obtain the equations

$$\begin{aligned} \sinh^2 \eta_0 - \rho^2 \left( \cosh \eta_0 - \frac{\sinh \eta_0}{\eta_0} \right)^2 &= \gamma^2 \left[ 1 + \frac{(J - \epsilon)^2}{1 - \epsilon^2} \right], \\ (1 - \rho^2) \frac{\sinh 2\eta_0}{2\eta_0} + \rho^2 \left[ 2 \left( \frac{\sinh \eta_0}{\eta_0} \right)^2 - 1 \right] &= 1 + \frac{2\gamma^2(1 - J^2)}{1 - \epsilon^2}, \end{aligned} \quad (10.10)$$

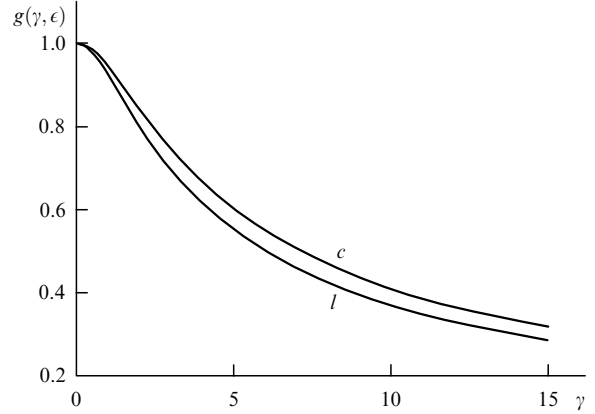


**Figure 19.** Results of the relativistic ionization theory: the function  $g(\gamma, \epsilon)$  in the case of linearly ( $l$ ) and circularly ( $c$ ) polarized radiation for the ground state of a hydrogen-like atom with  $Z = 60$  ( $\epsilon = 0.899$ ).

where  $\rho$  is the ellipticity of light ( $-1 \leq \rho \leq 1$ ,  $\rho = 0$  corresponds to linear polarization and  $\rho = \pm 1$  to the circular one). The function  $g(\gamma, \xi)$  calculated numerically is plotted in Fig. 19. With an increase in ellipticity, the function  $g = g(\gamma, \epsilon, \xi)$  monotonically increases and the ionization probability accordingly decreases. We give the expansion

$$g(\gamma, \epsilon, \rho) = 1 - \frac{1 - \rho^2/3}{10(1 - \xi^2/3)} \gamma^2 + O(\gamma^4), \quad (10.11)$$

which is valid in the adiabatic domain  $\gamma \ll 1$ . In the nonrelativistic limit ( $\xi \sim \alpha\sqrt{I} \ll 1$ ), this formula agrees with Ref. [5] for the case of arbitrary ellipticity  $\rho$  and with the results obtained in Refs [4, 5] for the case of circular polarization. The increase in light ellipticity leads to a lowering of the ionization probability  $w_R$ , while a decrease in  $\epsilon$ , i.e., a deepening of the bound level, conversely, raises it (for a fixed value of the reduced field  $F$ , which itself depends on the level energy).

The exponential factor (10.8) is independent of the particle spin. In the framework of the ITM, the spin correction to the action function is [121]

$$\begin{aligned} \delta S_{\text{spin}} &= \frac{ie}{2mc} \epsilon_{\alpha\beta\lambda\mu} \int F^{\alpha\beta} u^\lambda s^\mu dt \\ &= \frac{e}{mc} \int \{ (\mathbf{s}\mathbf{H}) - (\mathbf{v}\mathbf{s})(\mathbf{v}\mathbf{H}) + [\mathbf{v}\mathbf{s}]\vec{\mathcal{E}} \} dt. \end{aligned} \quad (10.12)$$

Taking into consideration that the sub-barrier trajectory (10.4) lies in the  $(x, y)$  plane and  $\mathcal{E} = \mathcal{H}$ , we obtain

$$\delta S_{\text{spin}} = \frac{e\mathcal{E}_0}{mc} \int_{t_0}^0 s_z a'(\eta)(1 - v_x) dt = -\frac{e\mathcal{E}_0 J}{mc} \int_0^{\eta_0} s_z a'(\eta) d\tau.$$

The rotation of the spin in an external electromagnetic field is defined by the Bargmann–Michel–Telegdi equation [122]. In the case of crossed fields it implies that  $s_z(t) = \text{const}$  and therefore

$$\delta S_{\text{spin}} = -\mu_B \frac{\mathcal{E}_0}{\omega} s_z a(i\eta_0). \quad (10.13)$$

For a constant field,

$$a(i\eta_0) = i \frac{\omega}{e\mathcal{E}_0} \sqrt{\frac{3\xi^2}{1 + \xi^2}};$$

furthermore, one should take into account that the exponential factor in formula (10.8) changes due to the splitting of the initial level  $\epsilon$  in the magnetic field. The splitting depends on the magnetic moment  $\mu$  of the bound electron, different from the Bohr magneton when  $Z\alpha \sim 1$  [123, 124]. Eventually we obtain the spin factor in the rate of the level ionization by a constant crossed field:

$$S_{\pm}^{\text{ITM}} = \exp \left[ \pm \frac{\sqrt{3}\xi}{\sqrt{1+\xi^2}} \left( 1 - \frac{\mu}{\mu_B} \right) \right], \quad (10.14)$$

where the  $\pm$  signs correspond to the  $\pm\hbar/2$  spin projections on the direction  $\mathcal{H}$ , and therefore states with different  $s_z$  possess different ionization rates.

Another way of calculating the spin correction involves squaring the Dirac equation.<sup>18</sup> In this case, instead of expression (10.14) we obtain

$$S_+ = S_-^{-1} = \frac{1+\sigma}{1-\sigma} \exp \left( -\frac{\sqrt{3}\xi}{\sqrt{1+\xi^2}} \frac{\mu}{\mu_B} \right), \quad (10.15)$$

$$\sigma = \frac{\sqrt{3}\xi}{1 + \sqrt{1+\xi^2}}.$$

The results of these two calculations are only slightly different. For instance, for the ground state  $1s_{1/2}$  in a hydrogen-like atom with a charge  $Z = 60$ , according to Breit [123], we have  $\mu = 0.933\mu_B$ , whence  $S_+ = 1.046$ , and  $S_+^{\text{ITM}}$  departs from it by only 1.5%.

When  $Z\alpha \ll 1$ ,  $S_{\pm} \approx S_{\pm}^{\text{ITM}} = 1 + O((Z\alpha)^3)$ , i.e., the tunneling probability is virtually independent of the electron spin projection. This is natural: the operator  $\hat{s}$  commutes with the Schrödinger Hamiltonian and the spin variable splits off.

The highest radiation intensities  $J$  are realized for IR lasers, where  $\gamma \ll 1$ . In this case, for the rate of tunnel ionization of the  $s$  level it is possible to derive a formula asymptotically exact in the weak-field limit ( $F \ll 1$ ):

$$w_R = \frac{mc^2}{\hbar} |C_{\lambda}|^2 G F^{3/2-2\nu} \exp \left[ -\frac{2}{3F} \left( 1 - \frac{\gamma^2}{10(1-\xi^2/3)} \right) \right], \quad (10.16)$$

$$\rho = 0, \quad \mathcal{E}_0 \ll \mathcal{E}_{\text{ch}},$$

where  $\nu = Z\alpha\epsilon/\sqrt{1-\epsilon^2}$  is the relativistic analog for the efficient principal quantum number  $n^* = Z/\sqrt{2I}$ , and  $C_{\lambda}$  is the asymptotic (at infinity) coefficient of the wave function of a free (in the absence of the wave field) atom, which can be determined numerically from the Hartree–Fock–Dirac equations. However, in the case of a hydrogen-like atom, there exists an analytical solution as well [120, 127]. For the ground  $1s_{1/2}$  state for arbitrary  $Z$ ,

$$\epsilon = \nu = \sqrt{1 - (Z\alpha)^2}, \quad C_{1s}^2 = \frac{2^{2\epsilon-1}}{\Gamma(2\epsilon+1)}. \quad (10.17)$$

Finally, we omit here the factor  $G = G(\epsilon, Z)$ , which is independent of the wave amplitude and has a rather cumbersome form. For an elliptical polarization, the exponential factor in formula (10.16) should be changed according to formula (10.11), while the index of the characteristic field  $F$  (in the pre-exponent) in the case of a circular polarization should be replaced with  $1-2\nu$ . In the nonrelativistic limit, formula (10.16) assumes the form of formula (13.3.1).

<sup>18</sup> This approach is similar to the one used in Refs [125, 126] for solving the relativistic Coulomb problem with  $Z > 137$ .

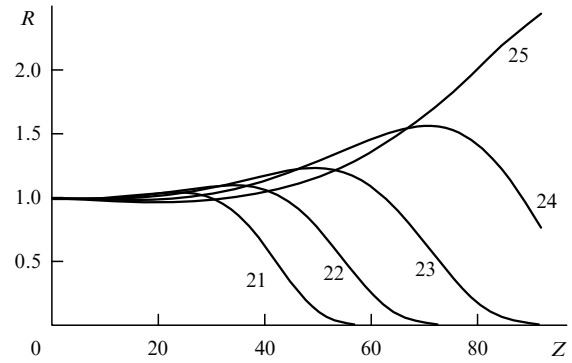


**Figure 20.** Ratio  $R = w_{\text{NR}}/w_R$  as a function of  $Z$  for the ground state of a hydrogen-like atom. The values of  $\lg J$ , where  $J$  is the radiation intensity [ $\text{W cm}^{-2}$ ], are indicated by the curves.

We now estimate the range of validity of the nonrelativistic ionization theory. With an exponential accuracy,

$$w_R \propto \exp \left[ -\frac{2(\sqrt{3}\xi)^3 \mathcal{E}_{\text{cr}}}{3(1+\xi^2)\mathcal{E}} \right],$$

$$w_{\text{NR}} \propto \exp \left( -\frac{2\kappa^3 \mathcal{E}_a}{3\mathcal{E}} \right) = \exp \left\{ -\frac{2}{3} [2(1-\epsilon)]^{3/2} \frac{\mathcal{E}_{\text{cr}}}{\mathcal{E}} \right\}. \quad (10.18)$$

Putting  $\epsilon = 1 - (1/2)\alpha^2\kappa^2 = \sqrt{1 - (Z\alpha)^2}$ , we find

$$R = \frac{w_{\text{NR}}}{w_R} \approx \exp \left[ -\frac{1}{36} (Z\alpha)^5 \frac{\mathcal{E}_{\text{cr}}}{\mathcal{E}} \right], \quad Z\alpha \ll 1. \quad (10.19)$$

One can see from Fig. 20 that the range of validity of the nonrelativistic Keldysh theory extends up to rather large  $Z$  values. For instance, for  $Z = 40, 60$ , and  $80$  and the radiation intensity  $J = 10^{23} \text{ W cm}^{-2}$ , the values of  $w_{\text{NR}}$  and  $w_R$  differ by respective factors of 1.15, 3, and 65. For  $Z \gtrsim 60$ , use must be made of the relativistic tunneling theory (see Fig. 20 and Ref. [128]).

It is pertinent to note that the ionization of a relativistic bound state by a constant crossed field was first considered by Nikishov and Ritus [4]. Using the exact solution of the Klein–Gordon equation these authors calculated the ionization probability for the  $s$  level bound by short-range ( $Z = 0$ ) forces in the case of a spin-zero particle. Their resultant expression for  $w_R$  actually coincides with the results of Refs [129–131] for  $Z = 0$ , although is written in a somewhat different form. The agreement of results obtained by two independent methods is of significance for the ITM: although this method possesses heuristic strength and physical clarity, it cannot, nevertheless, be considered as being rigorously substantiated from the mathematical standpoint, despite some attempts made along this line [121]. The Coulomb factor in the probability  $w_R$ , which is highly significant for  $Z \neq 0$ , was calculated in Ref. [130]. The recently published papers by Milosevic et al. [132, 133] are discussed in Refs [128, 134] and in Appendix 13.3.

## 11. Electron–positron pair production from a vacuum by the field of high-power optical and X-ray lasers

Quantum electrodynamics (QED) predicts the possibility of  $e^+e^-$ -pair production from a vacuum in a strong electric field.

This nonlinear and inherently nonperturbative effect, which was initially considered for a constant field [117–119], subsequently was theoretically studied for variable fields of the electric type:  $I_1 = (\mathbf{B}^2 - \mathbf{E}^2)/2 < 0$ ,  $I_2 = (\mathbf{E}\mathbf{B})/2 = 0$ . In particular, the model case of a spatially uniform field with a linear polarization<sup>19</sup>,

$$\mathbf{E}(t') = \{\mathcal{E}\varphi(t), 0, 0\}, \quad \mathbf{B}(t') = 0, \quad t = \omega t' \quad (11.1)$$

was comprehensively investigated for  $\varphi(t) = \cos t$  (see Refs [135–140]). Here,  $t'$  is the time,  $t$  is the dimensionless time,  $\mathcal{E}$  and  $\omega$  are the amplitude and characteristic frequency of the external electric field, while the function  $\varphi(t)$  defines the laser pulse shape. For simplicity it will be assumed that  $\varphi(-t) = \varphi(t)$  and  $|\varphi(t)| \leq \varphi(0) = 1$  for  $-\infty < t < \infty$  (the electric field attains its peak for  $t = 0$ , and at this instant  $e^+$  and  $e^-$  escape through the barrier [136]). It is assumed that  $\varphi(t)$  is an analytical function, which is required for the validity of the ITM.

With the aid of the ITM we describe the sub-barrier electron motion through the gap  $2mc^2$  between the upper and lower continua to obtain the production probability for a  $e^\pm$  pair with the momenta  $\pm \mathbf{p}$ :

$$w(\mathbf{p}) = \frac{d^3 W}{d^3 p^3} \propto \exp \left\{ -\frac{\pi}{\epsilon} \left[ \tilde{g}(\gamma) + \tilde{b}_1(\gamma) \frac{p_{\parallel}^2}{m^2} + \tilde{b}_2(\gamma) \frac{p_{\perp}^2}{m^2} \right] \right\}, \quad (11.2)$$

where  $\epsilon = \mathcal{E}/\mathcal{E}_{\text{cr}}$  is the reduced electric field,  $\mathcal{E}_{\text{cr}} = m_e^2 c^3 / e\hbar$ ,  $K_0 = 2m_e c^2 / \hbar\omega$  is the multiquantumness of the process and  $\gamma$  is the adiabaticity parameter:

$$\gamma = \frac{\omega}{\omega_t} = \frac{m_e c \omega}{eF} = \frac{\hbar\omega}{eF\lambda_e} = \frac{2}{K_0 \epsilon}. \quad (11.3)$$

Here,  $\omega_t = e\mathcal{E}/m_e \sim 1/T_t$ ,  $\lambda_e = \hbar/m_e c$ ,  $T_t$  is the characteristic tunneling time,  $T_t \sim b/c$ , and  $b = 2m_e c^2 / e\mathcal{E}$  is the barrier width. Hereinafter we assume that

$$\epsilon \ll 1, \quad K_0 \gg 1, \quad b \gg \lambda_e, \quad (11.4)$$

and the value of  $\gamma$  may be arbitrary in this case.

The function  $\tilde{g}(\gamma)$  appearing in expression (11.2) and the coefficients  $\tilde{b}_{1,2}(\gamma)$  of the momentum spectrum are determined by the shape of the field pulse  $\varphi(t)$ . The total  $e^\pm$ -pair production probability in the invariant Compton four-volume  $\lambda_e^4/c \approx 7.25 \times 10^{-53} \text{ cm}^3 \text{ s}$  (hereinafter  $\hbar = c = 1$ ) is obtained by integrating the expression (11.2) with respect to  $d^3 p$  with an account for the energy conservation law in the course of  $n$ -photon absorption. The corresponding formulas (rather cumbersome) can be found in Ref. [137].

Here, we restrict ourselves to the limiting cases of small and large  $\gamma$ . The former (low-frequency radiation,  $\hbar\omega \ll mc^2$ ) relates to the adiabatic domain:

$$w = c_1 m^4 \epsilon^{5/2} \exp \left[ -\frac{\pi}{\epsilon} \tilde{g}(\gamma) \right], \quad \gamma \ll 1, \quad (11.5)$$

where  $c_1 = 2^{-3/2} \pi^{-4} = 3.63 \times 10^{-3}$ ,

$$\begin{aligned} \tilde{g}(\gamma) &= 1 - \frac{1}{8} \gamma^2 + \frac{3}{64} \gamma^4 + \dots, \\ \tilde{b}_1 &= \frac{1}{2} \gamma^2, \quad \tilde{b}_2 = 1 - \frac{1}{4} \gamma^2. \end{aligned} \quad (11.6)$$

<sup>19</sup> Such a field, in principle, is formed at an antinode of a standing light wave, which results from the superposition of two coherent laser beams.

**Table 4.** Laser-driven  $e^+e^-$ -pair production from a vacuum.

$\lambda$ , nm	$\hbar\omega$ , eV	$N = 1$ ( $\mathcal{E}_{\text{th}}$ )	$N = 10^3$	$N = 10^6$	$N = 10^9$	Laser type
106(4)	0.117	0.739 0.481	0.838 0.521	0.967 0.570	1.14 0.627	CO <sub>2</sub>
1064(3)	1.165	0.873 0.521	1.02 0.570	1.21 0.628	1.49 0.698	Nd:YAG
785	1.580	0.899 0.527	1.05 0.577	1.25 0.636	1.56 0.707	Ti:Sa
694	1.786	0.912 0.530	1.06 0.58	1.27 0.64	1.59 0.71	Ruby
109	11.4	1.07 0.569	1.29 0.627	1.61 0.697	2.13 0.785	FEL
25	49.6	1.26 0.61	1.56 0.67	2.04 0.75	2.91 0.86	—

*Note.* Given in the table are the magnitudes of the electric field  $\mathcal{E}$  (in units of  $10^{15} \text{ V cm}^{-1}$ ) at which  $N$  pairs are produced in the focal volume  $V = \lambda^3$  during one field cycle (first line) and during 1 s (second line, for given values of  $\lambda$  and  $N$ ). The threshold field  $\mathcal{E}_{\text{th}}$  is sufficient for the production of one pair.

The numerical coefficients of these expansions correspond to the monochromatic laser field  $\varphi(t) = \cos t$ . In this case, the transverse (to the field) momentum  $e^\pm$  is always nonrelativistic:  $p_{\perp} \sim \sqrt{e\mathcal{E}} = m\sqrt{\epsilon} \ll m$ , but their longitudinal momentum  $p_{\parallel} \sim \gamma^{-1} p_{\perp} \sim K_0 \epsilon^{3/2} m$  may become relativistic when  $\gamma \lesssim \sqrt{\epsilon}$ .

In the other limiting case ( $\gamma \gg 1$ ) we obtain

$$\begin{aligned} \tilde{g}(\gamma) &= \frac{4}{\pi\gamma} \left[ \left( 1 + \frac{1}{4\gamma^2} \right) \ln \gamma + 0.386 \right], \\ \tilde{b}_1 &= \frac{2}{\pi\gamma} (\ln \gamma + 0.386), \quad \tilde{b}_2 = \frac{2}{\pi\gamma} (\ln \gamma + 1.39), \end{aligned} \quad (11.7)$$

and the pair production probability  $w$  is equal to the sum of the probabilities of  $n$ -photon processes  $w_n$ ,  $n > K_0$ . In this case,  $w_{n+1}/w_n \sim \gamma^{-2n} \ll 1$  and

$$w = \sum_{n=K_0}^{\infty} w_n \approx c_2 m^4 \left( \frac{\omega}{m} \right)^{5/2} \left( \frac{4\gamma}{e} \right)^{-2K_0}, \quad e = 2.718\dots, \quad (11.8)$$

where  $c_2 = (\sqrt{2}\pi)^{-3} = 0.0114$ .

The magnitudes of the threshold field  $\mathcal{E}_{\text{th}}$  required for the production of one  $e^+e^-$  pair in the volume<sup>20</sup>  $V = \lambda^3$  during one period  $T = 2\pi/\omega$  are collected in Table 4, where  $\lambda = 2\pi c/\omega$  is the wavelength and  $\mathcal{E}_{\text{th}}$  is measured in units of  $10^{15} \text{ V cm}^{-1}$ . The threshold for observing the Schwinger effect for infrared and optical lasers is reached at  $\mathcal{E} = (0.7-1.0) \times 10^{15} \text{ V cm}^{-1}$ , which is lower than  $\mathcal{E}_{\text{cr}}$  by one and a half orders of magnitude. For  $\mathcal{E} > \mathcal{E}_{\text{th}}$ , the number of pairs produced rises quite rapidly, which is evident from Fig. 21.

In the  $\gamma \gtrsim 1$  domain, the functions in expression (11.2) exhibit a strong dependence on the pulse shape  $\varphi(t)$ . Formulas similar to formula (4.2) hold; in particular [137, 140],

$$\tilde{g}(\gamma) = \frac{4}{\pi} \int_0^1 \chi(\gamma u) \sqrt{1-u^2} du = \frac{4}{\pi} \int_0^{\pi/2} \chi(\gamma \sin \theta) \cos^2 \theta d\theta, \quad (11.9)$$

<sup>20</sup> The diffraction limit for focusing the laser radiation with a wavelength  $\lambda$ .

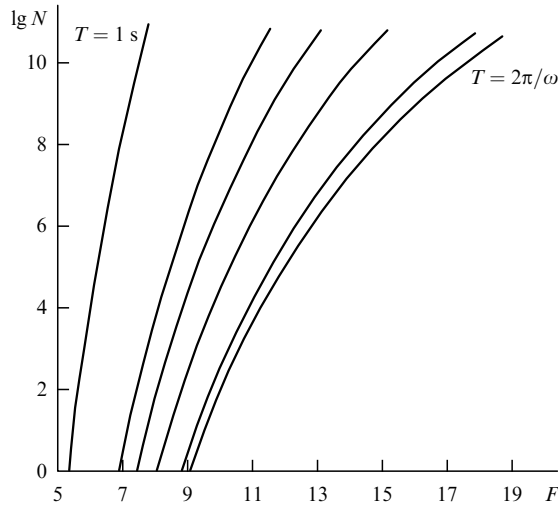


**Figure 21.** Number of electron – positron pairs  $N$  produced from a vacuum in the focal volume  $\lambda^3$  by the field of a Ti:Sapphire laser with a pulse duration  $T = 2/6$  fs (one field cycle), 10 fs, 1 ps, 100 ps, 10 ns, and 1 s (curves, from right to left).

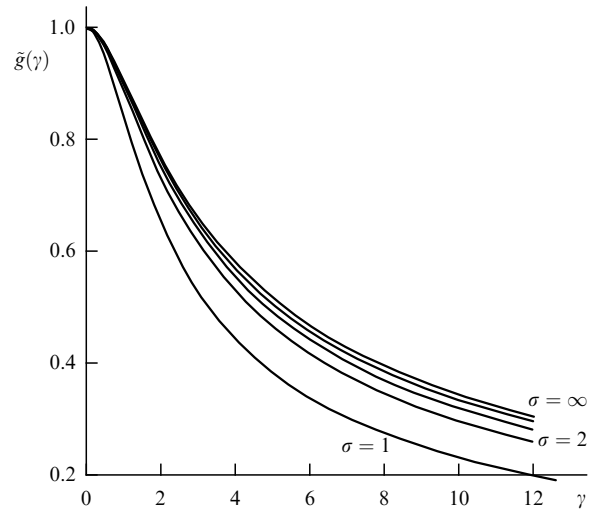


**Figure 22.** Function  $\tilde{g}(\gamma)$  for a modulated laser pulse of the form (4.5).

$\chi(u)$  being the same function as in the multiphoton ionization theory [see formula (4.2)].

In the case of monochromatic field,  $\chi(u) = 1/\sqrt{1+u^2}$ ,

$$\begin{aligned} \tilde{g}(\gamma) &= \frac{4}{\pi\sqrt{1+\gamma^2}} \mathbf{D}(v), & \tilde{b}_1(\gamma) &= \frac{2\gamma^2}{(1+\gamma^2)^{3/2}} \mathbf{D}(v), \\ \tilde{b}_2(\gamma) &= \frac{2}{\pi\sqrt{1+\gamma^2}} \mathbf{K}(v), & v &= \frac{\gamma}{\sqrt{1+\gamma^2}}, \end{aligned} \quad (11.10)$$

where  $\mathbf{K}$  and  $\mathbf{D}$  are complete elliptic integrals of the first and third kinds [135, 136]. Hence, there follow the asymptotics (11.5)–(11.7).

Another example is the soliton-like pulse  $\varphi(t) = 1/\cosh^2 t$ , for which  $\chi(u) = (1+u^2)^{-1}$ ,

$$\tilde{g}(\gamma) = \frac{2}{1+\sqrt{1+\gamma^2}}, \quad \tilde{b}_1 = \frac{\gamma^2}{(1+\gamma^2)^{3/2}}, \quad \tilde{b}_2 = \frac{1}{\sqrt{1+\gamma^2}}, \quad (11.11)$$

which is, in the quasiclassical limit (11.4), consistent with the exact solution obtained in Ref. [141]. The function  $\tilde{g}(\gamma)$  for the modulated pulse (4.5) is plotted in Fig. 22. Its  $\gamma$ -dependence is similar to the function  $g(\gamma)$  in the nonrelativistic ionization theory, but the adiabaticity parameter  $\gamma$  is different in the order of magnitude in these two cases.

In all cases considered,  $\tilde{g}(\gamma)$  decreases monotonically with  $\gamma$  and the probability  $w$  rises sharply (for a fixed field amplitude  $\mathcal{E}$ ). This effect shows up in the high-frequency domain  $\omega > \omega_t$  and is referred to [140] as the dynamic Schwinger effect. In recent years, the possibility of experimental observation of the Schwinger effect has become a question of considerable interest [116, 142–145].

A uniform electric field of the form (11.1) is an idealization, which overrates the number of resultant pairs  $N$ . A real wave always contains a magnetic field, which reduces  $N$  (in a purely magnetic field, as in a plane wave in a vacuum, the pairs are not produced at all [119]). Bulanov et al. [145] considered a realistic three-dimensional model of a focused laser pulse reliant on the exact solution of the Maxwell

equations derived by Narozhnyi and Fofanov [146]. Numerical integration of expression (11.5) over the entire four-momentum volume allowed studying the dependence of the resultant  $e^+e^-$ -pair number  $N$  on the parameters of the problem:  $R$  (the focal spot radius),  $L = R/\Delta$  (the diffraction length), and  $\Delta = c/\omega R = \lambda/2\pi R$  (the focusing parameter, which characterizes the difference of the laser pulse from a plane wave). The dependence of  $N$  on the peak radiation intensity  $J$  is extremely sharp: for instance, varying  $J$  from  $8 \times 10^{27}$  to  $3 \times 10^{28} \text{ W cm}^{-2}$ , i.e., only by a factor of four, increases the number of  $e^+e^-$  pairs produced by a single pulse from  $N = 0.03$  to  $N = 6 \times 10^9$  (for  $\Delta = 0.1$ ).

Recent years have seen rapid progress in shortening the wavelength  $\lambda$  of laser radiation and increasing its intensity  $J$  [116]. The values  $J \gtrsim 10^{21} \text{ W cm}^{-2}$  have already been achieved, which exceeds the atomic field  $\mathcal{E}_a$  by two orders of magnitude. Increasing further the power of infrared and optical lasers is supposedly the most promising way towards the experimental observation of the Schwinger effect.

Furthermore, there are projects to develop free-electron X-ray lasers, which are executed in DESY and SLAC [143]. When these lasers with  $\hbar\omega \gtrsim 1 \text{ keV}$  are commissioned and if their radiation is possible to focus in a diffraction-limited volume on the order of  $\lambda^3$ , the minimal laser power  $P$  required for the observation of the Schwinger effect will become significantly lower, because  $\mathcal{E} \sim \sqrt{P}/\lambda$ . In particular, for  $\lambda = 0.1 \text{ nm}$  and a pulse duration  $T = 0.1 \text{ ps}$ , the power  $P_{\min} \sim 10^{16} \text{ W}$  would be high enough for the production of one  $e^+e^-$  pair in a vacuum [143]. This power level has long been reached in optics, but the transition to the X-ray region calls for the solution of a number of difficult problems. These possibilities are now being discussed.

For charged particles other than  $e^\pm$ , it will hardly ever be possible to observe the Schwinger effect in a laboratory, because  $\mathcal{E}_{\text{cr}} \propto m^2$  and even for  $\pi$ -mesons it assumes a fantastic value of  $\sim 10^{21} \text{ W cm}^{-1}$ . However, the dispersion law in solid-state physics, in particular for semiconductors, can be approximately written as

$$\epsilon(p) = \Delta \sqrt{1 + \frac{p^2}{m_* \Delta}}, \quad (11.12)$$

where  $m_*$  is the effective mass and  $\Delta$  is the width of the gap separating the valence band from the conduction band. This expression formally possesses the same form as the expression for a free particle in relativistic mechanics:  $\epsilon(p) = \sqrt{m^2 + p^2}$ . That is why the results outlined above may be employed in the theory of multiphoton ionization of semiconductors by a laser pulse (for monochromatic light this has already been done in Ref. [1]). Since the part of the Schwinger field  $\mathcal{E}_{\text{cr}}$  is played here by the fields on the order of  $10^6 - 10^7$  V cm $^{-1}$ , the corresponding effects are much easier to investigate in experiments.

## 12. Conclusion

Let us make several concluding remarks.

**1. On the saddle-point technique and ITM.** According to Ref. [1], the ionization rate  $w_0$  is determined by the matrix element

$$V_{0\mathbf{p}} = \int \psi_{\mathbf{p}}^*(e\vec{\mathcal{E}}\mathbf{r}) \psi_0 d^3r, \quad (12.1)$$

where  $\psi_0(r) = \pi^{-1/2} \exp(-r)$  for the ground state of the hydrogen atom and  $\psi_{\mathbf{p}}$  is the Volkov [2] wave function of a free electron in the external field  $\vec{\mathcal{E}}(t) = \vec{\mathcal{E}}_0 \cos \omega t$ :

$$\begin{aligned} \psi_{\mathbf{p}}(\mathbf{r}, t) &= \exp \left\{ i \left[ \mathbf{Pr} - \frac{1}{2} \int_0^t \mathbf{P}^2(t') dt' \right] \right\}, \\ \mathbf{P}(t) &= \mathbf{p} + \frac{e\vec{\mathcal{E}}_0}{\omega} \sin \omega t. \end{aligned} \quad (12.2)$$

The expression for  $w_0$  comes out in the form of the sum of  $n$ -photon event probabilities, each of which contains the square of a rapidly oscillating integral (see formulas (14) and (15) in Ref. [1]). Applying the saddle-point technique gives the equation for the saddle points in the complex plane,

$$\begin{aligned} I_0 + \frac{1}{2} \left( \mathbf{p} + \frac{e\vec{\mathcal{E}}_0}{\omega} \sin \omega t \right)^2 &= 0, \quad I_0 = \frac{\kappa^2}{2}, \\ \sin \omega t_0 &= i\gamma\kappa^{-1} \left( \sqrt{\kappa^2 + p_{\perp}^2} + ip_{\parallel} \right) \end{aligned} \quad (12.3)$$

( $I_0$  is the ionization potential; for the  $1s$  level,  $\kappa = 1$ ), or

$$\begin{aligned} t_0 &= i\omega^{-1} \left\{ \operatorname{arcsinh} \gamma \right. \\ &\quad \left. + \frac{\gamma}{\sqrt{1+\gamma^2}} \left[ i \frac{p_{\parallel}}{\kappa} + \frac{1}{2\kappa^2} \left( \frac{\gamma^2}{1+\gamma^2} p_{\parallel}^2 + p_{\perp}^2 \right) \right] + O\left(\frac{p^3}{\kappa^3}\right) \right\}, \end{aligned} \quad (12.4)$$

which coincides exactly with the expression for the initial instant  $t_0$  of sub-barrier electron motion in the ITM [5]. These equations define the complex points  $t_0$  at which there occurs a transition from the bound state to the state described by the Volkov function (12.2). The contribution of a point  $t_0$  to the tunneling amplitude is [1], with an exponential accuracy

$$A_0 \propto \exp \left\{ \frac{i}{2\omega} \int_0^{\sin \omega t_0} \left[ \kappa^2 + \left( \mathbf{p} + \frac{e\vec{\mathcal{E}}_0}{\omega} v \right)^2 \right] \frac{dv}{(1-v^2)^{1/2}} \right\}. \quad (12.5)$$

It is easy to verify that this integral coincides with the imaginary part of the action function  $W(t_0, 0)$ , which leads to formula (2.1) when expression (12.5) is expanded in powers

of  $\mathbf{p}$  up to the second order inclusive [similar to expression (12.4)]. Therefore, as regards the exponential factor, both methods lead to the same result and are equivalent.<sup>21</sup> This conclusion, which was demonstrated by the above example of monochromatic light, is valid in the general case as well. In this connection, note that for pulses of the form  $\varphi(t) = 1/\cosh^2 t$  and  $(1+t^2)^{-1}$ , the corresponding exponents in the expression for  $w_0$  calculated [70, 71] independently by the two above techniques coincide [to within the accuracy of the quasiclassical approximation itself, i.e., for instance,  $\cosh S \approx (1/2) \exp S$  when  $S \gg 1$ ].

**2.** The question of the pre-exponent, however, arises, which we first discuss using the example of a constant electric field,  $\omega = 0$ . This problem was first considered and solved in the framework of quantum mechanics by Oppenheimer [147]. In this case, the wave function of the final state  $\psi_{\mathbf{p}}(\mathbf{r})$  can be expressed in terms of the Airy function [16, 20]. In Ref. [147],

$$w_0(\mathcal{E}) = 0.1093\mathcal{E}^{1/4} \exp \left( -\frac{2}{3\mathcal{E}} \right) \quad (12.6)$$

was obtained. Subsequently, however, it became clear that an error was made in the calculations of Ref. [147] ('a slight computational error'; see the remark on p. 885 in Ref. [148]). Upon correction it turns out that [148]

$$w_0(\mathcal{E}) = \frac{\pi}{2} \exp \left( -\frac{2}{3\mathcal{E}} \right), \quad (12.7)$$

but this formula is not correct, either. To the best of our knowledge, the correct asymptotics of  $w_0$  in a weak field for the  $1s$  level was first obtained by Landau and Lifshitz [149]:

$$w_0(\mathcal{E}) = 4\mathcal{E}^{-1} \exp \left( -\frac{2}{3\mathcal{E}} \right), \quad \mathcal{E} \rightarrow 0. \quad (12.8)$$

The ITM [8] with the inclusion of the Coulomb correction [6] leads to the same result. Collected in Table 1 in Ref. [148] is an impressive list of erroneous (in the pre-exponent) formulas for different states of the hydrogen atom published in the literature. Generally speaking, the asymptotics for  $w = -2 \operatorname{Im} E_{n_1 n_2 m}(\mathcal{E})$  in weak fields is of the form

$$w_{n_1 n_2 m}(\mathcal{E}) = C_{n_1 n_2 m} \exp \left( -\frac{2}{3n^3 \mathcal{E}} \right) \mathcal{E}^{-(2n_2 + |m| + 1)} [1 + O(\mathcal{E})], \quad (12.9)$$

where  $n_1$ ,  $n_2$ , and  $m$  are parabolic quantum numbers [16] and  $n = n_1 + n_2 + |m| + 1$  is the principal quantum number of the level. For the ground state ( $n_1 = n_2 = m = 0$ ) this formula turns into formula (12.8).

The exponential factors in expressions (12.6)–(12.8) coincide with one another, but the pre-exponents are significantly different. Therefore, a formula like (12.1) does not give the correct pre-exponent. The reason is clear enough: the external field  $\mathcal{E}$  is exactly taken into account in  $\psi_{\mathbf{p}}$ , but the Coulomb interaction between the outgoing electron and the nucleus (proton) is neglected. Since the method of calculation used in Ref. [1] is in essence the generalization of the Oppenheimer method to the case of variable field  $\mathcal{E}(t)$ , it is supposedly beyond reason to expect that the correct pre-

<sup>21</sup> Although the ITM is, in our view, physically more clear.

exponent in the probability  $w(\mathcal{E}, \omega)$  can be obtained in this case.

On the other hand, for  $Z = 0$  (the short-range potential) and  $\mathcal{E}(t) = \mathcal{E}_0 \cos \omega t$  the ITM leads to the same result as solving the Schrödinger equation with the saddle-point technique used at only the final stage of calculations [5]. In this case, not only the exponents, but also the expressions for the photoelectron momentum and energy spectra and the pre-exponential factors coincide [5, 8]. The same is generally true of elliptic polarization and arbitrary  $\gamma$  (compare formulas (23)–(28) of Ref. [5] with formulas (40)–(43) in Ref. [8]). Finally, in the problem of pair production by an electric field the ITM agrees [137] with the exact solution derived [141] for  $\mathcal{E}(t) = \mathcal{E}_0 / \cosh^2 \omega t$ . These facts, even if they do not furnish rigorous proof, nevertheless definitely count in favor of ITM validity and, in particular, show that the ITM may be used validly to calculate the pre-exponent. An attempt to substantiate the ITM (at the physical level of rigor) was undertaken in Ref. [121].

3. The extremal [8] sub-barrier path for a linearly polarized field  $\mathcal{E}(t)$  corresponds to the momentum  $\mathbf{p} = 0$  on escape from the barrier. For this path,  $t_0$  and the ‘time’  $t$  in the sub-barrier motion are purely imaginary (hence the origin of the name ITM). For the neighboring trajectories with  $p_{\parallel} \neq 0$ , the initial point  $t_0$  shifts from the imaginary time axis, but, as is evident from expression (12.4), this shift is small for all  $\gamma$ .

For a periodic field, for instance,  $\mathcal{E}_0 \cos \omega t$ , to every half-period there corresponds a saddle point of its own,  $t_k$ . Their contributions  $A_k$  to the transition amplitude are similar in magnitude, but are different in phase for  $p_{\parallel} \neq 0$  (because  $t_{k+1} - t_k \neq \pi\omega^{-1}$  due to the above-mentioned shift of the saddle points). The coherent composition of the amplitudes  $A_k$  is responsible for rapid oscillations in the photoelectron momentum spectrum, which was first noted in Ref. [5] [see formula (53) in this paper]. More recently, these oscillations were discussed in Refs [35, 70, 71]. At present, they are being investigated in experiment [43].

4. The case of negative-ion ( $Z = 0$ ) ionization is especially convenient for the experimental verification of the Keldysh theory. In Refs [150, 151], measurements were made of the photoelectron momentum distribution in the ionization of  $\text{H}^-$  and  $\text{F}^-$ . The energy spectra and the angular distributions agree nicely with the results of calculations by the formulas of Ref. [35] (which, in contrast to the formulas of Ref. [5], do not use the expansion of  $\text{Im } W$  in powers of  $\mathbf{p}^2$ ). It is pertinent to note that for a long time measurements were made only of the total photoelectron yield, although multiphoton ionization of atoms was observed as far back as the 1960s [22]. The spectrum of above-threshold ionization was first observed in Ref. [152], whose publication fostered numerous theoretical and experimental investigations in this area.

5. Remarkable advances have been made in laser physics and technology during the 40 years that have elapsed since the advent of Ref. [1]. At present, the investigations of nonlinear photoionization of atoms and ions constitute a vast and rapidly developing domain of atomic physics. In the 1960s, which saw the publication of the first theoretical papers in this field, it was hard to imagine that such subtle features of laser-induced atomic photoionization as the photoelectron momentum and angular distribution and quantum tunnel interference in the energy spectrum would become the subjects of comprehensive experimental studies. But, however, this has already happened! Further significant advances in this area would be expected to occur, including, for

instance, investigations of the structure and dynamics of molecules and clusters, solution of applied problems of quantum chemistry, or controlling molecular processes in a strong laser field [153].

Naturally, in the context of a relatively brief review it is impossible to comprehensively discuss the numerous applications and generalizations of the Keldysh theory. Our aim was to recall the early papers [1, 4–8], which have not lost their significance even now, to outline several new results obtained in the elaboration of ideas proposed in Ref. [1], including the relativistic ionization theory and the Schwinger effect in a varying electric field, and to briefly compare the Keldysh theory with experiment. It is beyond question that the pioneering work by Keldysh will long underlie the theoretical description of tunnel and multiphoton ionization effects in atomic and laser physics.

This review has its origin in the papers which the author reported at the 3rd International Sakharov Conference on Physics (Moscow, June 2002), the 11th JST International Symposium (Tokyo, September 2002), the International Conference ‘‘I Ya Pomeranchuk and Physics at the Turn of Centuries’’ (Moscow, January 2003), the 31st Winter School of the Institute of Theoretical and Experimental Physics (February 2003), and the XVIIth Conference ‘Basic Atomic Spectroscopy’ (Zvenigorod, December 2003).

The author is deeply grateful to L V Keldysh for stimulating discussions, the opportunity to see the manuscript of Ref. [70], and helpful comments on the contents of the present paper. I would like to express my sincere gratitude to S V Bulanov, S P Goreslavskii, K S Ikeda, B M Karnakov, V D Mur, A I Nikishov, L B Okun’, and S V Popruzhenko for fruitful discussions at different stages of this work and their advice, which I took into consideration as far as possible, as well as to S G Pozdnyakov for performing numerical calculations and to M N Markina for her unflinching assistance in the preparation of the manuscript.

This work was supported in part by the Russian Foundation for Basic Research (Projects Nos 01-02-16850 and 04-02-17157).

## 13. Appendices

### 13.1 Asymptotic coefficients for atoms and ions

Assuming that the atomic potential is  $U(r) \approx -Z/r$  for  $r \gg r_c$ , from the Schrödinger equation we obtain the asymptotics of the radial wave function at infinity:

$$\chi_{\kappa l}(r) \approx 2\kappa^{1/2} C_{\kappa l} e^{-\kappa r} (\kappa r)^v \left[ 1 - \frac{(v+l)(v-l-1)}{2\kappa r} + \dots \right],$$

$$r \gg \frac{1}{\kappa}, \quad (13.1.1)$$

where  $v = Z/\kappa \equiv n^*$  and the normalization condition is of the form  $\int_0^\infty \chi_{\kappa l}^2(r) dr = 1$ . The asymptotic coefficients  $C_{\kappa l}$  are frequently encountered in atomic and nuclear physics, the inverse problem of quantum scattering theory, etc. [13–17]. Their values are determined by solving the Hartree–Fock equations, the inaccuracy of numerical calculations for certain multielectron atoms and ions (for instance, for Ne, K, Ca, Rb,  $\text{Li}^-$ ,  $\text{K}^-$ , and so forth) ranging up to 10–30% or more [14].

According to Hartree [11], an approximate value of  $C_{\kappa l}$  is given by formula (2.7), its inaccuracy for the first  $s$  and  $p$  levels

in the rubidium atom amounting [11] to 2–2.5% (see also Table 1). When  $n^* \gg 1$  and  $l \sim 1$ , formula (2.7) takes on the form

$$C_{\kappa l} \approx \frac{1}{\sqrt{8\pi n^*}} \left(\frac{2e}{n^*}\right)^{n^*} \left(1 - \frac{l(l+1)}{2n^*} + \dots\right), \quad e = 2.718\dots \tag{13.1.2}$$

Recently, Mur et al. [19] obtained an effective radius expansion for these coefficients; for the  $s$  states, it has the form

$$C_{\kappa} = C_{\kappa}^{(0)} [1 - c_1 \kappa r_{cs} + O((\kappa r_{cs})^3)]^{-1/2}, \tag{13.1.3}$$

where

$$C_{\kappa}^{(0)}(v) = C_{\kappa}^H f(v), \quad c_1(v) = \frac{1}{2} \left[ \frac{\sin \pi v}{\pi v} f(v) \right]^2, \tag{13.1.4}$$

$$f(v) = \left\{ 1 - \left( \frac{\sin \pi v}{\pi v} \right)^2 \left[ v^2 \psi'(v) - \left( v + \frac{1}{2} \right) \right] \right\}^{-1/2},$$

$C_{\kappa}^H$  is the Hartree coefficient (2.7) for  $l = 0$ ,  $\psi(v) = \Gamma'(v)/\Gamma(v)$  is the logarithmic derivative of the gamma function, and  $r_{cs}$  is the effective nuclear-Coulombian [154] radius of the system. To the purely Coulombian spectrum ( $r_{cs} = 0$ ,  $v = n = 1, 2, \dots$ ) there correspond the values  $C_{\kappa}^{(0)} = C_{\kappa}^H = 2^{n-1}/n!$  and  $c_1 = 0$ , with  $C_{\kappa}^{(0)} = 1$  for the ground level.

In the atomic spectral domain ( $v \gtrsim 1$ ), the coefficients  $C_{\kappa}^{(0)}$  and  $C_{\kappa}^H$  are close while  $c_1(v)$  are numerically small, and therefore the correction for the effective radius can be ignored here [19]. This serves as a substantiation of the Hartree formula.<sup>22</sup> On the other hand, for  $v \rightarrow 0$  (the passage to the limit of a short-range potential) the expansion assumes the form

$$\frac{1}{2C_{\kappa}^2} = 1 - \kappa r_s + c_3 (\kappa r_s)^3 + \dots, \quad Z = 0, \tag{13.1.5}$$

or

$$C_{\kappa} = \frac{1}{\sqrt{2}} \left[ 1 + \frac{1}{2} \kappa r_s + \frac{3}{8} (\kappa r_s)^2 - \frac{1}{2} \left( c_3 - \frac{5}{8} \right) (\kappa r_s)^3 + \dots \right], \tag{13.1.5'}$$

where  $r_s = \lim_{Z \rightarrow 0} r_{cs}$  is the effective radius for the short-range potential. A few remarks are quite in order.

1. The quadratic terms in the effective radius are absent in the expansions for  $1/C_{\kappa}^2$ . This fact is nontrivial, because the Coulomb wave function for  $r \rightarrow 0$  and a non-integer  $v$  contains terms of the order [154, 155]  $r \ln r$ ,  $r^2 \ln r$ ,  $r^2$ , and  $r^3 \ln r$ , which mutually annihilate upon sewing together the outer and inner wave functions at the point  $r = r_c \ll a_B$ .

2. The first correction  $\propto r_{cs}$  (or  $r_s$ ) is independent of the form of potential for  $r < r_c$ . Calculations of the  $c_3$  coefficient for several model potentials showed [19] that it is numerically small, which broadens the domain of applicability of expansions (13.1.3) and (13.1.5).

3. For  $v = 0$ , the coefficient  $c_1 = 1$ , i.e., is two or three orders of magnitude greater than for  $v \gtrsim 1$  (see Table 1), and therefore the correction for the effective radius for negative ions is more significant than for neutral ions [108].

<sup>22</sup> Another substantiation of the Hartree formula was obtained with the aid of the quantum defect method [17, 18].

4. The asymptotic coefficients  $A$  given in reference book [14] are related to our coefficients as

$$A = 2\kappa^{v+1/2} C_{\kappa l}, \quad v = \frac{Z}{\kappa}, \tag{13.1.6}$$

the scatter of  $C_{\kappa}$  being substantially smaller than in the case of coefficients  $A$ . This formula was employed to calculate the numerical values of  $C_{\kappa}$  (see Table 1, the HF column).

### 13.2 The Keldysh function and its expansions

The frequency dependence of the ionization rate of an atom is determined primarily by the function  $f(\gamma, \xi)$  [see formulas (2.1) and (3.4)]. This function, which was first calculated in Ref. [1] for  $\xi = 0$  and in Ref. [5] for an arbitrary ellipticity  $\xi$ , will be referred to as the Keldysh function. We give the expansion terms next to expression (2.2); in this case, it is convenient to proceed from the representation (4.2). For  $\xi = 0$  we have

$$f(\gamma) = \sum_{n=0}^{\infty} (-1)^n f_n \gamma^{2n+1},$$

$$f_n = \frac{2}{3} g_n = \frac{(2n-1)!!}{n! 2^{n-1} (2n+1)(2n+3)}, \tag{13.2.1}$$

and similar series for the coefficients of the momentum spectrum  $c_{1,2}(\gamma)$ . Since  $f_n \propto n^{-5/2}$  for  $n \rightarrow \infty$ , the series converge for  $|\gamma| \leq 1$ . In the antiadiabatic domain,

$$f(\gamma) = \left( 1 + \frac{1}{2\gamma^2} \right) \ln \gamma + \sum_{n=0}^{\infty} a_n \gamma^{-2n}, \quad \gamma \rightarrow \infty, \tag{13.2.2}$$

where  $a_0 = \ln 2 - 1/2$ ,  $a_1 = \ln 2/2$ ,  $a_2 = 3/32$ ,  $a_3 = -5/192$ , and so on.

When  $\chi(u)$  is known in the analytical form, from expression (4.2) it is easy to obtain adiabatic expansions. In particular, putting

$$\chi(u) = (1 + u^2)^{-\rho}, \tag{13.2.3}$$

we obtain

$$f(\gamma) = \frac{2}{3} \gamma {}_2F_1 \left( \frac{1}{2}, \rho; \frac{5}{2}; -\gamma^2 \right),$$

$$f_n = \frac{2\Gamma(n+\rho)}{n!(2n+1)(2n+3)\Gamma(\rho)} \propto n^{\rho-3}, \tag{13.2.4}$$

and for  $\gamma \rightarrow \infty$

$$f(\gamma) \rightarrow \frac{\sqrt{\pi} \Gamma(\rho - 1/2)}{2\Gamma(\rho)}, \quad \rho > \frac{1}{2}, \tag{13.2.5}$$

while for  $\rho = 1/2$  the function  $f(\gamma)$  grows as  $\ln \gamma$ .

The shape of the field pulse corresponding to formula (13.2.3) is characterized by the asymptotics

$$\varphi(t) = 1 - \rho t^2 + \frac{1}{6} (7\rho^2 - 3\rho) t^4 + \dots, \quad t \rightarrow 0,$$

$$\varphi(t) \underset{t \rightarrow \infty}{\approx} \begin{cases} [2(\rho - 1)t]^{-\rho/(\rho-1)}, & \rho > 1, \\ 4 \exp(-2t), & \rho = 1, \end{cases}$$

with  $\varphi(t) = \cos t$ ,  $1/\cosh^2 t$ , and  $(1 + t^2)^{-3/2}$  corresponding to the values of  $\rho = 1/2$ , 1, and  $3/2$ , respectively. For an

arbitrary  $\varphi(t)$  we have the expansion

$$\chi(u) = 1 - \frac{1}{2} a_2 u^2 + \frac{5}{12} (a_2^2 - 0.1a_4) u^4 - \frac{7}{18} \left( a_2^3 - \frac{1}{5} a_2 a_4 + \frac{1}{280} a_6 \right) u^6 + \dots, \quad (13.2.6)$$

which gives, upon substitution into expression (4.2), the expansion of  $g(\gamma)$  and the coefficients of the momentum spectrum  $b_{1,2}(\gamma)$  in the adiabatic domain [here,  $a_n$  are the coefficients of the series (5.1)].

For the problem of pair production there exists formula (11.9), which is similar to expression (4.2). The expansion coefficients for  $f(\gamma)$  and  $\tilde{f}(\gamma)$  are therefore related as

$$\tilde{f}_n = \frac{4}{3\sqrt{\pi}} \frac{\Gamma(n+5/2)}{\Gamma(n+2)} f_n = \frac{(2n+3)!!}{(n+1)! 2^n \cdot 3} f_n, \quad (13.2.7)$$

this relation being valid for an arbitrary pulse shape  $\varphi(t)$ . In the asymptotics  $\tilde{f}_n \propto \sqrt{n} f_n, n \gg 1$ , and therefore the series for  $f(\gamma)$  and  $\tilde{f}(\gamma)$  possess the same radius of convergence.

The preceding formulas pertain to the case of linearly polarized radiation. For the case of elliptical polarization, the function  $f(\gamma, \xi)$  is defined by Eqns (3.5) and (3.6), which are simplified in the case of circular polarization:

$$\frac{\sinh 2\tau_0}{\tau_0} - \left( \frac{\sinh \tau_0}{\tau_0} \right)^2 = 1 + \gamma^2, \quad (13.2.8)$$

$$f_c(\gamma) = 2 \left[ \tau_0 - \frac{1}{2\gamma^2} (\sinh 2\tau_0 - 2\tau_0) \right],$$

where  $f_c(\gamma) \equiv f(\gamma, \xi = \pm 1)$ ; hence, it follows that

$$f_c(\gamma) = \frac{2}{3} \gamma \left( 1 - \frac{1}{15} \gamma^2 + \frac{13}{945} \gamma^4 - \frac{517}{127575} \gamma^6 + \dots \right), \quad \gamma \rightarrow 0, \quad (13.2.9)$$

$$f_c(\gamma) = \ln(\gamma \sqrt{\ln \gamma}) - \frac{1}{2} (1 - \ln 2) - \frac{1}{4 \ln \gamma} + \dots, \quad \gamma \rightarrow \infty. \quad (13.2.10)$$

The dependence of  $\tau_0(\gamma, \xi)$  and  $f(\gamma, \xi)$  on the ellipticity of light becomes significant on passing to the circular polarization, as is evident from Fig. 3.

The Keldysh function for the case of linear polarization can be written in the form similar to expressions (13.2.8):

$$f(\gamma, 0) = \tau_0 - \frac{1}{4\gamma^2} (\sinh 2\tau_0 - 2\tau_0), \quad (13.2.11)$$

where  $\tau_0 = \operatorname{arcsinh} \gamma$  [see Eqn (3.6) for  $\xi = 0$ ].

### 13.3 Remarks on the ‘ADK theory’.

Some authors compare the results of their experiments on tunnel ionization with the so-called<sup>23</sup> ‘ADK formulas’ or ‘ADK theory’ (Ammosov, Delone, Krainov [115]). We make several remarks here on this ‘theory’ and its relation to earlier papers.

In the case of the ionization of an  $s$ -level by low-frequency ( $\gamma \ll 1$ ) laser radiation with a linear polarization, formula

<sup>23</sup> These terms, which were introduced in Ref. [156], are quite frequently used in the literature, including by the authors themselves (see, for instance, Refs [50, 51, 132, 157]).

(2.5) is simplified:

$$w_a = \kappa^2 C_\kappa^2 \sqrt{\frac{3F}{\pi}} 2^{2n^*} F^{1-2n^*} \exp \left[ -\frac{2}{3F} \left( 1 - \frac{1}{10} \gamma^2 \right) \right], \quad (13.3.1)$$

and for the case of circular polarization,

$$w_a = \kappa^2 C_\kappa^2 2^{2n^*} F^{1-2n^*} \exp \left[ -\frac{2}{3F} \left( 1 - \frac{1}{15} \gamma^2 \right) \right], \quad \xi = \pm 1 \quad (13.3.2)$$

(here,  $l = 0, C_\kappa \equiv C_{\kappa 0}, F = \mathcal{E}/\kappa^3 \mathcal{E}_a$  is the reduced electric field, and  $\hbar = m = e = 1$ ). Specifically, for the ground state of the hydrogen atom,  $\kappa = n^* = 1, F \equiv \mathcal{E}$ , and the tunnel ionization rate (in atomic units) is

$$w_a = 4 \sqrt{\frac{3}{\pi \mathcal{E}}} \exp \left[ -\frac{2}{3\mathcal{E}} \left( 1 - \frac{1}{10} \gamma^2 \right) \right], \quad \xi = 0. \quad (13.3.3)$$

These formulas are asymptotically exact in the weak-field limit<sup>24</sup> like the well-known formula [16] for the ground state of the hydrogen atom in a constant electric field [see formula (12.8)].

We note that the factor  $\sqrt{3F/\pi}$  appearing in formula (13.3.1) for the case of linear polarization and absent in the case of circular polarization emerges due to the averaging of  $w_{st}(F(t))$  over a period of laser radiation subject to the condition  $\gamma \ll 1$  [see Eqn (3.20)]. This factor was derived in Ref. [5]. In this case, it was suggested that the asymptotic coefficients  $C_{\kappa l}$  from numerical calculations for a free ( $\mathcal{E} = 0$ ) atom be borrowed, for instance from tables like those in Ref. [14].

On the other hand, the ADK formula is written as follows [51, 156, 157]:

$$w_{\text{ADK}} = \sqrt{\frac{3n^{*3} \mathcal{E}}{\pi Z^3}} \frac{\mathcal{E} D^2}{8\pi Z} \exp \left( -\frac{2Z^3}{3n^{*3} \mathcal{E}} \right), \quad D = \left( \frac{4eZ^3}{n^{*4} \mathcal{E}} \right)^{n^*}, \quad (13.3.4)$$

where  $e = 2.718\dots, n^*$  is the effective principal quantum number of the level, and  $Z = 0, 1, 2, \dots$  is the atomic core charge. On passing to the variables

$$F = \frac{n^{*3} \mathcal{E}}{Z^3}, \quad \kappa = \frac{Z}{n^*} = \sqrt{\frac{I}{I_H}},$$

it is easily seen that the ADK formula differs from formula (13.3.1) in only the expression for the asymptotic coefficient  $C_\kappa$  and in that the correction  $\propto \gamma^2$  in the exponent is neglected:

$$w_{\text{ADK}} \equiv \kappa^2 (C_\kappa^{\text{ADK}})^2 \sqrt{\frac{3F}{\pi}} 2^{2n^*} F^{1-2n^*} \exp \left( -\frac{2}{3F} \right), \quad (13.3.5)$$

where<sup>25</sup>

$$C_\kappa^{\text{ADK}} = \frac{1}{\sqrt{8\pi n^*}} \left( \frac{2e}{n^*} \right)^{n^*} \quad (13.3.6)$$

<sup>24</sup> Special investigation is invited by the question: up to what values of  $F$  and with what accuracy can use be made of these asymptotics valid for  $F \rightarrow 0$ ? For the hydrogen atom it was carried out in Refs [72, 82] and for a short-range potential, in Ref. [105].

<sup>25</sup> The numerical values of  $C_\kappa^{\text{ADK}}$  usually exceed the exact coefficients  $C_\kappa$  by 10–15%. Specifically, for the ground state of the hydrogen atom,  $C_\kappa^2 = 1$  and  $(C_\kappa^{\text{ADK}})^2 = e^2/2\pi \approx 1.18$ ; the difference for the helium atom amounts to 47%, for potassium 30%, for cesium 35%, etc.

[compare with formula (13.1.2)]. Note that formula (13.3.6) follows directly from the Hartree formula<sup>26</sup>

$$C_{\kappa}^H = \frac{2^{n^*-1}}{\Gamma(n^*+1)}, \quad l=0, \quad (13.3.7)$$

if the Stirling approximation,  $\Gamma(n^*+1) \approx \sqrt{2\pi n^*} (n^*/e)^{n^*}$  is substituted for the gamma function in the Hartree formula. The generalization of formula (13.3.6) to the case of arbitrary  $l$  was given in Ref. [115] and results from expression (2.7), proposed by Hartree, with the use of the same Stirling formula,

$$\begin{aligned} C_{nl}^2 &= \frac{2^{2n-2}}{n\Gamma(n+l+1)\Gamma(n-l)} \rightarrow (C_{nl}^{\text{ADK}})^2 \\ &= \frac{1}{8\pi n} \left( \frac{4e^2}{n^2 - l^2} \right)^n \left( \frac{n-l}{n+l} \right)^{l+1/2} \end{aligned} \quad (13.3.8)$$

and the subsequent replacement of  $n$  and  $l$  with the effective quantum numbers  $n^*$  and  $l^*$ . This trivial transformation exhausts the original contribution of the authors of the ‘ADK theory’ compared to the earlier works [4, 5, 11]. Eventually, a rather cumbersome expression results for the ionization rate  $w$  (see Eqn (30) in Ref. [156], in which the term ‘ADK theory’ was introduced).

It is pertinent to note that the very notation for  $w$  in the form (13.3.4) is unnatural: the seemingly straightforward implication is that the main factor  $\exp(-2Z^3/3n^{*3}\mathcal{E})$  depends sharply on the charge of the atomic core  $Z$  and, moreover, the passage to the case  $Z=0$  (the ionization of negative ions like  $\text{H}^-$ ,  $\text{Na}^-$ , etc.) is not obvious. Meanwhile, this factor does not depend on  $Z$  whatsoever and is determined only by the bound-state energy  $E_0 = -\kappa^2/2$  (in which it is possible to include the Stark shift of the level) and the external electric field  $\mathcal{E}$ , which is easily seen even with the simplest one-dimensional model:

$$w \propto \exp\left(-2 \int_0^b \sqrt{\kappa^2 - 2\mathcal{E}x} dx\right) = \exp\left(-\frac{2\kappa^3}{3\mathcal{E}}\right), \quad (13.3.9)$$

where the barrier width is  $b = \kappa^2/2\mathcal{E} \gg \kappa^{-1}$ . The dependence on  $Z$  enters Eqns (13.3.1), (13.3.2) via  $n^* = Z/\kappa$  and begins (in the exponent) with the Coulomb correction  $2n^* \ln F$ , which is small in comparison with the principal term  $2/3F$  for  $F \ll 1$ . In the ADK formula (13.3.4), this fact is masked by the designation adopted in it, making it less clear. Moreover, this formula offers no computational advantages in comparison with formula (13.3.1). The latter actually is even simpler (with the understanding that the asymptotic coefficients  $C_{\kappa}$  are borrowed from Ref. [14] or similar tables) and is no less accurate. Therefore, one cannot agree with the statement that “the formulas obtained in Refs [4, 5] ... did not completely satisfy the demands of experiment. In Ref. [115], the formula derived in Ref. [5] was recast in the form most convenient for practical use in the cases of tunnel ionization of atoms and their multiply charged ions” (see Ref. [157], p. 228). The entire

‘recasting’ consisted of replacing the factorials in expressions (2.5), (2.7) with the Stirling approximation, which was done for no good reason (for the quantum numbers  $n$ ,  $l$  are ordinarily on the order of unity).

We also note that the photoelectron momentum distribution in the case of linear polarization [5] for  $\gamma \ll 1$  turns directly into formula (3.13) obtained by a separate calculation in Refs [48, 49]. The distribution (2.9) for circularly polarized radiation follows from the formulas in Refs [4, 5] valid for all values of  $\gamma$  and has already been written in explicit form (see Eqn (29'') in Ref. [4]). The Coulomb interaction was taken into account by employing the quasiclassical perturbation theory in Refs [49–51], the corresponding mathematical manipulation being a replication of Ref. [5]. Lastly, we note that formula (2.5) derived in Ref. [5] is valid for an arbitrary level of any atom and not exclusively for the hydrogen atom. Nor does it necessitate generalization with the aid of the quantum defect method – contrary to what is stated in Refs [51, 115].

Therefore, all results of the ‘ADK theory’ follow from the formulas of Refs [4–7], which are valid for arbitrary  $\gamma$ , in the special case  $\gamma \ll 1$ . However, this is not noted in Refs [50, 51, 156] or elsewhere, although Refs [4–7] are familiar to these authors and are occasionally cited by them but not concerning this point.

In summary, we enlarge on Refs [132, 133] concerned with the ‘semiclassical Dirac theory of tunnel ionization’. Reference [132] contains formula (8) for the ionization rate  $w_r$  of the ground state in constant crossed fields. This formula (which is considered [132] the ‘main result’ of this work) can be written in the form

$$w_r = \frac{mc^2}{\hbar} C_{\lambda}^2 P Q \text{Exp}, \quad (13.3.10)$$

where the factors Exp [see (10.8), (10.11)], the Coulomb factor  $Q$ , and the pre-exponent  $P$  are identically equal to the expressions previously obtained in Refs [4, 129–131] and the coefficient  $C_{\lambda}^2$  can be found in any textbook on quantum mechanics [120, 127].

Neither the spin factor (10.14) in the tunneling probability, nor the correction of the order of  $\gamma^2$  in the exponent (10.11) were calculated in Ref. [132]. Nor was the adiabatic correction included [5], which changes the power of the field in the pre-exponent. Formula (8) of Ref. [132] might therefore bear relation only to the case of constant fields. However, in this case, too, the authors actually assume that the Dirac bispinor  $\hat{S}$ , which defines the electron polarization and is predetermined near the atomic nucleus, remains invariable in the course of sub-barrier motion (see formulas (1), (2), and (5) in Ref. [132]), which is wrong [128] [see formulas (10.14) and (10.15)]. The original contribution of the authors of Ref. [132] reduces to the multiplication of the factors Exp,  $Q$ , and  $P$  derived in the earlier works [4, 129–131], which is nowhere mentioned, though. In this case, the asymptotic coefficient  $C_{\lambda}^2$  refers to the spin  $s = 1/2$  and the spin correction to the action is not considered, and therefore formula (8) of Ref. [132] is physically senseless.

‘The main result’ of that paper is mere rewriting of the formulas from our papers with retention of the notation, including the passage from the energy level  $\epsilon = E_0/mc^2$  to the convenient auxiliary variable  $\xi$  (10.9) introduced in Ref. [129], which emerges in a natural way in the ITM. Added to this in Ref. [133] were the formulas of the relativistic theory of

<sup>26</sup> See Eqn (7.6) in Ref. [11], where formula (2.7) was derived from the analysis of the recurrence relations satisfied by the normalization integrals  $\int \chi_{n,l}^2(r) dr$  with the neighboring values of quantum numbers  $n^*$ ,  $n^* \pm 1$  in the Coulomb field distorted at short distances  $r \lesssim r_c$ . Subsequently, a more rigorous derivation of the Hartree formula (with an estimate of corrections to it) was made employing the quantum defect method [17, 18] and from the effective range expansion [19].

ionization by a constant electric field, which were entirely borrowed from Ref. [130] (compare, for instance, formula (35) in Ref. [133] with expressions (6) and (32) in Ref. [130]), the necessary references also missing from Ref. [133]. Considering this situation to be not only strange but also at contradiction with the elementary principles of scientific ethics, I would like to draw the attention of the scientific community to these facts.

## References

- Keldysh L V *Zh. Eksp. Teor. Fiz.* **47** 1945 (1964) [*Sov. Phys. JETP* **20** 1307 (1965)]
- Volkov D M *Z. Phys.* **94** 250 (1935); *Zh. Eksp. Teor. Fiz.* **7** 1286 (1937)
- Berestetskiĭ V B, Lifshitz E M, Pitaevskiĭ L P *Relyativistskaya Kvantovaya Teoriya* (Relativistic Quantum Theory) Pt. 1 (Moscow: Nauka, 1968) [Translated into English (Oxford: Pergamon Press, 1971)]
- Nikishov A I, Ritus V I *Zh. Eksp. Teor. Fiz.* **50** 255 (1966) [*Sov. Phys. JETP* **23** 162 (1966)]
- Perelomov A M, Popov V S, Terent'ev M V *Zh. Eksp. Teor. Fiz.* **50** 1393; **51** 309 (1966) [*Sov. Phys. JETP* **23** 924 (1966); **24** 207 (1967)]
- Perelomov A M, Popov V S *Zh. Eksp. Teor. Fiz.* **52** 514 (1967) [*Sov. Phys. JETP* **25** 482 (1967)]
- Nikishov A I, Ritus V I *Zh. Eksp. Teor. Fiz.* **52** 223 (1967) [*Sov. Phys. JETP* **25** 145 (1967)]
- Popov V S, Kuznetsov V P, Perelomov A M *Zh. Eksp. Teor. Fiz.* **53** 331 (1967) [*Sov. Phys. JETP* **26** 240 (1968)]; Preprint No. 517 (Moscow: Institute of Theoretical and Experimental Physics of the USSR Academy of Sciences, 1967)
- Nikishov A I *Tr. Fiz. Inst. Akad. Nauk SSSR* **111** 152 (1979)
- Kotova L P, Perelomov A M, Popov V S *Zh. Eksp. Teor. Fiz.* **54** 1151 (1968) [*Sov. Phys. JETP* **27** 616 (1968)]
- Hartree D R *Proc. Camb. Philos. Soc.* **24** 89 (1927)
- Bates D R, Damgaard A *Philos. Trans. R. Soc. London* **242** 101 (1949)
- Hartree D R *The Calculation of Atomic Structures* (New York: J. Wiley, 1957)
- Radziĭ A A, Smirnov B M *Parametry Atomov i Atomnykh Ionov* (Moscow: Energoatomizdat, 1986) [Translated into English (earlier edition) as *Reference Data on Atoms, Molecules, and Ions* (Berlin: Springer-Verlag, 1985)]
- Sobelman I I *Vvedenie v Teoriyu Atomnykh Spektrov* (Moscow: Nauka, 1977) [Translated into English as *Atomic Spectra and Radiative Transitions* (Berlin: Springer-Verlag, 1979)]
- Landau L D, Lifshitz E M *Kvantovaya Mekhanika: Nerelyativistskaya Teoriya* (Quantum Mechanics: Non-Relativistic Theory) (Moscow: Fizmatlit, 2001) [Translated into English (Oxford: Pergamon Press, 1977)]
- Rapoport L P, Zon B A, Manakov N L *Teoriya Mnogofotonnykh Protseessov v Atomakh* (Theory of Multiphoton Processes in Atoms) (Moscow: Atomizdat, 1978)
- Seaton M J *Mon. Not. R. Astron. Soc.* **118** 504 (1958); *Rep. Prog. Phys.* **46** 167 (1983)
- Mur V D, Karnakov B M, Popov V S *Dokl. Ross. Akad. Nauk* **365** 329 (1999) [*Dokl. Phys.* **44** 156 (1999)]; *Zh. Eksp. Teor. Fiz.* **115** 521 (1999) [*JETP* **88** 286 (1999)]
- Abramowitz M, Stegun I A (Eds) *Handbook of Mathematical Functions with Formulas, Graphs, and Mathematical Tables* (New York: Dover Publ., 1965) [Translated into Russian (Moscow: Nauka, 1979)]
- Popov V S *Pis'ma Zh. Eksp. Teor. Fiz.* **70** 493 (1999) [*JETP Lett.* **70** 502 (1999)]; *Zh. Eksp. Teor. Fiz.* **118** 56 (2000) [*JETP* **91** 48 (2000)]; *Laser Phys.* **10** 1033 (2000)
- Voronov G S et al. *Pis'ma Zh. Eksp. Teor. Fiz.* **2** 377 (1965) [*JETP Lett.* **2** 237 (1965)]; Voronov G S, Delone N B *Zh. Eksp. Teor. Fiz.* **50** 78 (1966) [*Sov. Phys. JETP* **23** 54 (1966)]; Voronov G S, Delone G A, Delone N B *Zh. Eksp. Teor. Fiz.* **51** 1660 (1966) [*Sov. Phys. JETP* **24** 1122 (1967)]
- Faisal F H M *J. Phys. B: At. Mol. Phys.* **6** L89 (1973)
- Reiss H R *Phys. Rev. A* **22** 1786 (1980); **42** 1476 (1990); *Prog. Quantum Electron.* **16** (1) 1 (1992)
- Reiss H R *J. Opt. Soc. Am. B* **7** 574 (1990)
- Brabec T, Krausz F *Rev. Mod. Phys.* **72** 545 (2000)
- Delone N B, Kraĭnov V P *Multiphoton Processes in Atoms* (Berlin: Springer-Verlag, 1994; 2nd ed. — Berlin: Springer, 2000)
- Fock V A *Z. Phys.* **98** 145 (1935)
- Bargmann V *Z. Phys.* **99** 576 (1935)
- Bander M, Itzykson C *Rev. Mod. Phys.* **38** 330, 346 (1966)
- Perelomov A M, Popov V S *Zh. Eksp. Teor. Fiz.* **50** 179 (1966) [*Sov. Phys. JETP* **23** 118 (1966)]
- Popov V S “O ‘skrytoĭ’ simmetrii atoma vodoroda” (“On the ‘hidden’ symmetry of the hydrogen atom), in *Fizika Vysokikh Energii i Teoriya Elementarnykh Chastits* (High-Energy Physics and Theory of Elementary Particles) (Ed. V P Shelest) (Kiev: Naukova Dumka, 1967) p. 702
- Smirnov B M, Chibisov M I *Zh. Eksp. Teor. Fiz.* **49** 841 (1965) [*Sov. Phys. JETP* **22** 585 (1966)]
- Demkov Yu N, Drukarev G F *Zh. Eksp. Teor. Fiz.* **47** 918 (1964) [*Sov. Phys. JETP* **20** 614 (1965)]
- Gribakin G F, Kuchiev M Yu *Phys. Rev. A* **55** 3760 (1997)
- Goreslavskii S P, Shvetsov-Shilovskii N I, Shcherbachev O V, in *Nauchnaya Sessiya MIFI-2004, Moskva, 26–30 Yanvarya 2004 g.* (Scientific Session of the Moscow Engineering Physics Institute-2004, Moscow, 26–30 January 2004) Vol. 5 (Moscow: MIFI, 2004) p. 158; *Zh. Eksp. Teor. Fiz.* **127** (1) (2005) ¶
- Goreslavskii S P, Popruzhenko S V *Zh. Eksp. Teor. Fiz.* **110** 1200 (1996) [*JETP* **83** 661 (1996)]
- Goreslavskii S P, Popruzhenko S V *Laser Phys.* **6** 780 (1996); Goreslavskii S P, Popruzhenko S V *Laser Phys.* **7** 700 (1997)
- Mur V D, Popruzhenko S V, Popov V S *Zh. Eksp. Teor. Fiz.* **119** 893 (2001) [*JETP* **92** 777 (2001)]
- Kraĭnov V P *J. Phys. B: At. Mol. Opt. Phys.* **32** 1607 (1999)
- Paulus G G et al. *Phys. Rev. Lett.* **80** 484 (1998)
- Becker W et al. *Laser Phys.* **8** 56 (1998)
- Paulus G G et al. *Phys. Rev. Lett.* **84** 3791 (2000)
- Corkum P B, Burnett N H, Brunel F *Phys. Rev. Lett.* **62** 1259 (1989)
- Pont M, Shakeshaft R, Potvliege R M *Phys. Rev. A* **42** 6969 (1990); Pont M et al. *Phys. Rev. A* **45** 8235 (1992)
- Dykhne A M *Zh. Eksp. Teor. Fiz.* **38** 570 (1960); **41** 1324 (1961) [*Sov. Phys. JETP* **11** 411 (1960); **14** 941 (1962)]
- Delone N B, Kraĭnov V P *Atom v Sil'nom Svetovom Pole* (Atom in a Strong Light Field) 2nd ed. (Moscow: Energoatomizdat, 1984) [Translated into English: *Atoms in Strong Light Fields* (Berlin: Springer-Verlag, 1985)]
- Delone N B, Kraĭnov V P *J. Opt. Soc. Am. B* **8** 1207 (1991)
- Kraĭnov V P *J. Opt. Soc. Am. B* **14** 425 (1997)
- Kraĭnov V P, Ristic V M *Zh. Eksp. Teor. Fiz.* **101** 1479 (1992) [*Sov. Phys. JETP* **74** 789 (1992)]
- Delone N B, Kraĭnov V P *Usp. Fiz. Nauk* **168** 531 (1998) [*Phys. Usp.* **41** 469 (1998)]
- Popov V S *Usp. Fiz. Nauk* **169** 819 (1999) [*Phys. Usp.* **42** 733 (1998)]
- Bashkansky M, Bucksbaum P H, Schumacher D W *Phys. Rev. Lett.* **60** 2458 (1988)
- Basile S, Trombetta F, Ferrante G *Phys. Rev. Lett.* **61** 2435 (1988)
- Shvetsov-Shilovskii N I, Goreslavskii S P, Popruzhenko S V, in *Nauchnaya Sessiya MIFI-2004, Moskva, 26–30 Yanvarya 2004 g.* (Scientific Session of the Moscow Institute of Engineering Physics-2004, Moscow, 26–30 January 2004) Vol. 5 (Moscow: MIFI, 2004) p. 208; *Phys. Rev. Lett.* **93** 233002 (2004) ¶
- Hehenberger M, McIntosh H V, Brändas E *Phys. Rev. A* **10** 1494 (1974)
- Yamabe T, Tachibana A, Silverstone H J *Phys. Rev. A* **16** 877 (1977)
- Benassi L, Grecchi V *J. Phys. B: At. Mol. Phys.* **13** 911 (1980)
- Franceschini V, Grecchi V, Silverstone H J *Phys. Rev. A* **32** 1338 (1985)
- Vainberg V M et al. *Pis'ma Zh. Eksp. Teor. Fiz.* **44** 9 (1986) [*JETP Lett.* **44** 9 (1986)]; *Zh. Eksp. Teor. Fiz.* **93** 450 (1987) [*Sov. Phys. JETP* **66** 258 (1987)]
- Popov V S et al. *Phys. Lett. A* **124** 77 (1987); **149** 418 (1990); Popov V S, Mur V D, Sergeev A V *Phys. Lett. A* **193** 159 (1994)

62. Fernández F M *Phys. Rev. A* **54** 1206 (1996)
63. Barenblatt G I, Zel'dovich Ya B *Usp. Mat. Nauk* **26** 115 (1971) [*Russ. Math. Surv.* **26** 45 (1972)]
64. Zel'dovich Ya B, Sokolov D D *Usp. Fiz. Nauk* **146** 493 (1985) [*Sov. Phys. Usp.* **28** 608 (1985)]
65. Benassi L et al. *Phys. Rev. Lett.* **42** 704, 1430 (1979)
66. Popov V S *Phys. Lett. A* **173** 63 (1993)
67. Yaffe L G *Rev. Mod. Phys.* **54** 407 (1982)
68. Doren D J, Herschbach D R *Phys. Rev. A* **34** 2654 (1986)
69. Tsipis C A et al. (Eds) *New Methods in Quantum Theory* (Dordrecht: Kluwer Acad., 1996)
70. Keldysh L “Multiphoton ionization by a very short laser pulse” (private commun.)
71. Popov V S *Laser Phys.* **10** 1033 (2000); *Pis'ma Zh. Eksp. Teor. Fiz.* **73** 3 (2001) [*JETP Lett.* **73** 1 (2001)]; *Zh. Eksp. Teor. Fiz.* **120** 315 (2001) [*JETP* **93** 278 (2001)]
72. Popov V S, Karnakov B M, Mur V D *Phys. Lett. A* **229** 306 (1997); *Zh. Eksp. Teor. Fiz.* **113** 1579 (1998) [*JETP* **86** 860 (1998)]
73. Baz' A I, Zel'dovich Ya B, Perelomov A M *Rassseyanie, Reaktsii i Raspady v Nerelativistskoĭ Kvantovoi Mekhanike* (Scattering, Reactions and Decays in Nonrelativistic Quantum Mechanics) 2nd ed. (Moscow: Nauka, 1971) [Translated into English 1st ed. (Jerusalem: Israel Program for Scientific Translations, 1969)]
74. Popov V S *Zh. Eksp. Teor. Fiz.* **61** 1334 (1971); **63** 1586 (1972) [*Sov. Phys. JETP* **34** 709 (1972); **36** 840 (1973)]
75. Landau L D *Phys. Z. Sowjetunion* **1** 88; **2** 46 (1932); *Sobranie Trudov* (Collected Works) Vol. 1 (Moscow: Nauka, 1969) pp. 71, 81
76. Lifshitz E M *Zh. Eksp. Teor. Fiz.* **8** 930 (1938)
77. Nikitin E E, Pitaevskii L P *Usp. Phys. Nauk* **163** (9) 101 (1993) [*Phys. Usp.* **36** 851 (1993)]
78. Landau L D, Lifshitz E M *Mekhanika* (Mechanics) (Moscow: Fizmatlit, 2001) [Translated into English (Oxford: Pergamon Press, 1976)]
79. Gaponov A V, Miller M A *Zh. Eksp. Teor. Fiz.* **34** 242 (1958) [*Sov. Phys. JETP* **7** 168 (1958)]
80. Muller H G, Tip A, van der Wiel M J *J. Phys. B: At. Mol. Phys.* **16** L679 (1983)
81. Goreslavsky S P, Narozhny N B, Yakovlev V P *J. Opt. Soc. Am. B* **6** 1752 (1989)
82. Popov V S, Sergeev A V *Pis'ma Zh. Eksp. Teor. Fiz.* **63** 398 (1996) [*JETP Lett.* **63** 417 (1996)]
83. Drukarev G F, Monozon B S *Zh. Eksp. Teor. Fiz.* **61** 956 (1971) [*Sov. Phys. JETP* **34** 509 (1972)]
84. Dyson F J *Phys. Rev.* **85** 631 (1952)
85. Kazakov D I, Shirkov D V *Fortschr. Phys.* **28** 465 (1980)
86. Itzykson C, Zuber J-B *Quantum Field Theory* (New York: McGraw-Hill Intern. Book Co., 1980) [Translated into Russian: Vol. 2 (Moscow: Mir, 1984) Ch. 9]
87. Kazakov D I, Popov V S *Zh. Eksp. Teor. Fiz.* **122** 675 (2002) [*JETP* **95** 581 (2002)]
88. Popov V S, Sergeev A V *Zh. Eksp. Teor. Fiz.* **113** 2047 (1998) [*JETP* **86** 1122 (1998)]
89. Popov V S, Sergeev A V, Shchablykin A V *Zh. Eksp. Teor. Fiz.* **102** 1453 (1992) [*Sov. Phys. JETP* **75** 787 (1992)]; Popov V S, Sergeev A V *Zh. Eksp. Teor. Fiz.* **105** 568 (1994) [*JETP* **78** 303 (1994)]
90. Popov V S, Sergeev A V *Phys. Lett. A* **172** 193 (1993); **193** 165 (1994)
91. López-Cabrera M et al. *Phys. Rev. Lett.* **68** 1992 (1992)
92. Kais S, Herschbach D R *J. Chem. Phys.* **98** 3990 (1993)
93. Karnakov B M, Mur V D, Popov V S *Pis'ma Zh. Eksp. Teor. Fiz.* **65** 391 (1997) [*JETP Lett.* **65** 405 (1997)]; Popov V S, Karnakov B M, Mur V D *Zh. Eksp. Teor. Fiz.* **115** 1642 (1999) [*JETP* **88** 902 (1999)]
94. Sakharov A D et al. *Dokl. Akad. Nauk SSSR* **196** 65 (1965)
95. Sakharov A D *Usp. Fiz. Nauk* **88** 725 (1966) [*Sov. Phys. Usp.* **9** 294 (1966)]
96. Pavlovskii A I, in *Akademik A.D. Sakharov. Nauchnye Trudy* (Academician A.D. Sakharov. Scientific Works) (Eds B L Al'tshuler et al.) (Moscow: Tsentrkom OTF FIAN, 1995) p. 85
97. Fabrika S N, Balyavin G G, Preprint No. 129 (Nizhniĭ Arkhyz: Special Astrophysical Observatory of the Russian Academy of Sciences, 1998)
98. Nikishov A I *Zh. Eksp. Teor. Fiz.* **60** 1614 (1971) [*Sov. Phys. JETP* **33** 873 (1971)]; *Tr. Fiz. Inst. Akad. Nauk SSSR* **113** 211 (1979)
99. Manakov N L et al. *J. Phys. B: At. Mol. Opt. Phys.* **33** R141 (2000)
100. Bunkin F V, Prokhorov A M *Zh. Eksp. Teor. Fiz.* **46** 1090 (1964) [*Sov. Phys. JETP* **19** 739 (1964)]
101. Zel'dovich Ya B *Zh. Eksp. Teor. Fiz.* **51** 1492 (1966) [*Sov. Phys. JETP* **24** 1006 (1967)]; *Usp. Fiz. Nauk* **110** 139 (1973) [*Sov. Phys. Usp.* **16** 427 (1973)]
102. Ritus V I *Zh. Eksp. Teor. Fiz.* **51** 1544 (1966) [*Sov. Phys. JETP* **24** 1041 (1967)]
103. Manakov N L, Rapoport L P *Zh. Eksp. Teor. Fiz.* **69** 842 (1975) [*Sov. Phys. JETP* **42** 430 (1976)]; Manakov N L, Ovsiannikov V D, Rapoport L P *Phys. Rep.* **141** 319 (1986)
104. Berson I J *J. Phys. B: At. Mol. Phys.* **8** 3078 (1975)
105. Mur V D et al. *Pis'ma Zh. Eksp. Teor. Fiz.* **75** 294 (2002) [*JETP Lett.* **75** 249 (2002)]; *Yad. Fiz.* **66** 2014 (2003) [*Phys. At. Nucl.* **66** 1964 (2003)]
106. Zel'dovich Ya B *Zh. Eksp. Teor. Fiz.* **39** 776 (1960) [*Sov. Phys. JETP* **12** 542 (1961)]
107. Andreev S P, Karnakov B M, Mur V D *Pis'ma Zh. Eksp. Teor. Fiz.* **37** 155 (1983) [*JETP Lett.* **37** 187 (1983)]; Andreev S P et al. *Zh. Eksp. Teor. Fiz.* **86** 866 (1984) [*Sov. Phys. JETP* **59** 506 (1984)]
108. Mur V D et al. *Phys. Lett. A* **316** 226 (2003)
109. Manakov N L et al. *Pis'ma Zh. Eksp. Teor. Fiz.* **72** 426 (2000) [*JETP Lett.* **72** 294 (2000)]
110. Borca B et al. *Phys. Rev. Lett.* **88** 193001 (2002); Manakov N L et al. *J. Phys. B: At. Mol. Opt. Phys.* **36** R49 (2003)
111. Xiong W, Chin S L *Zh. Eksp. Teor. Fiz.* **99** 481 (1991) [*Sov. Phys. JETP* **72** 268 (1991)]
112. Fittinghoff D N et al. *Phys. Rev. Lett.* **69** 2642 (1992)
113. Moshhammer R et al. *Phys. Rev. Lett.* **84** 447 (2000)
114. Mohideen U et al. *Phys. Rev. Lett.* **71** 509 (1993)
115. Ammosov M V, Delone N B, Kraĭnov V P *Zh. Eksp. Teor. Fiz.* **91** 2008 (1986) [*Sov. Phys. JETP* **64** 1191 (1986)]
116. Tajima T, Mourou G *Phys. Rev. ST Accel. Beams* **5** 031301 (2002)
117. Sauter F Z. *Phys.* **69** 742; **73** 547 (1931)
118. Heisenberg W, Euler H Z. *Phys.* **98** 714 (1936)
119. Schwinger J *Phys. Rev.* **82** 664 (1951)
120. Akhiezer A I, Berestetskii V B *Kvantovaya Elektrodinamika* (Quantum Electrodynamics) (Moscow: Nauka, 1981) [Translated into English from the 2nd Russian ed. (New York: Interscience Publ., 1965)]
121. Marinov M S, Popov V S *Yad. Fiz.* **15** 1271 (1972); *Fortschr. Phys.* **25** 373 (1977)
122. Bargmann V, Michel L, Telegdi V L *Phys. Rev. Lett.* **2** 435 (1959)
123. Breit G *Nature* **122** 649 (1928)
124. Perelomov A M, Popov V S *Yad. Fiz.* **14** 661 (1971)
125. Popov V S *Yad. Fiz.* **12** 429 (1970); **14** 458 (1971); **64** 421 (2001) [*Phys. At. Nucl.* **64** 367 (2001)]
126. Zel'dovich Ya B, Popov V S *Usp. Fiz. Nauk* **105** 403 (1971) [*Sov. Phys. Usp.* **14** 673 (1972)]
127. Schiff L I *Quantum Mechanics* 2nd ed. (New York: McGraw-Hill, 1955) [Translated into Russian (Moscow: IL, 1957)]
128. Popov V S, Karnakov B M, Mur V D *Pis'ma Zh. Eksp. Teor. Fiz.* **79** 320 (2004) [*JETP Lett.* **79** 262 (2004)]
129. Popov V S, Mur V D, Karnakov B M *Pis'ma Zh. Eksp. Teor. Fiz.* **66** 213 (1997) [*JETP Lett.* **66** 229 (1997)]; *Phys. Lett. A* **250** 20 (1998)
130. Mur V D, Karnakov B M, Popov V S *Zh. Eksp. Teor. Fiz.* **114** 798 (1998) [*JETP* **87** 433 (1998)]
131. Karnakov B M, Mur V D, Popov V S *Yad. Fiz.* **62** 1444 (1999) [*Phys. At. Nucl.* **62** 1363 (1999)]
132. Milosevic N, Krainov V P, Brabec T *Phys. Rev. Lett.* **89** 193001 (2002)
133. Milosevic N, Krainov V P, Brabec T *J. Phys. B: At. Mol. Opt. Phys.* **35** 3515 (2002)
134. Karnakov B M, Mur V D, Popov V S, quant-ph/0405158
135. Brezin E, Itzykson C *Phys. Rev. D* **2** 1191 (1970)
136. Popov V S *Pis'ma Zh. Eksp. Teor. Fiz.* **13** 261 (1971) [*JETP Lett.* **13** 185 (1971)]; *Zh. Eksp. Teor. Fiz.* **61** 1334 (1971) [*Sov. Phys. JETP* **34** 709 (1972)]
137. Popov V S *Pis'ma Zh. Eksp. Teor. Fiz.* **18** 453 (1973) [*JETP Lett.* **18** 255 (1973)]; *Yad. Fiz.* **19** 155 (1974)
138. Narozhnyi N B, Nikishov A I *Zh. Eksp. Teor. Fiz.* **65** 862 (1973) [*Sov. Phys. JETP* **38** 427 (1974)]
139. Mostepanenko V M, Frolov V M *Yad. Fiz.* **19** 885 (1974)

140. Popov V S *Pis'ma Zh. Eksp. Teor. Fiz.* **74** 151 (2001) [*JETP Lett.* **74** 133 (2001)]; *Zh. Eksp. Teor. Fiz.* **121** 1235 (2002) [*JETP* **94** 1057 (2002)]
141. Nikishov A I *Nucl. Phys. B* **21** 346 (1970); Narozhnyi N B, Nikishov A I *Yad. Fiz.* **11** 1072 (1970) [*Sov. J. Nucl. Phys.* **11** 596 (1970)]
142. Alkofer R et al. *Phys. Rev. Lett.* **87** 193902 (2001)
143. Ringwald A *Phys. Lett. B* **510** 107 (2001)
144. Popov V S *Phys. Lett. A* **298** 83 (2002)
145. Bulanov S S et al. *Phys. Lett. A* (2004) (in press)
146. Narozhny N B, Fofanov M S *Zh. Eksp. Teor. Fiz.* **117** 867 (2000) [*JETP* **90** 753 (2000)]; *Phys. Lett. A* **295** 87 (2002)
147. Oppenheimer J R *Phys. Rev.* **31** 66 (1928)
148. Yamabe T, Tachibana A, Silverstone H J *Phys. Rev. A* **16** 877 (1977)
149. Landau L D, Lifshitz E M *Kvantovaya Mekhanika* (Quantum Mechanics) 2nd ed. (Moscow: Fizmatlit, 1963) p. 327 [Translated into English (Oxford: Pergamon Press, 1965)]
150. Reichle R, Helm H, Kiyan I Yu *Phys. Rev. Lett.* **87** 243001 (2001)
151. Kiyan I Yu, Helm H *Phys. Rev. Lett.* **90** 183001 (2003)
152. Agostini P et al. *Phys. Rev. Lett.* **42** 1127 (1979)
153. *JST Intern. Symp. on Control of Molecules in Intense Laser Fields, Tokyo, Japan, Sept. 9–10, 2002*, Program and Abstracts (Tokyo, 2002)
154. Goldberger M L, Watson K M *Collision Theory* (New York: Wiley, 1964) [Translated into Russian (Moscow: Mir, 1967)]
155. Curtis A R *Coulomb Wave Functions* (Cambridge: Univ. Press, 1964)
156. Krainov V P, Xiong W, Chin S L *Laser Phys.* **2** 467 (1992)
157. Delone N B, Kraїnov V P *Nelineinaya Ionizatsiya Atomov Lazernym Izlucheniem* (Nonlinear Atom Ionization by Laser Radiation) (Moscow: Fizmatlit, 2001)